MORPHOLOGY OF THE INNER STRUCTURES OF THE FACIAL SKELETON IN *HOMO NEANDERTHALENSIS* AND THE CASE-STUDY OF THE NEANDERTHAL FROM ALTAMURA (BARI, ITALY)

PhD candidate
Costantino Buzi

Tutor
Prof. Giorgio Manzi

SAPIENZA
UNIVERSITÀ DI ROMA

Sapienza University of Rome
Department of Environmental Biology
PhD course in Environmental and Evolutionary Biology
(curriculum Anthropology)
XXXII PhD program

Alla mia famiglia

A mio padre

CONTENTS

ACKNOWLEDGMENTS

I would like to thank the Department of Environmental Biology of the Sapienza University of Rome for allowing me to conduct this research and, more in general, granting me an ideal environment to start a career in research. I thank my friend and colleague Antonio Profico very much, for his unlimited patience, resourcefulness and inspiring enthusiasm in investigation. I also thank my other friends and colleagues from the Laboratory of Paleoanthropology and Bioarcheology: Ileana Micarelli, Fabio Di Vincenzo, Mary Anne Tafuri, Sara Bernardini, Robert Paine, Carlotta Zeppilli, Sofia Panella, Roberta Manzollino, Elisabetta Aloisi Masella. The work for this research included activities on the field which would not have been possible without the permission of the "Soprintendenza A.B.A.P. per la città metropolitana di Bari" (formerly "Soprintendenza Archeologia per la Puglia"), the national park "Parco Nazionale dell'Alta Murgia", and the municipality of Altamura. To work in the Lamalunga Cave, on the other hand, would have been impossible without the speleologist of C.A.R.S. (Centro Altamurano Ricerche Speleologiche) and without Vincenzo Martimucci (Società Speleologica Italiana) or would have been even worse without the commitment, the assistance and friendship of Marco Boggioni. For a great part of this work I am debtor to Mario Micheli, Andrea Borsato, Marco Samadelli, Paolo Piras, Andrea Papini, Stefan Schlager, Marco Antonucci (Olympus Italia), Stefano Tamburrini (Olympus Europe) and Simone Amici (Leica Geosystems). The materials of the comparative sample were kindly provided by Museo Preistorico Etnografico "Luigi Pigorini", Rome (now part of the "Museo delle Civiltà"); Natural History Museum, London; Tel Aviv University; Musée de l'Homme, Paris; Aristotle University of Thessaloniki; Museo di Antropologia "Giuseppe Sergi", Rome; Museo de la Evolución Humana, Burgos; Naturkunde Museum, Stuttgart; NESPOS Pleistocene People and Places; in the same way I thank Christoph P. E. Zollikofer, Lynn Copes, Amélie Vialet and Adrie and Alfons Kennis. In the last three years I've been lucky to meet, exchange

ideas and sometimes to collaborate with some of the greatest experts in the study of human evolution and prehistory, I would like to thank here in a strict alphabetical order: Juan Luis Arsuaga, Giovanni Boschian, José Miguel Carretero, Steven E. Churchill, Stefano Grimaldi, Dominique Grimaud-Hervé, Carlos Lorenzo Merino, Damiano Marchi, Ignacio Martínez Mendizábal, Fidelis T. Masao, Jacopo Moggi-Cecchi, Paul O'Higgins, Rolf Quam, Pasquale Raia, Ian Tattersall. I would like to thank all the friends and colleagues I had the pleasure to meet - and work with - in Spain, on excavation or during my stays as visiting student in Madrid; among them, Maicu Ortega, Mercedes Conde-Valverde, Laura Rodriguez, Rebeca García-González and Yuliet Quintino. I would like to thank Elena Santos very much, for her friendship and her invaluable help in the study of the maxillary sinuses. During my PhD I had the chance to participate to wonderful meetings and conferences in which I could count on the help, the advices and - more importantly - the great company of a group of friends and colleagues among which I would like to thank Alessio Veneziano, Federica Landi, Antonia Del Bove, Tommaso Mori, Lumila Menendez, Vito Sparacello and Alessandro Riga, also a 'brother in arms' at Lamalunga Cave. I also would like to thank my good friend Nico Radi and my good friend Marco Cherin, to whom I owe a lot. I thank my non-academic friends, some of which – Daniele, Gabriele, Simone, Emiliano - I can count on since very long time. I can't thank enough my girlfriend – and accidentally lawyer - Rachele Fortuni, without whom I probably would not have achieved anything of which I'm proud of today. Lastly, I'm very grateful to Prof. Giorgio Manzi for having given me the opportunity to start this career and an international range in which pursue it, for having granted me his trust for work on an incomparable specimen and, ultimately, for being my mentor and advisor.

LIST OF TABLES AND FIGURES

1 INTRODUCTION

Gonna end up a big ole pile a them bones.

Jerry Cantrell, *Them Bones*

The present thesis reports the results of an investigation performed both 'on the field' and in laboratory activities of Virtual Anthropology. The subject of the investigation is a unique human specimen still preserved in the place of its deposition: the so-called "Altamura Man", or, more simply, Altamura.

Altamura is a nearly complete skeleton of an archaic or 'early' Neanderthal – of exceptional antiquity, actually – which is still preserved, covered in karstic concretions, inside the Lamalunga Cave, in Southern Italy. Altamura is potentially the most complete Neanderthal specimen in the fossil record, but the lesser known at the same time. There are a number of reasons for this: the lack of an in-depth study between its discovery in 1993 and the last years of activities, the difficult access to the place of deposition, in association to the peculiar condition of preservation of the specimen, which resulted in a nearly perfect condition of the skeletal structures, but in their exceptional fragility at the same time. Also, to a lesser degree, are to be mentioned some 'socio-political' circumstances, occurred because in the town of Altamura the discovery of a Neanderthal skeleton triggered a debate on its potential in terms of public fruition before raising a discussion on its scientific relevance.

Nowadays, a multidisciplinary project of National concern (the K.A.R.S.T. project), involving an international research group directed by prof. G. Manzi, is underway and this thesis has the aim to present some of the outputs coming from the activities carried out in the last three years. These activities prelude to a future extraction of the entire skeleton from the Lamalunga Cave and possibly to an extended study of the karstic system as a whole, including the faunal fossil record it preserves. At present, the project

has been aimed at the most complete characterisation of both the specimen *in situ* and the cave environmental conditions which determined its unique preservation.

The peculiar case study of Altamura led to the development of new techniques of Virtual Anthropology, that are presented in this thesis: i - two tools for the automatic segmentation of inner cavities of the cranium; ii - a statistics-based method for the digital alignment of disassembled skeletal objects; iii - a method for the combined analysis of separate portions – or norms – of the same object of study.

Lastly, the remarkable preservation of the facial skeleton in Altamura has led to the investigations on the inner cavities of the cranium (i.e. maxillary sinuses) influencing the facial morphology, which deserved a preliminary observation on the Mid-to-Late Pleistocene human fossil record, although still not including the case study itself.

The scenario outlined by the analysis reported in this thesis is that of an exceptionally archaic Neanderthal, bearing more traits in common with earlier Neanderthal-related Mid-Pleistocene samples (i.e., Atapuerca Sima de Los Huesos), than those shared with the Neanderthals *sensu stricto*, from 'early' to 'classic' Neanderthals.

Cutting-edge techniques of Virtual Anthropology – Paleoanthropology, in this case – were applied to investigate the cranium – not yet extracted - and to offer the most faithful reconstruction of its morphology, both in general and in some of the details of the facial skeleton. Therefore, along with the activities currently held in the context of the K.A.R.S.T. project, this thesis represents part of a work aimed to the most complete documentation and digital acquisition of a paleoanthropological specimen in its place of deposition, where little has probably changed in the environmental conditions from about 180 ka to the date of the discovery.

1.1 THE HUMAN CRANIUM

The head is one of the elements that most defines us as a species: it carries a unique assemblage of features that cannot be found in any other mammal, vertebrate or animal more in general (Lieberman, 2011). The many functions performed by the head are reflected in the complex structure of the skull, which represents for this reason – in humans and in the majority of vertebrates as well - the most diagnostic district of the skeleton. Moreover, the shape of the head in *H. sapiens*, carries traits that allow an almost immediate recognition from other species of its genus, as for example the vertical forehead, the globular braincase and the distinct presence of a chin (Lieberman, 1998).

In anthropology, the skull is one of the key element to look at for determining sex, age and lifestyle, whereas paleoanthropologist can extract from it crucial information on phylogeny and the evolution of aspects as locomotion, diet, cognition, encephalization (White and Folkens, 2005; Ponce De León et al., 2008; Gunz et al., 2010; Bruner et al., 2016; Profico et al., 2017).

The human cranium is composed by 28 bones (ossicles of the medium ear included) and can be subdivided in three regions (fig.1.1), deriving from embryologically distinct regions: the splanchnocranium, the neurocranium and the basicranium (Lieberman, 2000), with the sphenoid bone being the structural 'pivot' around which the three modules develop - or even are affected by - during ontogeny (Lieberman et al., 2000; Profico et al., 2017). The basicranium, or cranial base, is the primal foundation for the development of the rest of the skull; it is composed, in adults, by portions of sphenoid, occipital, temporals and ethmoid and its formation starts during the embryonic development, from condensations of parachordal cartilages (Lieberman, 2011). The neurocranium, or cranial vault, is mainly formed by the parietals, with the contributions of the squamous portions of temporals, occipital and frontal bones, and portions of the sphenoid; its formation starts at the edge of the already formed

basicranial bones, with an upwards migration of the mesodermal cells and subsequent covering of the meningeal mesenchymal layers (Yoshida et al., 2008). The splanchnocranium, or facial skeleton, grows below the brain and the cranial base and is originated around the oral cavity and pharynx, mainly from the branchial pharyngeal arches at the back of the embryonic head (Lieberman, 2011). The frontal bone, although contributing to the structure of the face with the supraorbital ridge, is generally not considered part of the splanchnocranium, that is thus composed by lacrimal, nasal, zygomatic, palatine bones, the maxillae, the inferior nasal conchae, and the vomer; the mandible and the hyoid bone are often considered part of the facial skeleton as well.

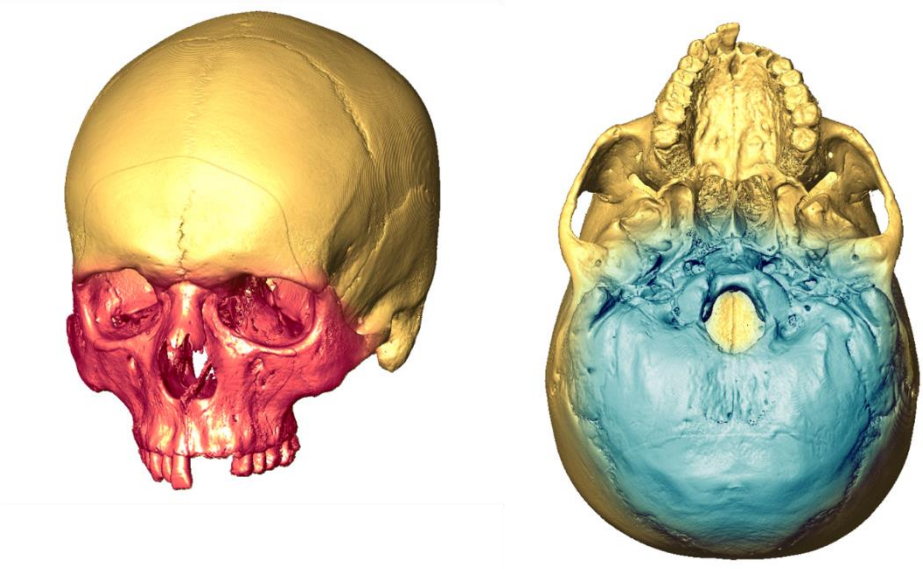

Figure 1.1 - Cranial districts. In yellow, neurocranium; in red, splanchnocranium; in blue, basicranium

In primates, apart from constraints related with developmental processes, the three regions are morphologically influenced in a differential way by the presence of sensory organs and functional demands as masticatory stress, vocalization, posture, equilibrium (Profico et al., 2017). This determines that although connected, the three regions show different patterns of development both in ontogeny and phylogeny, which can be explained by the concepts of integration and modularity (Klingenberg, 2013; Esteve-

Altava, 2017). The evolution of primates, as well as that of human species, is characterized by great modifications in the cranial anatomical regions (Bruner, 2007; Cardini and Elton, 2008), which led to the recognition, by some authors, of a strong integration between facial skeleton and cranial base (Bastir et al., 2010; Gkantidis and Halazonetis, 2011; Neaux, 2017), whereas additional studies found that the same regions respond to different evolutionary pressures and their status of distinct modules is determined by different aspects: locomotion and posture on the cranial base and, on the face, size, sexual election and the rate of airorhynchy, a structural pattern of the cranium the function of which is still debated (Tattersall, 1972; Bruner et al., 2004; Profico et al., 2017).

1.2 THE INNER CAVITIES OF THE CRANIUM

As already mentioned in the previous section, the cranium represents the most informative region of the skeleton: it is a complex structure, which encloses vital organs and tissues - among which can be cited the brain and the majority of sensory organs - and its morphology reflects functional demands and/or constraints, as those related with posture, mastication or encephalization. It goes without saying that like the actual bony structure, much of the informative value of the cranium is carried by the hollow spaces enclosing organs and tissues and the traces left by these on the inner surfaces of the bone.

The major cavities of the human cranium are the neurocranial cavity and the maxillary sinuses. The latter are comprised among the paranasal sinuses along the smaller frontal, ethmoidal and sphenoidal sinuses (White et al., 2011) (fig. 1.2). Other highly informative cavities are those housing the sensory organs (i.e. orbits, inner nose, inner and medium ear), as well as the canals where the sensory nerves pass through. Lastly,

there are the many air-filled cells forming the pneumatization of some bones (e.g. temporal bones) (Preuschoft et al., 2002).

Figure 1.2 - Inner cavities of a human cranium extracted by automatic segmentation. Are visible the endocast, the paranasal sinuses and other pneumatization

The attention of paleoanthropologists to the inner cavities of the human skull is longstanding, tracing back at least to Taung child's natural endocast discovered in South Africa and described by Raymond Dart (1925), while, more in general, the cranial cavities of the human cranium have been of interest for scholars since the dawn of anatomical studies. According to Keir (2009), the study of paranasal sinuses can be traced back to Galen of Pergamon (129 – c. 200 AD), which is credited with the first acknowledgement by Vesalius and Fallopius, as reported by Wright (1914). Flottes and colleagues (1960) attribute the discovery of paranasal sinuses to Leonardo Da Vinci (1452–1519) which identified frontal and maxillary sinuses in his classic illustrations

"Two views of the skull" and "View of a skull"(1489 ca., fig 1.3) and also proposed that the maxillary sinus 'contains the humor which nourishes the teeth' (Keir, 2009).

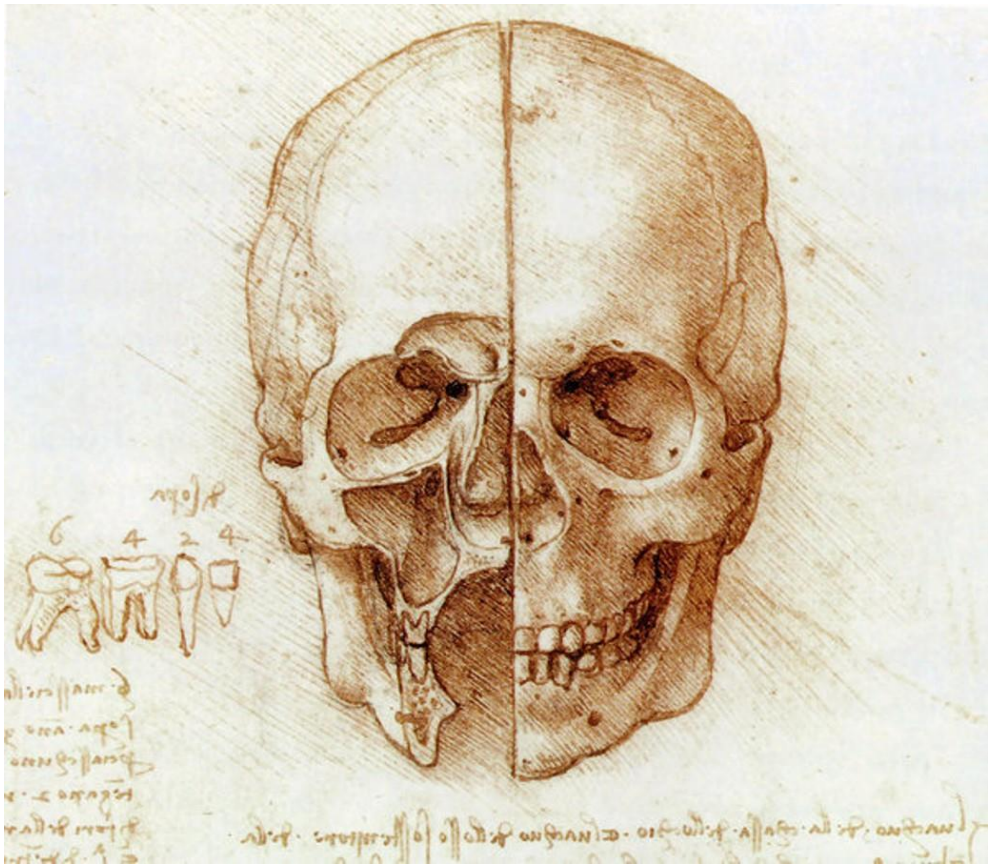

Figure 1.3 - Leonardo Da Vinci, "View of a skull"(1849 ca.). Are recognizable the frontal and maxillary sinuses

The introduction of x-ray-based technology (Röntgen, 1896) allowed to start to look at the internal structures of the skeleton without dissecting it, a procedure that meant the damage or even the destruction of the object of study. In palaeoanthropology, X rays are applied since 1902 – the first application was carried out on the Neanderthal sample from Krapina (Gorjanović-Kramberger, 1906) - and the use of digital acquisition techniques is nowadays essential for the purpose of preserving and studying in detail unique specimens. The use of CT scans is now very common for the digitization of skeletal and fossil specimens and led to the ever-increasing availability of web-based repositories (e.g., Nespos, Digital Morphology Museum, KUPRI, MorphoSource). Thanks to this technology, the number of studies dedicated to the sizes and shape of

inner cavities of skeletal specimens has increased in the last few years. Such studies include investigations on inner ear structure (Spoor and Zonneveld, 1995; Spoor et al., 2003; Quam et al., 2015; Conde-Valverde et al., 2018), cranial nerve organization (Ibrahim et al., 2014), trabecular bone geometry (Ryan and Ketcham, 2002; Chirchir et al., 2015), and, of course, the volume and shape of brain endocasts (Falk et al., 2005; Beaudet and Bruner, 2017; Diniz-Filho and Raia, 2017). It is thus possible nowadays to study inner cavities in a non-invasive, non-destructive way and with a highly increased detail by the widely used protocol of segmentation, that will be discussed in Chapter 2.

1.2.1 The maxillary sinuses

The maxillary sinuses are the greater among the paranasal sinuses and surround the nasal cavity in eutherian mammals and archosaurs (Witmer, 1999; Rae et al., 2002). Like paranasal sinuses in general, maxillary sinuses originate during ontogeny by resorption of cartilage, starting from the extension of recesses in the nasal cavity, and the subsequent expansion of nasal epithelium (Maier, 2000). Each of these air-filled cavities is connected to the nasal cavity by an *ostium*, located above the inferior nasal concha (Rae et al., 2002).

From a comparative perspective, the distribution of the paranasal sinuses among catarrhine primates varies from totally absent in cercopithecoid monkeys - with the exceptions of macaques, which have only the maxillary sinuses - to partly present in some hominoid taxa, where only maxillary and sphenoidal sinuses are present, to the presence of all four kind of paranasal sinuses, recorded only among African apes, humans included (Rae and Koppe, 2004).

The occurrence of paranasal sinuses in fossil and extant species helps tracing the evolutionary history of the primate face. Rossie and colleagues (2002) proposed a revision of the relationship between proconsulids and hominoids on the basis of the

analysis of ethmo-frontal sinuses in the fossil catarrhine *Aegyptopithecus zeuxis* from the Oligocene of Fayum (Egypt): in the well-preserved fossil face of the specimen DPC 2803 it is possible to recognize also the maxillary sinuses (Rossie, 2005). The presence of ethmo-frontal sinuses could be a primitive condition for catarrhines, whereas the loss of the same complex in orangutans and the related fossil genus *Sivapithecus* may represent a synapomorphy (Rossie et al., 2002), besides being a further example of the variability in the distribution of paranasal sinuses in primates.

The maxillary sinuses are the paranasal sinuses that are the most present in mammal species, probably being a relic feature from the first eutherians (Rae and Koppe, 2004); nonetheless it is interesting to point out that maxillary sinuses were lost in some groups of primates to independently re-emerge in some taxa, one of the best example properly represented by the genus *Macaca*. Paranasal pneumatization, in fact, is almost completely absent in cercopithecoids, although the maxillary recess forms during foetal ontogeny but not furtherly develops later (Maier, 2000). The lack of paranasal sinuses seems to be a synapomorphy of the cercopithecoids, determined by a loss of the pneumatization occurred in basal species (Rae and Koppe, 2004), as can be seen in a complete cranium (KNM MB 29100) of *Victoriapithecus macinnesi* from the Miocene of Kenya, which approaches the Colobinae/Cercopithecinae divergence (Rae et al., 2002). In the genus *Macaca*, on the contrary, is present a maxillary pneumatization, not homologous to the maxillary sinuses of other mammals, which represents a remarkable case of convergence, the reason of which is still unclear (Rae et al., 2002).

The ontogeny of paranasal sinuses is a critical aspect to discern the status of a 'sinus' from that of a recess of the nasal cavity (which may represent, in turn, the preliminary stage of a sinus). The development is also taken into consideration by Maier (2000) for the definition of paranasal sinuses (Rossie, 2006). The formation of a sinus during development is a defining criterion also for Cave (1967), who defines it by its evolution from an outgrowth of a meatus of the nasal fossa to a pneumatization of the diploe, connected to the meatus by an *ostium* remaining open during growth. These recesses of

the nasal cavity represent a primary pneumatization taking place prenatally; subsequently, after birth, resorption of cartilage and osteoclastic activity allow the secondary pneumatization, which determines the emergence of proper sinuses (Rossie, 2006).

One of the main topics of debate concerning the maxillary sinuses in humans is whether they bear a function or not and, if so, which it may be. Many hypotheses have been proposed by scholars, but those more considered as adequately supported by evidences fall within two main groups: those related with respiratory functions and those related with the biomechanics of the skull (Rae and Koppe, 2004).

The first group of hypotheses ranges from thermoregulation to the contribution to the moistening or immune defence of the nasal cavity, to the increasing of the olfactory area (Keir, 2009). The contribution of the sinuses to the air flow of the nasal cavity has been calculated to be minimum (Mlynski et al., 2003; Rae and Koppe, 2004) and thus both the functions of moistening and warming - or cooling - of the inspired air seem unlikely (Keir, 2009); a complete exchange of the air present in the sinuses, moreover, is achieved at a significantly slower rate than that of the nasal cavity (Aust et al., 1994; Keir, 2009). For the same reason, the involvement of maxillary sinuses in thermoregulation can be excluded: this suggestion, for some reasons traditionally linked with the increased volume of maxillary sinuses in Neanderthals, is in contrast with the trend seen in other fossil species (e.g. African *H. heidelbergensis*, Zollikofer et al., 2008) and the negative development of sinuses seen in cold climate adapted humans (Shea, 1977) and macaques (Rae et al., 2003). On the other hand, the same negative development is not incompatible with a concurrence in the brain cooling by the additional vascularization present in the sinuses (Rae and Koppe, 2004). Another physiological function maxillary sinuses seem to contribute to is the production of nitric oxide (NO) in the nasal cavity, which plays a role in inhibiting pathogens (Lundberg, 2008); NO production seems to be negatively affected by the size of the *ostia* (Kirihene et al., 2018) and has been taken into consideration in the study of the correlation between Neanderthal sinuses and

adaptation to a harsh lifestyle (Marquez et al., 2002). On the contrary, the contribution to the olfactory function is unlikely, for humans at least, since the sinuses are lined with non-olfactory epithelium, thinner and less vascular in respect to that of the nasal cavity, a fact that also make them more prone to diseases (Blaney, 1990).

The structural hypotheses have been focusing in the last years on the correlation between forces (e.g. stress, strain) related with mastication and the presence/absence and development of paranasal sinuses in primates and fossil humans, stressing the efficiency of their general geometry and the curved walls in dissipating forces (Demes, 1987; Bookstein et al., 1999). Studies of dentistry and orthodontics carried out by finite element analysis (FEA) (e.g. Koca et al., 2005; Huang et al., 2008) take into consideration the structure of the sinuses as a reference for the optimization of efficiency of prosthetics and the same models have been applied to the evolutionary context, coming to similar conclusions (Preuschoft et al., 2002). On the contrary, studies carried out on sister primate species feeding respectively on heavier and softer foods (e.g. in the genus *Cebus*) found no relation between chewing stress and variation in maxillary sinuses (Rae and Koppe, 2008). Also, in fossil species characterized by robust dentition (i.e. robust australopiths) and thus traditionally linked to high dietary stresses, the maxillary region - including the pneumatization - does not appear to be significantly different from that of the more gracile relative species (Villmoare and Kimbel, 2011).

According to Witmer (1997) the soft tissue (i.e. the epithelium) is a key factor to look at for defining whether maxillary sinuses have a functional explanation: in the light of such approach, that sees the epithelium as passively expanding into adjacent cavities, sinuses appear to be 'opportunistic' empty spaces expanding into the bone until it is allowed by the biomechanics of the bony structure. The result would be a progressive optimization of the skull by a balance between the increasing expansion of the pneumatization and the deposition of bone (Witmer, 1997). This seems likely also by looking at the development of the sinuses in Neanderthals (more on it in section 1.3.2). Lastly, by looking at the distribution of a maxillary pneumatization of some sort among

extant and fossil eutherians, a plain retention of their presence from sinus-bearing ancestors can be easily suggested for the anthropoids primates (Rae and Koppe, 2004). The evolution and the variability of the maxillary pneumatization among human species has been studied in the light of the facial morphology and the nasal cavity, with which it seems to be highly integrated independently from function (Holton et al., 2013).

1.2.2 The nasal cavity

The inner structure of the nose is of major interest in palaeoanthropology because of its relation to crucial aspects of the adaptation; this is particularly true for Neanderthals and their ancestors when looking at aspects related with their dispersal and response to climate condition (de Azevedo et al., 2017). In addition, the peculiar facial morphology of Neanderthals is highly characterized by the shape and size of the nose (see section 1.3.2), although in fossils is rarely preserved the inner structure and are never preserved the most fragile structures (e.g. turbinates; Schwartz and Tattersall, 2002), although a remarkable exception is represented by the case study of the present thesis, Altamura. The skeletal structure of the nasal cavity, in fact, is composed by bones that are generally thin and highly pneumatized.

The greater part of the nasal cavity (i.e. the anterior part of the walls and floor) is formed by the medial portion of the maxillae, thus the frontal and palatine processes (White et al., 2011). The posterior borders of the palatine bones contribute to the floor, while the roof is constituted by the cribriform plate of the ethmoid; this latter bone bears the processes forming the upper and medial nasal conchae (Lieberman, 2011) and accommodates the olfactory nerves in small canals that, together with the many air cells, make the ethmoid one of the most fragile bones (White et al., 2011). The nasal cavity is divided by a septum that is partly formed by a thin layer of bone, the vomer,

articulating superiorly with the likewise laminar perpendicular plate of the ethmoid; lastly, the lateral part of the inner nose is occupied by the spongy inferior nasal conchae (White et al., 2011). The nasal bones close superiorly the anterior part of the nasal cavity (fig. 1.4).

During life, the inner surface of the whole nose is covered by a thin layer of mucosa, or respiratory epithelium, which also expands onto the inner walls of the maxillary sinuses: it is highly vascularized and secretes mucus for various functions, among which the most important is to provide immunity by trapping dust and pathogens (Lieberman, 2011). The only area of the nasal cavity not covered by the nasal mucosa is located on the roof, in correspondence with the cribriform plate, that is covered instead by an olfactory epithelium formed by the ciliated olfactory neurons and other type of cells involved in support and chemoreception (Moran et al., 1982; Morrison and Costanzo, 1990).

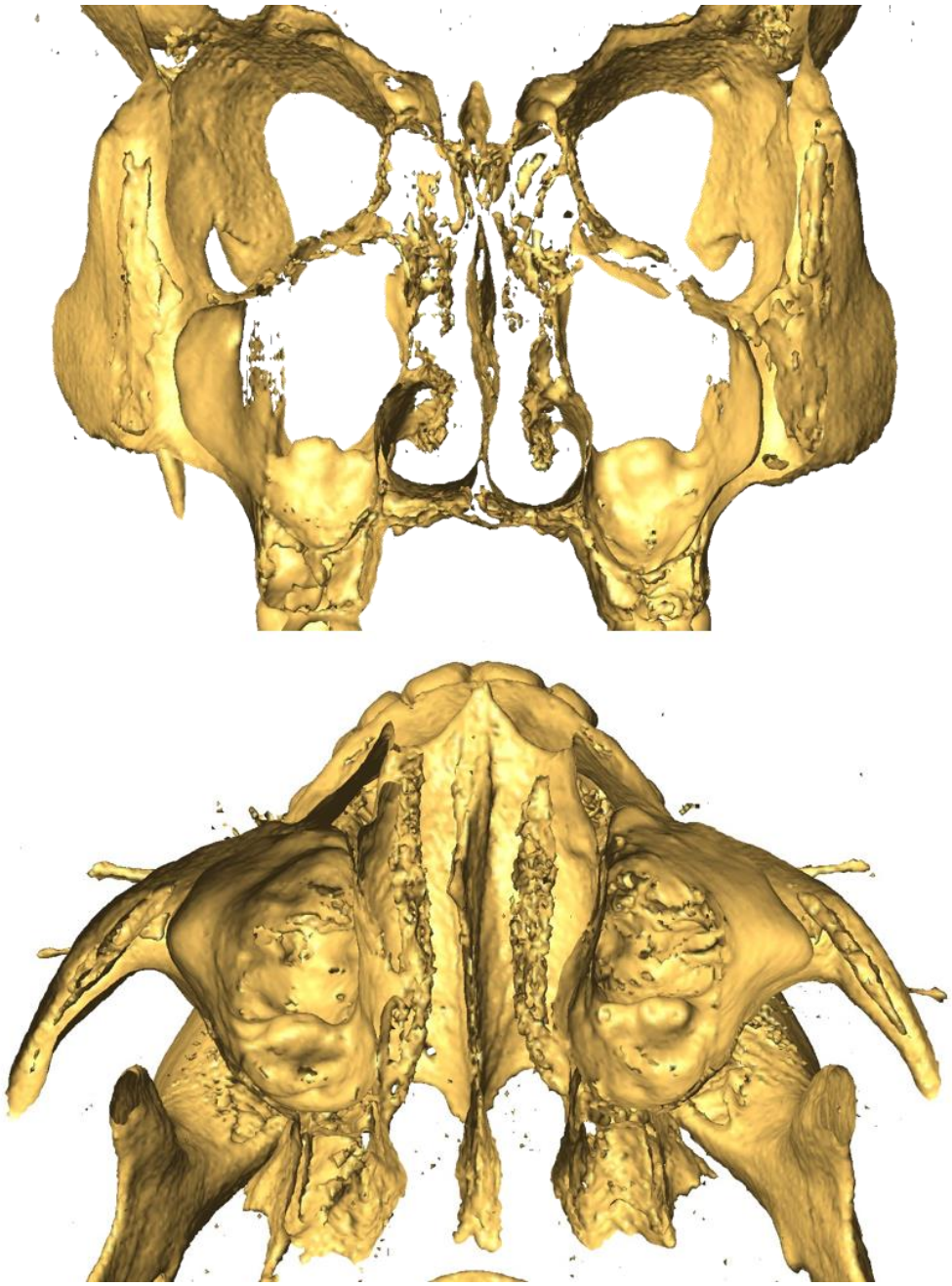

Figure 1.4 - Nasal cavity. Coronal section (above), view from front; transverse section (below), view from above.

The nasal conchae – or turbinates – located in the lateral walls of the nasal cavity, are covered with a thicker layer of respiratory epithelium and occupy part of the cavity itself; they give place to three meatuses located under each concha, which expand the surface-area-to-volume ratio inside the nasal cavity, thus obtaining a more efficient function of conditioning of the inspired air (Lieberman, 2011) (fig. 1.5).

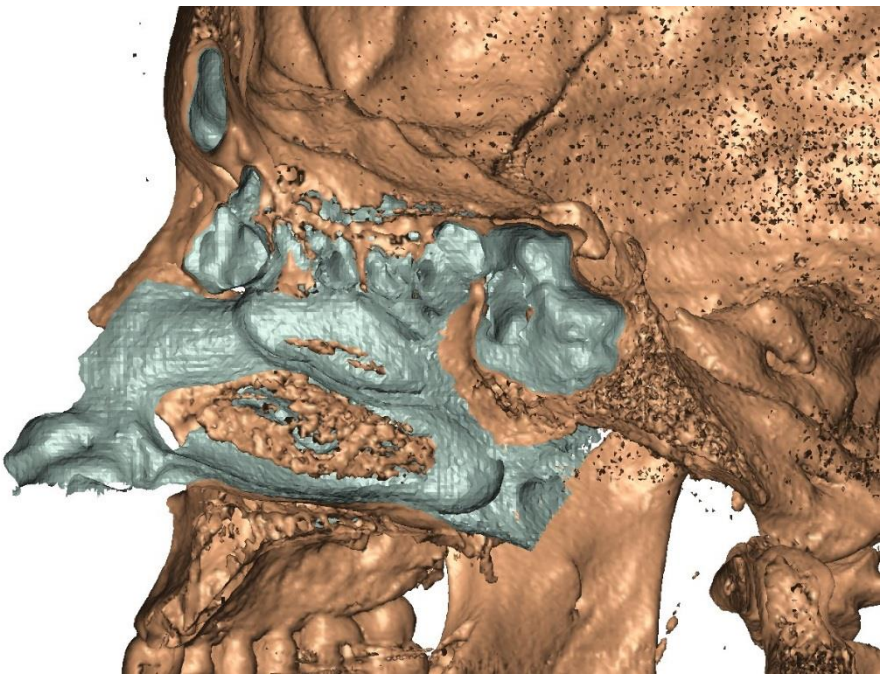

Figure 1.5 - Sagittal section of the human nasal cavity, parallel to the vomer. In brown, the cranium and bony structures; in grey, soft tissues and epithelium. Can be recognized the three turbinates

The surface area of turbinates scales isometrically with the body mass in mammals and birds and the variation of their ratio can be put in relation with the climate of the habitat: primates – as can be expected from animals adapted to tropical conditions - have small nasal surface areas relatively to body mass, with humans displaying some of the smallest values among mammals (Owercowicz et al., 2015). A condition which reflects the tropical origin of our species, besides the huge reduction of the snout (Lieberman, 2011).

The superior and medial conchae form, in the majority of mammals, an 'olfactory labyrinth' located in a blind recess of the upper part of the nasal cavity; in humans they have lost their olfactory epithelium in favour of the respiratory function, a probable consequence of the cranial base reorganization due to the upright posture (Jankowski, 2011).

In human ontogeny, the nose starts from nasal placodes appearing in the fifth week of embryonic development and, by the seventh week, the cartilaginous nasal capsule is formed and the general structure of two connected canals – nasal and oral, separated by the palate - is already distinct; by the tenth week, on each side of the nasal capsule appear six sulci, from which the turbinates will develop before birth (Jankowski, 2011).

The shape of the human nose and of the nasal cavity is influenced by the adaptation to climate (Weiner, 1954). Different populations of modern humans share a similar set of features of the inner nose; for this reason, the shape and size of the nasal aperture have been often studied in terms of linear measurements (e.g. the nasal index) or mucosal surface-area-to-air-volume ratio (SA/V, Yokley, 2009). The changes are driven by both temperature and humidity and can be described as follows: the 'cold climate morphology' features a nasal aperture that is narrower laterally and more elongated supero-inferiorly, whereas for the 'hot climate' one it is larger and shorter; the nasal cavity is respectively shorter antero-posteriorly and higher along the mid-sagittal plane in the 'cold morphology' and longer, slightly narrower and less developed vertically in the 'hot morphology' (Noback et al., 2011) (fig. 1.6).

Humidity seems to influence nasal morphology if taken into consideration as a relative value in combination with temperature (Maddux et al., 2016), and the changes reflects a lower SA/V - thus a better condition for an efficient heat dissipation - in populations adapted to warm climates (Yokley, 2009). In cold climate-adapted populations, on the contrary, a narrow nasal aperture contribute to an increased air turbulence, which favours, in a nasal cavity with higher walls, the contact with the respiratory epithelium and the conditioning of the inspired air (Noback et al., 2011).

It is important to point out that these differences in the nasal morphology are difficult to detect, given the relatively low facial variability of our species; they can be better identified by looking at very distinct populations, historically isolated and living in very different climatic contexts of which the most extreme expressions (e.g. extreme

cold, extreme dry seasons) are the conditions driving the adaptation (Evteev et al., 2014).

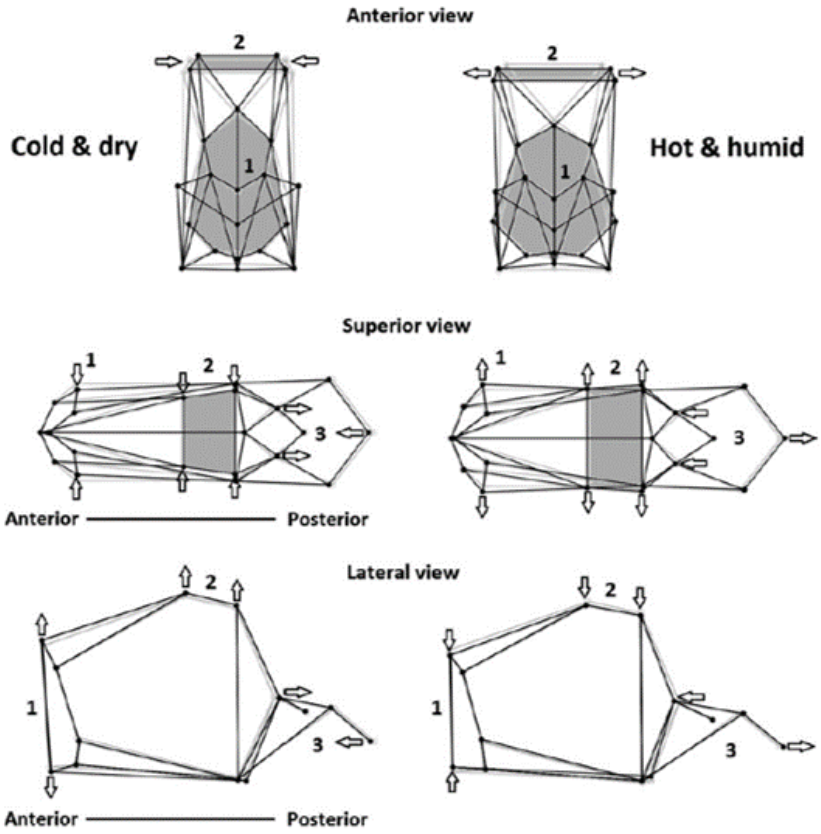

Figure 1.6 - Comparing shape differences between ''cold and dry'' and ''warm and humid" populations. From Noback et al., 2011.

1.3 *H. NEANDERTHALENSIS*

Since the proposal of Neanderthals as a separate species by William King, in 1864, there have been several major topic of debate animating scholars' discussions around them. One of these issues is still discussed in the scientific community and can be resumed by the question: when it is possible to start to talk of Neanderthals while looking at the fossil record? In other words, is there a precise time span when is dealt with specimens/populations that can be referred to as *H. neanderthalensis*?

Like other biological species, *H. neanderthalensis* has been subjected to selective pressures and other evolutionary mechanisms which determined its emergence, development and extinction. One of the aspects of the afore-mentioned debate is centred on 'continuity vs. discontinuity': Neanderthal lineage could have been either determined by a slow change of a population into another, in a "evolutionarily dynamic lineage of chronospecies" (Churchill, 2014), or by a series of events (i.e. bottle-necks), related with climate changes, which led to a progressive reduction of the variability (Dennell et al., 2011).

Paleoanthropologists studying the cranial morphology rely on a complex of features of the skull characterizing the so-called 'classic' Neanderthals (Howell, 1957). This complex includes a large nasal aperture, rounded orbits, an inflated maxillary region, horizontal zygomatic arches, aligned with the acoustic meatus: all features contribute to the peculiar trait of the facial morphology we commonly refer to as *mid-facial prognathism* (Harvati, 2015). But it is possible to identify a Neanderthal even from small fragments because of the unique shape of the neurocranium: Neanderthal traits of the braincase include small mastoids, a peculiar shape of the occipital torus, a clearly expressed suprainiac fossa, antero-posteriorly and laterally extended parietal and occipital bones, in sum, the well-known morphologies that can be resumed by the French terms *chignon* and *en bombe* shape (Cartmill and Smith, 2009).

The evolutionary history of these Neanderthal features is of major interest because is characterized by their differential development during the chronology from earliest forms thought to be related with the lineage (Manzi, 2004, 2016); this represent the basis for the "accretion model" developed - among others - by Hublin (Dean et al., 1998), which suggest that *H. neanderthalensis* evolved in partial (or complete) genetic isolation so as to accumulate some distinctive morphological traits, while reducing their variability (Hublin, 2005). The integration and mutual influence of the same traits has been taken into consideration for further variations of the model (e.g. the "organismic model", Rosas et al., 2008).

In the light of the accretion model it is possible to discern a peculiar stage of expression of the complex of features typical of this species, which chronologically corresponds to the Marine Isotopic Stages (MIS) 7 to 5 (Bruner and Manzi, 2006a). In this phase, some of the 'classic' Neanderthal features are incipient, while others are either present or absent; moreover, the significant values of encephalization borne by the classic Neanderthals is, in the archaic ones from the MIS 7-5, yet to be expressed (Howell, 1957). Evidences of these earlier Neanderthal populations comes from several sites in Middle east (e.g. Tabun) and Europe (e.g. Ehringsdorf, Krapina, Apidima), with some of the most remarkably preserved specimens coming from Italy (e.g. Saccopastore 1, Altamura).

In the case of the two crania from Saccopastore, the stratigraphic studies conducted after the two discoveries – respectively in 1929 and 1935 - ascribed the two specimens to 100 - 130 ka, although a recent reconsideration of stratigraphic correlations suggests an earlier dating, still within the chronological interval from MIS 7 to 5 (Marra et al., 2015).

By looking at Saccopastore 1, the anthropologist Sergio Sergi, who first studied it, recognized Neanderthal features but differing from those of the majority of Neanderthal specimens known until then, to the point that he proposed a name for a distinct subspecies: *H. neanderthalensis aniensis* (Sergi, 1936).

Nowadays more recent findings could be encompassed in this 'early Neanderthal' stage, both for the common morphology and the dating bracketed between the MIS 7 to 5: one of the most important is in Italy and is represented by the nearly complete skeleton from Altamura, recently dated to the range between 172 ± 15 ka and 130 ± 2 ka (Lari et al., 2015). Despite its morphology is in part obscured by karstic concretions, on Altamura it is possible to recognize a number of traits closer to a plesiomorphic condition of Neanderthals (Giacobini and Manzi, 2018), like the neurocranium relatively smaller in respect to the facial complex and lacking a full expression of the *en bombe* shape, despite several well visible Neanderthal traits as the morphology of mastoids and the clear presence of a suprainiac fossa. On the other side, some of the archaic features of the face of Altamura can be detected in the frontal bone Lazaret 24 from France, whose chronology is close to about 170 ka, which shows an outline of the brow ridges slightly discontinuous in correspondence of the mid of each orbit (de Lumley et al., 2018).

Similar to Lazaret 24 is the frontal bone of Neanderthal morphology nicknamed "Pàus", found re-deposited in a seasonal alluvium along the course of the Po river near Cremona, in Italy (Manzi et al., 2014; Tuniz et al., 2014); despite being only a fragment of difficult dating, Pàus carries nonetheless some traits that can plausibly place him among the European humanity of MIS 5 to 7, along with the crania from Saccopastore in Italy, those from Biache-Saint-Vaaste and La Chaise in France, Ehringsdorf and Salzgitter-Lebenstedt in Germany, Krapina in Croatia and the Apidima skulls from Greece (Bruner and Manzi, 2006a; Giacobini and Manzi, 2018). Lastly, among these, could be included the skull from Forbes' Quarry, Gibraltar, one of the first Neanderthal specimen to be discovered, which is of unknown dating (Schwartz and Tattersall, 2002), but displays an archaic morphology (Condemi, 1992) and has been recently subjected to a molecular study that characterized it as genetically similar to the Neanderthals comprised between 60 and 120 ka (Bokelmann et al., 2019). One plausible scenario is that of a population of early Neanderthals which spread across Europe and Middle East

with a relatively homogenous set of morphological traits, although emerging differentially thanks to a context of higher variability (Condemi, 1992) (fig. 1.7).

By cross-referencing the archaeological data, the skeletal morphology and dating of the specimens, it is possible to identify a distinction between the less variable 'classic' Neanderthals of the MIS 4 to 3 and the 'early' Neanderthals of the MIS 5 to 7, showing a set of features not present in earlier European specimens (e.g. Petralona, Sima de Los Huesos) if not in a 'mosaic' pattern (Dean et al., 1998; Bruner and Manzi, 2006a; Harvati, 2015). Some authors recognize the morphology of the archaic Neanderthals in more recent specimens from the Middle East and consider it a retention from the earlier populations (Stringer, 1990; Rak, 1993; Harvati, 2015).

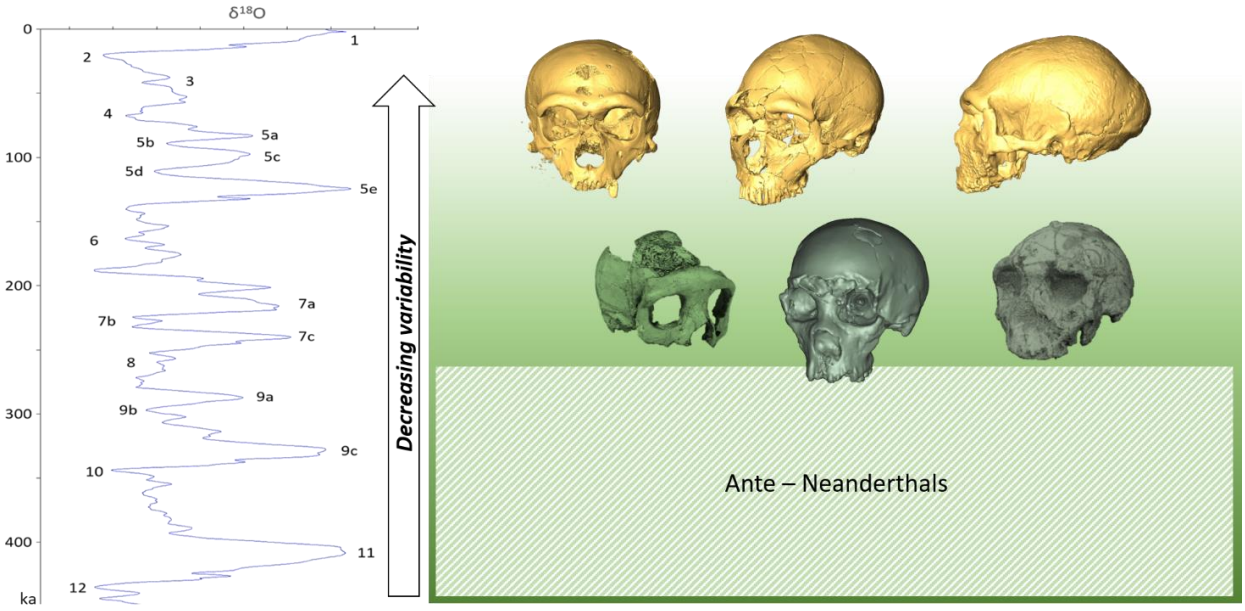

Figure 1.7 - Marine Isotopic Curve with some Neanderthal specimens (from above, left to right: La Chapelle-aux-Saints 1, La Ferrassie 1, Guattari 1; Krapina 3, Saccopastore 1, Apidima 2).

1.3.1 Neanderthal facial morphology

The distinctive morphology of the facial skeleton in 'classic' Neanderthals has been animating a debate around its nature, whether adaptative or the result of a derived architecture (Rak, 1986). The Neanderthal skull is a mixture of traits retained from more archaic human species (e.g. the last common ancestor with *H. sapiens*) and highly derived characters: to the former belong, among the others, the antero-posterior elongation of the low cranial vault, the distinct presence of a supraorbital torus and the lack of a chin; among the latter can be cited the mid-facial prognathism, the highly convex occipital – forming the 'chignon' – and the retromolar space of the mandible (Harvati, 2015).

Derived features seem to determine in Neanderthals cascading effects to the rest of morphology. This is particularly true for the cranial capacity – greater in respects to other human species, modern humans included – and averaging 1470 cc (Tobias, 1971), which determined an expansion of the neurocranium along the preferential directions of the 'archaic human framework': laterally, this determines the expansion of both parietals and temporals, with a consequent squeeze of the mastoids, their apparent reduction, the emergence of a juxtamastoid crest (Trinkaus, 2007; Lieberman, 2011) and maybe the autapomorphy of the middle ear (Spoor et al., 2003; Lieberman, 2011). Posteriorly, the expansion of the neurocranium in an archaic 'blueprint' determines the development of the occipital bun - or *chignon* – and the consequent flattening of the lambdoid region (Gunz and Harvati, 2007), with the setting of a well distinct suprainiac fossa (fig. 1.8). The significant development of the occipital region could be related with a differential timing of the brain growth (Trinkaus and Lemay, 1982), in an ontogenetic context probably characterized by a more rapid development (Ramírez-Rozzi and Bermúdez De Castro, 2004).

Figure 1.8 – The Neanderthal cranium Guattari 1

The other side of the 'neanderthalization' is the development of mid-facial prognathism, which seems to follow a parallel path seemingly not related with encephalization but driven by adaptation and/or genetic isolation: its emergence and driving factors are among the major topics of debate among paleoanthropologist (Rak, 1986). The enlarged, forward projected nasal cavity has been long considered the result of adaptation to cold climate, although it is one of the aspects of a more complex system of causal relationships (Condemi, 1998).

The projection of nose along the sagittal axis is accompanied by a backward shifting of the zygomatic arches (Churchill, 2014), so as the infraorbital plates are rotated in a slight parasagittal orientation, followed by the rims of the piriform aperture which, as a result, is larger laterally (Rak, 1986; Lieberman, 2011); to this is associated an 'inflation' of the infraorbital plates, to the point that they lack a clear canine fossa (Rak, 1986) and the infraorbital foramina appear 'stretched'. The frontal region is not affected by the same forward shift, determining as a result an upward rotation of the anterior margins of the nasal bones, which acquire a sub-horizontal orientation (Rak, 1986) (fig. 1.9).

The derived facial morphology is reflected also on the dentition: the incisors are thicker antero-posteriorly and often display a strong wear on the labial surface (Lieberman, 2011); the mandibular joints seem shifted backward, along with the masticatory muscles (Churchill, 2014) but the optimal occlusion is achieved by the anterior migration of the inferior dental arch, which leaves a space behind the third molar (Lieberman, 2011).

The fossil record is lacking of the internal structures of the Neanderthal nose, so as up to now has been difficult to describe how the mid-facial prognathism could have affected the inner nose, although some studies tried to describe it by looking at best preserved portions or by virtual modelling (Schwartz and Tattersall, 2002; de Azevedo et al., 2017). A first description of some inner nasal structures is provided in this thesis, thanks to the remarkable preservation of the Altamura cranium (see Chapter 3). For what concerns the maxillary sinuses in the Neanderthal lineage, they seem to passively accompany the forward projection of the maxillary bones, apparently by giving place to additional *loculi* (Heim, 1989; Zollikofer et al., 2008), and thus consistently with the afore-mentioned view of sinuses as 'opportunistic' structures (Witmer, 1997).

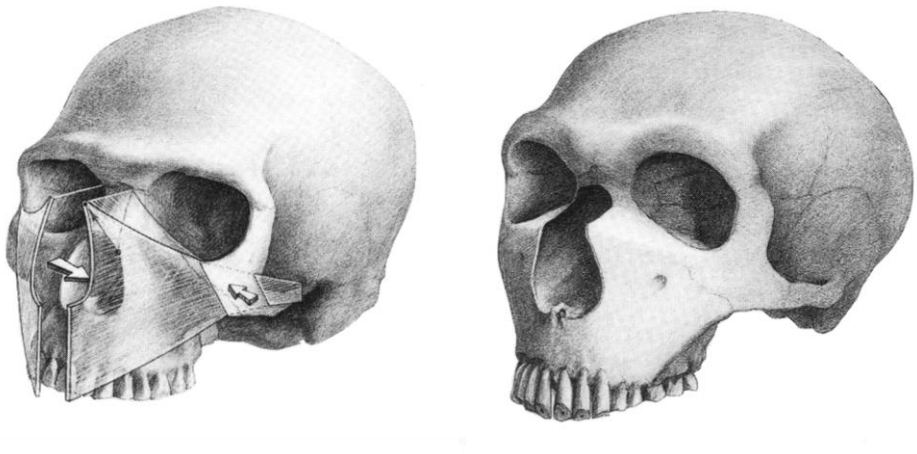

Figure 1.9 - The transformation of the generalized human face into the 'classic' Neanderthal face. Mod. from Rak (1986)

The two driving forces of the Neanderthal cranial shape, the mid-facial projection and the encephalization, have been subject to studies concerning their integration, mutual influence and respective emergence either in ontogeny or phylogeny (see for example Maureille and Bar, 1999; Lieberman et al., 2000; Bastir et al., 2007; Rosas et al., 2008); there is general consensus on the emergence of mid-facial prognathism prior to the encephalization, excluding the latter from the factors determining the derived Neanderthal facial morphology, as also suggested by the fossil record of 'early' Neanderthals (Bruner and Manzi, 2006a) and of the populations seen as ancestral to Neanderthals (e.g. Sima de los Huesos, Arsuaga et al., 1997, 2014).

1.4 THE SKELETON FROM ALTAMURA

Nicknamed "Altamura Man", the skeleton discovered in October 1993 in the Lamalunga karst system near the town of Altamura, in Puglia (Southern Italy), is an exceptionally preserved and nearly complete fossil skeleton of Neanderthal morphology deposited in a small cavity around 130 – 180 ka and today still embedded in calcite concretions (Di Vincenzo et al., 2018) (fig. 1.10). The skeleton is the only human individual found in the system - with no association nor presence in the cave, of lithic tools - and the bones are localized in a single niche in the cavity, renamed after the discovery "Apse of Man" ("*Abside dell'Uomo*"); the bones show no signs of transportation, thus it can be inferred that the individual remained trapped in the karstic system and died right in the place is still found today (Lari et al., 2015). The stable microclimatic condition of the cave may have contributed to the excellent condition of preservation of the bones (Borsato et al., 2010).

Figure 1.10 - The 'niche' of the Man inside the Lamalunga Cave. Photo: A. Profico

The cave is closed to the public since the discovery and is nowadays opened twice a year, only for scientific purpose and in controlled conditions.

The discovery, made jointly by speleologists of a local and a regional group (respectively, the C.A.R.S., Centro Altamurano Ricerche Speleologiche and "Vespertilio" of the Italian Alpine Club of Bari) who opened the before closed – although not completely sealed – karstic system in 1993 (Pesce Delfino and Vacca, 1994), has been followed by the first studies made mainly by the University of Bari and focused on the general structure of the cave and the taphonomy of the human remains (Vacca, 2006).

Since then, no more in depth studies of the skeletal material followed, with very few communications produced on the subject (Manzi et al., 2010), while a three-dimensional topographic survey of the cave has been performed, with the first digital mapping of

some of the bones (Vacca and Pesce Delfino, 2004). Other activities by the University of Bari focused on public fruition of the specimen, with the realization of a multimedia remote experience based on lights and cameras installed in the cave (S.A.R.A.S.T.R.O. project), which failed shortly and contributed to the increase of the impact on the microclimate – already made unstable by the opening of the cave in 1993 - that is currently threatening the preservation of the fossils (Piperno, 2010).

New studies started since 2009, with the contribution of Sapienza University of Rome among the different institutions involved, which led to the first extraction of skeletal materials (some fragments of the right scapula, Di Vincenzo et al., 2018) and performed the first sampling of mtDNA and dating by Uranium-Thorium, which respectively confirmed the belonging to a Neanderthal haplotype (although the genetic material extracted was very few) and provided a chronology ranging from 172 ± 15 ka to 130.1 ± 1.9 ka (Lari et al., 2015).

Since 2016 the activities in the Lamalunga cave have been conducted in the context of the Project of National Concern (PRIN) named K.A.R.S.T. project (*Knowing the Altamura man thRough Science & Technology)*, led by Prof. Giorgio Manzi and involving Sapienza University of Rome, Roma Tre University, Università degli Studi di Firenze, Università di Pisa, University of Newcastle (Australia).

The new studies, to which the candidate contributed, have been focused on the long-term observation of the microclimatic changes in the cave, while, on the skeletal materials *in situ* have been conducted direct investigations, both by measurements and digital acquisition, aimed also at the evaluation and preparation of a future extraction, still not feasible. A consistent part of the data reported in the present thesis has been achieved on the field activities carried out on the Altamura skeleton in the last three years.

1.4.1 The Lamalunga karst system

The Lamalunga cave is a complex karstic system which extends, for approximately 130 - 160 m with a sub-horizontal slope and NE direction, at a small depth below the surface (reaching roughly 30-25 m in the deeper regions, Agostini, 2010; Martimucci et al., 2010; Vanghi et al., 2017).

The complex represents one of the typical structures characterizing the karst of the "Murge" plateau, in Puglia (Southern Italy), which often feature large and massive phenomena (e.g. sinkholes, ravines Agostini, 2010). Nowadays, the landscape is dominated by open vegetation (e.g. grassland) highly influenced by human activities and established on a thin layer of soil, often developed in pockets between the exposed rocks (Vanghi et al., 2017). Among the karstic structures of the region, are the "*lame*" (singular, "*lama*", italian word for "blade"), namely shallow erosional sulci of high porosity, bearing stream water under the surface with a limited superficial runoff (Zezza and Zezza, 1999). The Lamalunga cave cuts the "Calcare di Altamura" formation, consisting in well-defined strata of white biostromal radiolite limestone - with some notable rudist-bearing layers – formed in cyclic sequences of deposition in different facies during the Upper Cretaceous (Azzaroli et al., 1968; Agostini, 2010) (fig. 1.11).

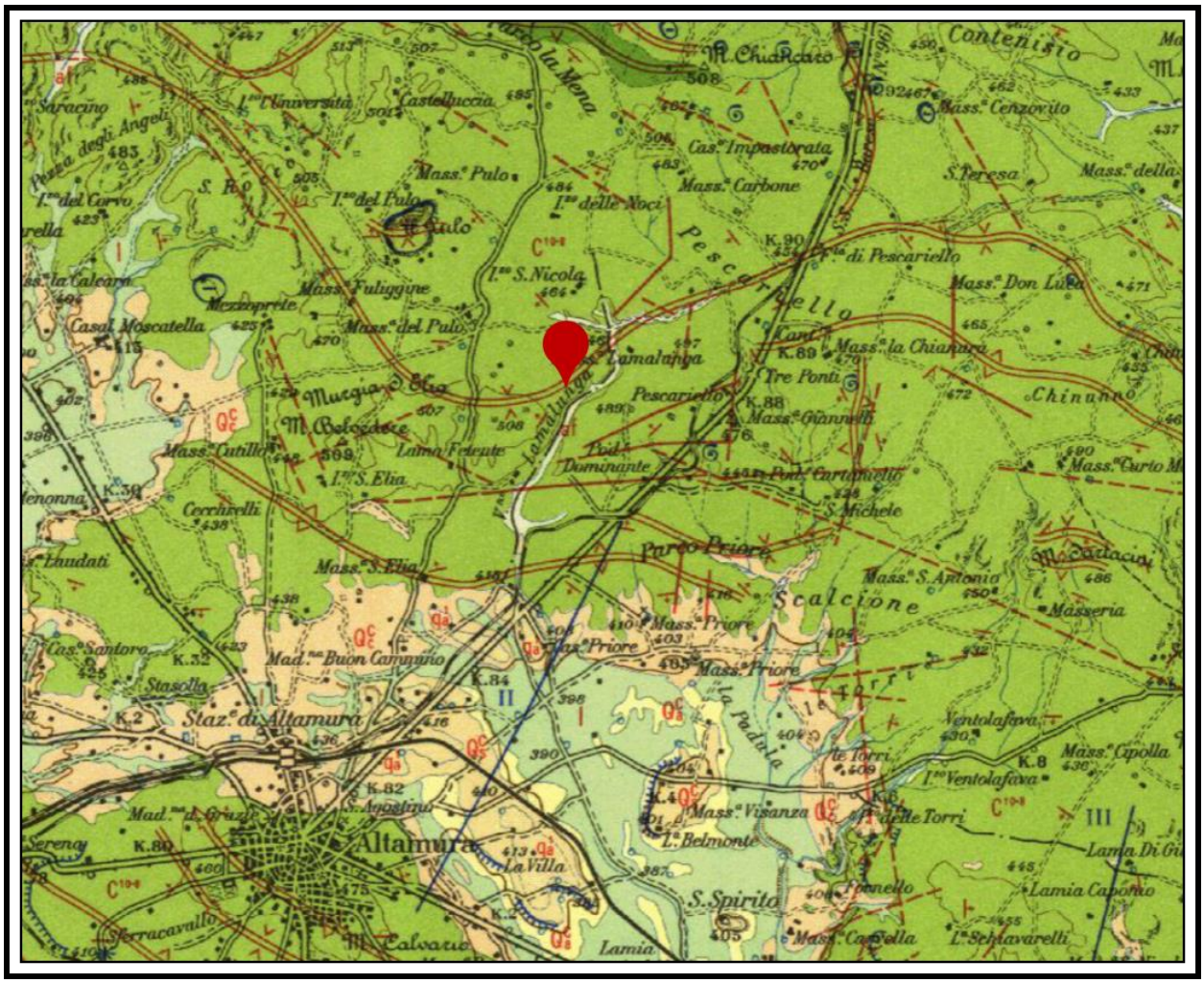

Figure 1.11 - Excerpt from the "Carta Geologica d'Italia"; sheet 189, Altamura. In deep green is represented the "Calcare di Altamura" formation, consisting mainly in debris and biostromal limestone. In red, is indicated the location of the Lamalunga Cave

The karst system is divided in two main branches (Northern and Southern) which present different characteristics, in addition to being respectively without fossils (the Northern one) and with a rich paleontological record (Southern one). The latter is a bifurcated interstratal gallery long approximately 80 m or less and generally closer to the surface; its easternmost, narrower branch, ends with the "Apse of Man", a small cavity (around 6 m^2 wide) at a depth of 6.5 m ca. The current entrance of the Lamalunga cave is an artificial well 8 m deep that has been opened right after the discovery and is located roughly at the midway point of the karstic system (fig. 1.12).

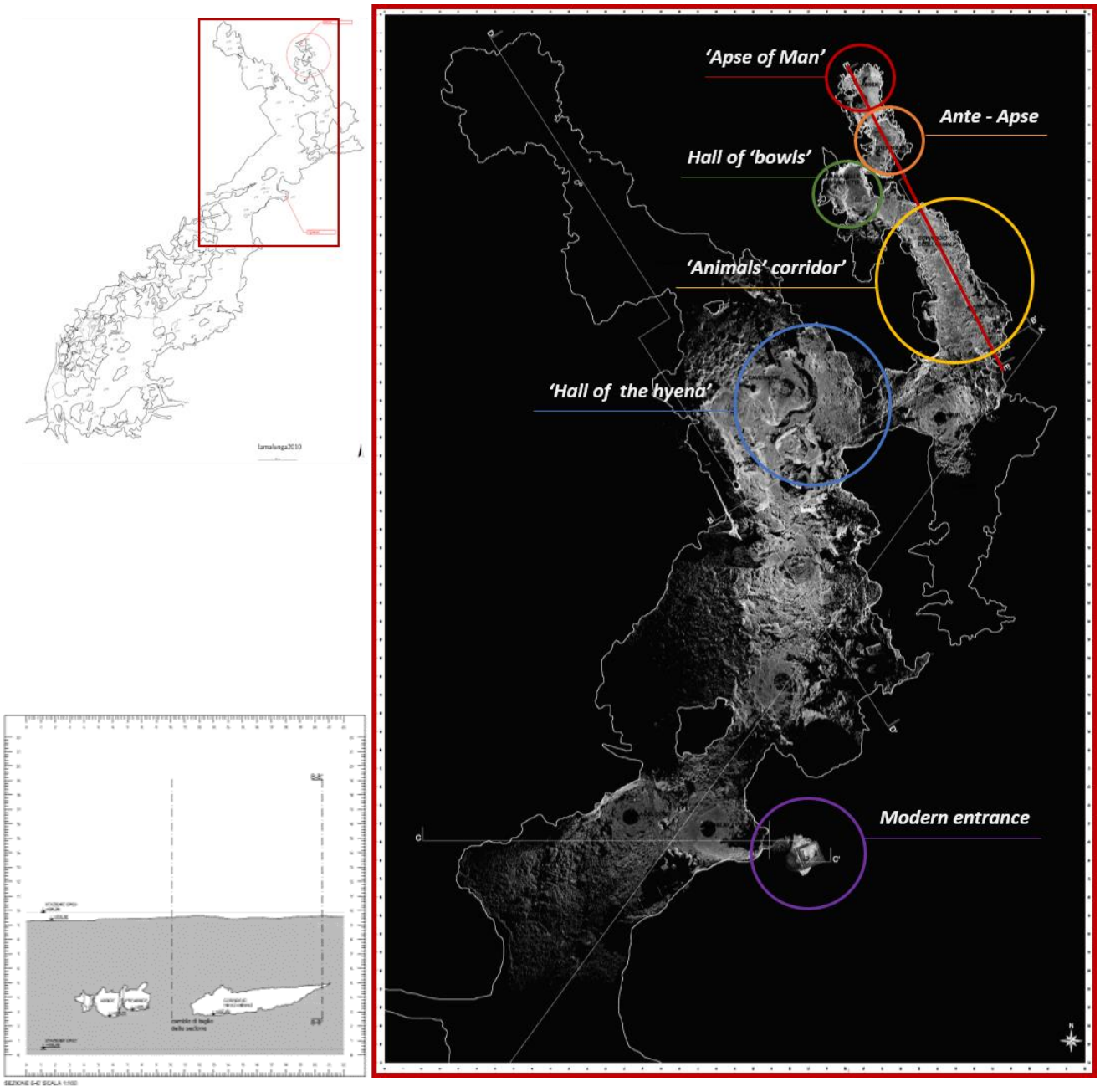

Figure 1.12 - Map of the Northern branch of the Lamalunga Cave (above). Are reported the names of the different zones of the system. the profile (on the left) is relative to the final segment of the cave (red line), where are human fossils. Topography: Sat Survey (www.satsurvey.com). Elaboration of the author.

Being closer to the surface, the Northern branch has been more subject to fractures which favoured collapses and the detachment of blocks from the ceiling (Vanghi et al., 2017). By contrast are clearly visible at least three talus cones, formed by debris corresponding to ancient openings that might have acted as natural traps: the one that might have been the actual entrance for the human individual is still unclear (fig. 1.13).

Figure 1.13 - Talus cones closing ancient sinkholes, near the current entrance (above) and before the 'Animals' corridor'(below). Photo: G. Boschian

From the "Hall of hyena" ("*Sala della iena*"), heading to the "Apse of Man", the gallery begins to narrow, until three small and difficult passages which lead to the Apse and the human skeleton.

The cave is still active, with rainfalls percolating from the fractured bedrock and seasonal trends of water infiltration (Vanghi et al., 2017); the cave environment is dominated by speleothems as stalactites, stalagmites, columns and flowstones but is characterized by coralloid formations, often covering the numerous faunal bones as well as the human ones, formed mainly by calcite deposited by hydroaerosol due to the fragmentation of water drips; this mechanism of deposition of the concretions suggest that the cave, although closed before the discovery, still was subject to a limited ventilation by fractures in the cave, which provided the presence of air without an oriented flow (Vanghi et al., 2017).

1.4.2 The skeleton

The skeleton is deposited in a small elongated niche located in the north-western quadrant of the Apse; the niche is delimited by flowstones which encompass some of the bones. The northern wall of the niche is formed by three major flowstones covered by coralloid formations and with a 'cauliflower-like' general structure; on the sides, the flowstones reach the floor of the niche, while the one at the centre ends approximately at the contact with the cranium, located at the bottom of the niche (see figure 1.10).

The flowstones, together with some columnar structures, separate the Apse from a northernmost small chamber, roughly 2 m^2 wide and with the floor approximately situated 60 cm lower than the bottom of the niche; in this blind chamber, not actually accessible from the Apse if not by probes, can be found other human bones coming from the skeleton, some of which are the only human skeletal materials extracted from the cave (i.e. fragments of the right scapula, Di Vincenzo et al., 2018) (fig. 1.14).

Figure 1.14 - On the left, the niche: are visible the holes connecting the Apse to the smaller chamber behind; on the upper right of the wall are visible the passages where is possible to insert the photographic probes; on the right, a frame of the chamber taken from those passages: are recognizable the occipital and the humerus on the floor.

The skeleton seems to be complete, although many of the bones are not accessible or clearly visible. The bones of the uppermost part of the assemblage have been mapped (Vacca and Pesce Delfino, 2004) and have been the subject of a review in the last descents; a list of the recognised bones is reported in table 1.1 and illustrated in figure 1.15.

As can be seen from figure 1.15, some of the bones present a variable layer of concretions, which vary from thin and smooth, to coralloid accumulations, often located on the reliefs of the bones; some other bones are partially or totally encompassed in the flowstones.

In general, the assemblage appears to be 'welded' together by the concretions, so as the majority of the bones are not removable, with very few exceptions (i.e. the broken proximal portion of the left fibula, the left first rib, a cervical vertebra).

It is important to point out the critical role of the concretions in preserving the bones; on some portions it can be seen how the absence of the cover led to the consumption of the cortical bone to expose the trabecular bone (Vacca, 2006). This process has been observed escalating because of some past activities held in the cave (e.g. the S.A.R.A.S.T.R.O. project) and, more in general, because of the environmental changes occurred consequently to the very first opening (fig. 1.16).

Figure 1.15 - Graphic elaboration of the niche with the superficial bones highlighted. Red: right radius; yellow: right ulna; blue: right fibula (up), left fibula (center); dark green: mandible; light pink: right femur (above), left femur (on the right); grey: left tibia; light green: left humerus; violet: left clavicle; in white: profile of the pelvis and of a lumbar vertebra. The other bones visible are ribs.

Table 1.1 - List of the skeletal elements of Altamura. The colours refer to those used in Fig 1.15. The blank elements are not visible either because absent or covered by concretions/other bones

Visible elements (niche)
Cranium
Mandible
Left clavicle
Left humerus
Right radius
Right ulna
Right femur
Left femur
Right fibula
Left fibula
Left tibia
Recognised elements
Atlas
First right rib
Right scapula
Right humerus
Sacrum
Iliac bones
Elements not recognised
Cervical vertebrae
Ribs (12)
Thoracic vertebrae (2)
Lumbar vertebrae (2)

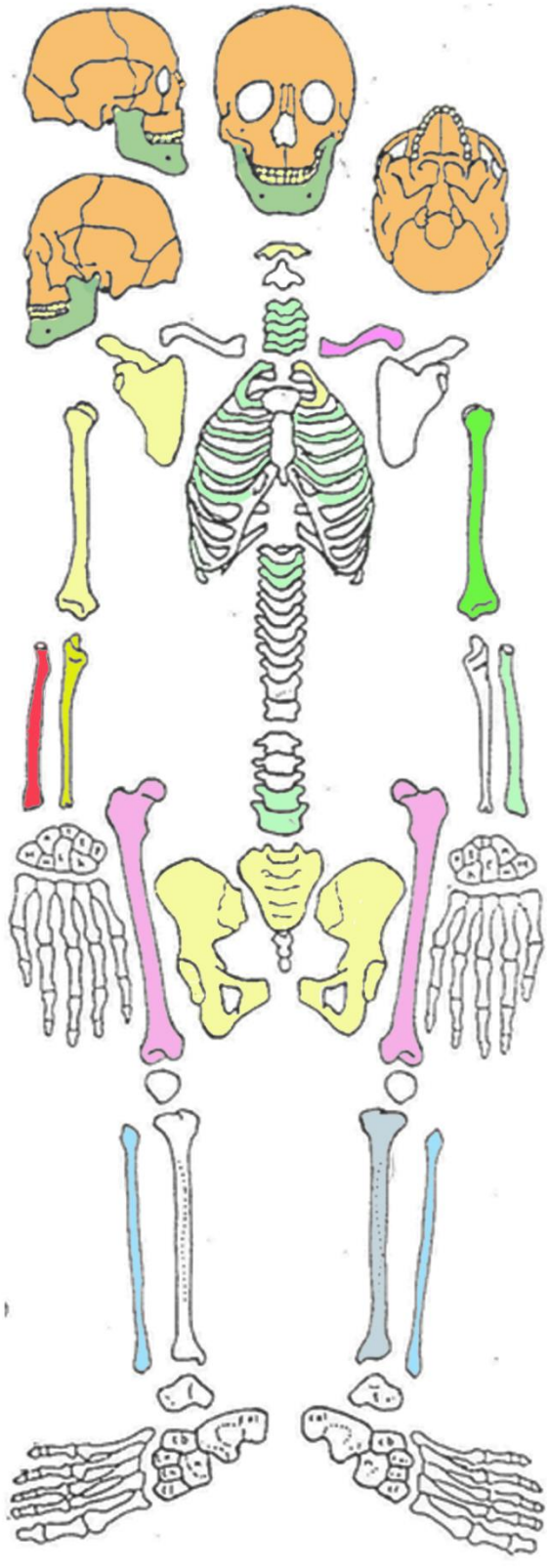

Figure 1.16 - Detail of the proximal epiphysis of the femurs, showing the detaching of the concretions.

The cranium is located at the border between the niche and the chamber behind, laid on a radius below and appears attached by only few points of contact to the framing flowstones. It is slightly tilted on the left and rests on the posterior part of its left parietal, so as only the anteriormost parts of the face and the frontal and part of the left side of neurocranium are visible from the Apse (fig.1.17). The palate, the occlusal surface of the teeth as well as the cranial base and the right posterior part of the neurocranium are not easy visible from the Apse, while are accessible by probes from behind; unfortunately the very few points of contact visible between the two visible portions of the cranium are hidden by speleothems to an efficient acquisition. General observations carried out on the skeleton suggest it belonged to an adult male Neanderthal presenting some archaic features (Alciati et al., 2005; Vacca, 2006), which is consistent with the study on the extracted scapula and the dating of the specimen (Lari et al., 2015; Di Vincenzo et al., 2018).

The taphonomy of the skeleton and the position of the bones suggest that the individual died in the place of deposition, possibly in a crouched position; during the decay the bones from the limbs fell ahead of the pelvis and the cranium tilted forward, remaining framed by some already formed speleothems, while some other bones fell in the chamber further ahead (e.g. right scapula, right humerus) or in the middle of the same assemblage (e.g. mandible). No transportation seems to have occurred afterwards.

Figure 1.17 - Detail of the cranium (reversed)

1.5 VIRTUAL PALEOANTHROPOLOGY

Fossil specimens can reveal cultural and biological information and the exploitation of their potential depends on the conditions at the moment of discovery and the combination of the subsequent steps of management (e.g. study, conservation and disclosure). For skeletal remains, the circumstances leading to their preservation are often exceptional, as they typically undergo various post-mortem phenomena that may alter their original morphology (Schlager et al., 2018). Since these remains can represent the only source of information available on important, or even crucial, phases of human evolution, diffusion and civilization, it becomes extremely important to extract all possible information by studying their features extensively and preventing, meanwhile, interventions that could potentially damage the skeletal elements in an irreversible manner and preclude future studies (Weber, 2001, 2014; Pollefeys, 2004; Cunningham et al., 2014).

Digital acquisition techniques, based on X-rays, structured-light and photogrammetry, allow nowadays to 'freeze' the morphology of unique remains or other relevant aspects related to their finding (e.g. excavation surfaces) (Bukreeva et al., 2016; Wilson et al., 2017; Micarelli et al., 2018); the digitised model can be studied in a totally virtual environment, without compromising the conservation of the actual specimens and their appreciation by a larger audience (Scopigno et al., 2015; Buzi et al., 2018).

The use of 3D models determined a 'revolution' in the study of fossils, thanks to an ensemble of methodologies and protocols which make up the field of "Virtual Anthropology"(Weber, 2001): the specimen is now represented by a 3D object formed by a net of oriented triangular facets (surface mesh), individually defined by the coordinates of their vertices and by their connections, the collection of which translates the shape of the object in the computer language (Weber and Bookstein, 2011; Profico et al., 2018b).

Further analytical tools, based on statistical and multivariate methods for the study of skeletal variability, allow palaeontologist and paleoanthropologist to analyse, on the digital models, evolutionary, functional and ecological processes sometimes inaccessible on the remains of study (Bruner and Manzi, 2006b).

Moreover, the development of 3D imaging techniques led to the definition of protocols addressed to the virtual restoration of damaged and/or deformed remains (Bates et al., 2010; Falkingham, 2012; Cunningham et al., 2014), thus not only decreasing the possibility of damages caused to the original specimen during study, but providing reproducible protocols of virtual restoration aimed at repairing damaged or deficient regions (Shipman, 1981; Lyman, 1994). These techniques can be used to restore morphologies and to reproduce the original item in an indefinite number of copies as detailed physical casts by using a 3D printer (rapid prototyping). This issue is central for research purposes and fosters the sharing of information in view of preservation, conservation and dissemination (Parry, 2016). In addition, responding to the increasing need of studying objects in their inner structures at a high detail, X ray-based imaging techniques guarantee a totally non-invasive investigation technique (Tafforeau et al., 2006).

Traditional restoration of a fossil often consists in the re-assemblage of fragmented portions and consolidation using fixing materials; an archaeological specimen can undergo more than once this kind of restoration, with added physical and chemical stresses; on the contrary, by working on its digital model, it is possible to perform other procedures such as the retrodeformation (Zollikofer et al., 2005; Tallman et al., 2014; Di Vincenzo et al., 2017; Schlager et al., 2018) and/or to add portions coming from similar specimens, digitally replicated and adapted to fill the missing ones with further anatomical accuracy (Weber, 2001; Friess et al., 2002; Ni et al., 2012; Profico et al., 2016; Veneziano et al., 2018). One of the procedures specifically designed for the case study of Altamura allows to align disarticulated fragments of the same specimen on the basis of a reference sample of statistical significance (Profico et al., 2019a).

1.5.1 Digital acquisition

Tomography is an imaging technique based on the use of X rays (Röntgen, 1896). As mentioned in section 1.2, the use of X-rays in paleoanthropology dates to the beginning of 20th century, when Gorjanović-Kramberger (1906) first published the X-ray images of Neanderthal fossils found in Krapina (Croatia). Subsequently, the first use of tomography in palaeoanthropology follows the rapid development of medical imaging in the 1980s (Conroy and Vannier, 1984, 1987; Wind, 1984; Wind and Zonneveld, 1985, 1989). In the early '90s were developed techniques and protocols specifically devoted to the virtual reconstruction of fossil hominin remains (Spoor et al., 1993; Zollikofer et al., 1995, 1998; Weber et al., 1998; Weber and Bookstein, 2011).

X-ray tomography provides a series of 2D cross-sectional images (slices), spaced by a constant inter-slice distance, which defines the resolution of the acquisition. The application of the 'Marching cubes' algorithm allows the extraction of a polygonal mesh (isosurface) from a 3D-array (Lorensen and Cline, 1987). The starting object is placed on a table that moves along the rotation axis of a rotating ring, where are mounted an X-ray source on one side and a line of detectors on the opposite side. The attenuation of the radiation passing through the object provide the information about its radio density, expressed in Hounsfield units (Buzi et al., 2018). The entire volume is divided in discrete units called voxels, defined by four variables: the first three are based on the resolution of the scan and the fourth quantify the grey values of radio density. Once the proper Hounsfield range is set, it is possible to calculate a 3D model by the application of the 'Marching cubes' algorithm (Livnat et al., 1996; Weber, 2001).

Micro CT is a variant of CT-scan which returns digital object at a higher detail: the resolution can reach 10 μm – in contrast to the 0.5 mm usually reached by medical tomography - which means more slices or sections captured; is often used in dentistry and has the limit to be applicable only on relatively small objects. The highest detail for digital acquisition is nowadays reached by synchrotron tomographic scans, which are

carried out by particle accelerators. Synchrotron tomography can reach resolutions of less than 0.5 μm; the characteristics of the synchrotron beam - monochromaticity, high intensity and partial coherence – allow to overcome the low absorption contrast typical of the high mineralised fossils, and thus to discriminate textures at microscopic level as well as efficiently digitise any kind of fossil organism (Tafforeau et al., 2006).

A 3D laser scanner is a device that acquires a surface as a points cloud through a Charge Coupled Device (CCD) sensor, by transmitting a laser light intercepting the surface at a known distance. The scans performed by a number of viewpoints allow a digital reconstruction of the virtual version of the physical object via triangulation (Pavlidis et al., 2007) with its colour information and recording the coordinates of the triangles composing the mesh. Another kind of laser scanning technology is the LIDAR scan, that is increasingly used for broad range observations (e.g. aerial imagery) on archaeological sites (van Zijverden and Laan, 2003; Opitz and Nuninger, 2014), as well as in other disciplines, as geomorphology and sedimentology (Burton et al., 2011).

Photogrammetry allows to reconstruct a 3D model from multiple images (Buzi et al., 2018); by using this technique, the operator acquires one or more series (chunks) of photos of the specimen in different views. The first processing step is the definition and the removal of the background from each picture; in this way other sources of noise are removed. Then, by using a dedicated software (e.g. Agisoft Photoscan, https://www.agisoft.com/) the pictures are aligned and, by triangulation, the location of the camera is determined in each of the photos taken, to generate a sparse point cloud (Nicolae et al., 2014) and to subsequently produce a dense point cloud. Eventually, the dense point cloud can be used as the baseline to build a mesh using a triangulation algorithm (Lee and Schachter, 1980). A detailed texture can be processed from the photographs acquired. Unlike CT-scanning and laser scanning, the dimension of the 3D model obtained via photogrammetry does not replicate the original scale, hence a metric reference is needed (Falkingham, 2012).

2 MATERIALS AND METHODS

Dead men don't lie.

Akira Kurosawa, *Rashōmon*

2.1 THE SAMPLE

2.1.1 The collections

The work for this thesis has been based on a comparative sample used as the reference for both the reconstruction of the Altamura cranium and for comparative analyses. Being the investigation focused on the cranium of an adult Neanderthal individual (Di Vincenzo et al., 2018) and concerning the variability of biological structures in adult individuals, only crania of adults were incorporated in the sample.

The open source approach that has been recently spreading in the scientific community provided invaluable aid in data collection both for materials and for tools (e.g. R software, R Development Core Team, 2016). The paleoanthropological investigation, also thanks to the increasing use of digital acquisition, is benefiting of online databases of 3D models, where it is possible to obtain digital versions of extant and fossil specimens (e.g. Nespos [https://www.nespos.org/display/openspace/Home, Bradtmöller et al., 2010], Morphosource [https://www.morphosource.org, Boyer et al., 2016], Digimorph [http://www.digimorph.org], Morphomuseum [http://morphomuseum.com/, Lebrun and Orliac, 2016], Digital Morphology Museum, KUPRI [http://dmm3.pri.kyotou.ac.jp/dmm/WebGallery/index.html]).

The work for the present thesis took advantage of 3D models coming from different Museum collections, thanks to efficient researchers who took care of the digitization.

The digital databases accessed are the following:

- Nespos – Pleistocene people and places: https://www.nespos.org/display/openspace/Home
- Lynn Copes' CT scans of modern *H. sapiens* (Copes, 2012): https://www.lynncopes.com/human-ct-scans.html

The digitally acquired specimens not coming from an online database have been obtained by the Palaeoanthropology and Bioarchaeology Lab (Department of Environmental Biology, Sapienza University of Rome) from the owning institutions who kindly provided them; specimens and owning institutions are reported in detail in table 2.1 (fossil humans) and in table 2.2 (modern humans), with reference to the section (chapter or subchapter) of the present thesis in which have been used.

Table 2.1 - List of the fossil specimens of the reference sample

SPECIMEN	SPECIES	SECTION	INSTITUTION	DATABASE
AMUD 1	*H. neanderthalensis*	3.2.2	Tel Aviv University	
KABWE (OR 'BROKEN HILL'; BH)	*H. heidelbergensis*	3.1; 3.2.2; 3.2.3	Natural History Museum, London	NESPOS
GIBRALTAR (FORBES' QUARRY)	*H. neanderthalensis*	3.1	Natural History Museum, London	NESPOS
GUATTARI 1	*H. neanderthalensis*	3.1; 3.2.2; 3.2.3	Museo Preistorico Etnografico "Luigi Pigorini", Rome	NESPOS
LA CHAPELLE-AUX-SAINTS 1	*H. neanderthalensis*	3.1; 3.2.2; 3.2.3	Musée de l'Homme, Paris	
LA FERRASSIE 1	*H. neanderthalensis*	3.2.2; 3.2.3	Musée de l'Homme, Paris	
PETRALONA	*H. heidelbergensis*	3.1; 3.2.2; 3.2.3	Aristotle University of Thessaloniki	
SACCOPASTORE 1 (SCP1)	*H. neanderthalensis*	3.1; 3.2.2; 3.2.3	Museo di Antropologia "Giuseppe Sergi", Rome	
SACCOPASTORE 2 (SCP2)	*H. neanderthalensis*	3.1	Museo di Antropologia "Giuseppe Sergi", Rome	
SIMA DE LOS HUESOS 5 (SH5)	*H. heidelbergensis*	3.1; 3.2.2; 3.2.3	Museo de la Evolución Humana, Burgos	

Table 2.2 - List of the modern human specimens of the reference sample. *(Copes, 2012); °(Marangoni et al., 2011)

SPECIMEN	ORIGIN	SEX	SECTION	INSTITUTION	DATABASE
ADU06	*Europe*	F	3.3	Université Paul Sabatier, Toulouse	NESPOS
ULAC012	*Europe*	M	3.2.2; 3.2.3	Anatomisches Institut, Universität Leipzig (UL)	NESPOS
ULAC013	*Europe*	F	3.2.2; 3.2.3	UL	NESPOS
ULAC016	*Europe*	M	3.2.2; 3.2.3	UL	NESPOS
ULAC019	*Europe*	M	3.2.2; 3.2.3	UL	NESPOS
ULAC033	*Europe*	M	3.2.2; 3.2.3	UL	NESPOS
ULAC039	*Europe*	F	3.2.2; 3.2.3	UL	NESPOS
ULAC057	*Europe*	M	3.2.2; 3.2.3	UL	NESPOS
ULAC060	*Europe*	M	3.2.2; 3.2.3	UL	NESPOS
ULAC066	*Europe*	F	3.2.2; 3.2.3	UL	NESPOS
ULAC904	*Europe*	M	3.2.2; 3.2.3	UL	NESPOS
ULAC909	*Europe*	M	3.2.2; 3.2.3	UL	NESPOS
ULAC920	*Europe*	F	3.2.2; 3.2.3	UL	NESPOS
ULAC953	*Europe*	M	3.2.2; 3.2.3	UL	NESPOS
ULAC954	*Europe*	M	3.2.2; 3.2.3	UL	NESPOS
ULAC955	*Europe*	M	3.2.2; 3.2.3	UL	NESPOS
VA014	*Africa*	F	3.1	Evan Society, Vienna (ES)	Evan
VA017	*Australia*	M	3.1	ES	Evan
VA019	*Africa*	F	3.1	ES	Evan
VA023	*Africa*	M	3.1	ES	Evan
VA024	*Africa*	F	3.1	ES	Evan
99.1/92	*Alaska*	m	3.1	American Museum of Natural History, New York (AMNH)	Lynn Copes*
99.1/502	*Alaska*	m	3.1	AMNH	Lynn Copes
99.1/510	*Alaska*	f	3.1	AMNH	Lynn Copes
99.1/514	*Alaska*	f	3.1	AMNH	Lynn Copes
226088	*Australia*	f	3.1	National Museum of Natural History, Washington D.C. (NMW)	Lynn Copes
226090	*Australia*	f	3.1	NMW	Lynn Copes
227805	*Greenland*	m	3.1	NMW	Lynn

					Copes
242693	*Greenland*	f	3.1	NMW	Lynn Copes
242694	*Greenland*	f	3.1	NMW	Lynn Copes
242697	*Greenland*	m	3.1	NMW	Lynn Copes
242699	*Greenland*	f	3.1	NMW	Lynn Copes
242724	*Greenland*	f	3.1	NMW	Lynn Copes
242725	*Greenland*	f	3.1	NMW	Lynn Copes
242726	*Greenland*	m	3.1	NMW	Lynn Copes
329778	*Australia*	f	3.1	NMW	Lynn Copes
331242	*Australia*	m	3.1	NMW	Lynn Copes
3116	*Tierra del Fuego (TF)*	f	3.1	Museo di Storia Naturale, Università di Firenze° (UF)	
3119	*TF*	f	3.1	UF	
3122	*TF*	m	3.1	UF	
3129	*TF*	m	3.1	UF	
3130	*TF*	u	3.1	UF	
3133	*TF*	m	3.1	UF	

2.1.2 The landmark configurations

For the analyses of this thesis have been used different landmark configurations aimed at the specific objectives of any analysis.

The list of the landmarks used is reported in table 2.3, which reports also the relative section of the thesis; the non-anatomical point (i.e. concretion tips or margin of Altamura) are not specified in the table. The criteria used for the definition of the landmark configurations, with reference to the analysis performed are the following:

- ***Section 3.1 – Maxillary sinuses analysis in 2D:***
  The 2D analysis required two configurations, respectively one of extremal points (type 3, see section 2.2, Bookstein, 1997) and thus the most lateral, anterior and posterior of the sinus profile and one of 100 equidistant semilandmarks (Bookstein, 1997b) by function *equidistantCurve()* (package Morpho) along the sinus profile (fig. 2.1).

- ***Section 3.2.2 – Digital alignment – section 3.2.3 – 'combin3d'***:
  For the Digital alignment, landmarks were sampled on the surface acquisitions of the front and rear sides of Altamura; were chosen only anatomical points with no concretions and/or easily recognizable through the concretions, subsequently acquired on the reference sample (fig. 2.2). The same configuration was used for the application of the *combinland()* tool.

- ***Section 3.2.4 – Alignment of the nasal cavity***
  For the alignment of the anterior portion of the nose and of the coanae on the reconstructed cranium of Altamura two configurations were used: the anterior was made by points with no anatomical criterion (i.e. tips of concretions recognizable on both face and nose models, see figure 2.3, left); the posterior

made mainly by anatomical points recognizable on both the rear side and the coanae (fig 2.3, right).

- ***Section 3.3 –Reconstruction of the nasal cavity***

  The second step of the reconstruction required the warping of a modern human nose: the landmark configuration was made by anatomical points of the inner nose preserved and recognisable in the nose of Altamura (fig. 2.4).

Table 2.3 - List of the landmarks used. Pairing refers to the landmarks being located on the mid-sagittal plane (MS) or on both sides (bilateral, BL); left (L) and right (R) refers to landmarks sampled only on that side

Landmark name/description	PAIRING	SECTION
Most anterior point maxillary sinus (section)	BL	3.1
Most lateral point maxillary sinus (section)	BL	3.1
Most posterior point maxillary sinus (section)	BL	3.1
Supra-glabellar depression (medial point)	MS	3.2.2; 3.2.3
Nasion	MS	3.2.2; 3.2.3
Rhinion	MS	3.2.2; 3.2.3
Nasospinale	MS	3.2.2; 3.2.3
Prosthion	MS	3.2.2; 3.2.3
Supraorbital notch	BL	3.2.2; 3.2.3
Frontomalare orbitale	BL	3.2.2; 3.2.3
Zygoorbitale	BL	3.2.2; 3.2.3
Lacrimale	BL	3.2.2; 3.2.3
Alare	BL	3.2.2; 3.2.3
Infraorbital foramen	BL	3.2.2; 3.2.3
Lambda	MS	3.2.2; 3.2.3
Projection on occipital squama of the medial point of the chord between lambda and inion	MS	3.2.2; 3.2.3
Inion	MS	3.2.2; 3.2.3
Opisthion	MS	3.2.2; 3.2.3
Basion	MS	3.2.2; 3.2.3
Hormion	MS	3.2.2; 3.2.3
Posterior margin of the palatine foramen	MS	3.2.2; 3.2.3
Orale	MS	3.2.2; 3.2.3
Condylion laterale	L	3.2.2; 3.2.3

Asterion	BL	3.2.2; 3.2.3
Mastoidale	BL	3.2.2; 3.2.3
Posteriormost point of the maxillary dental arch	BL	3.2.2; 3.2.3
Staphilion	MS	3.2.4
Middle point of the posterior border of the vomer	MS	3.2.4
Superior margin of the meeting point of the wings of the vomer	MS	3.2.4
Notch between the wings of the vomer	MS	3.2.4
Posterolateral corner of the hard palate	BL	3.2.4
Medial point of the medial pterygoid plate	R	3.2.4
Postero-lateral margin of the basisphenoid	BL	3.2.4; 3.3
Point of the medial pterygoid plate meeting with the suture between sphenoid and temporal	L	3.2.4
Inner projection of the Rhinion	MS	3.3
Anterior margin of the medial nasal concha	BL	3.3
Posterior margin of the medial nasal concha	BL	3.3
Medial point of the medial nasal concha	BL	3.3
Anterior margin of the inferior nasal concha	BL	3.3
Posterior margin of the inferior nasal concha	BL	3.3

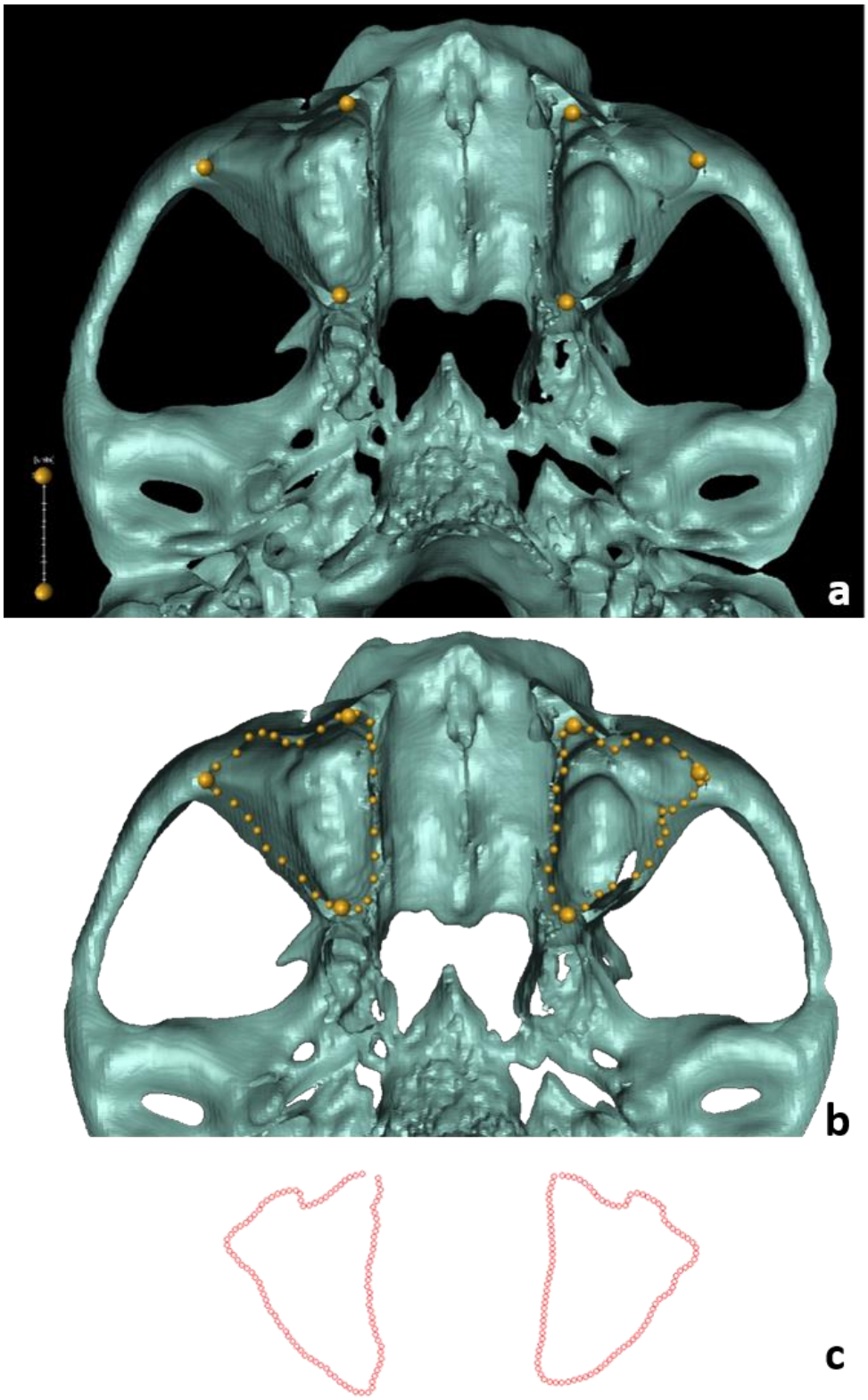

Figure 2.1 - Configuration for Section 3.1, maxillary sinuses analysis in 2D. ***a:*** *first configuration of extremal points for the scaling (first two points on the metric reference);* ***b:*** *sinus profile sampled in Amira;* ***c:*** *example of the configuration of 100 equidistant semilandmarks defined by the function equidistantCurve() in R*

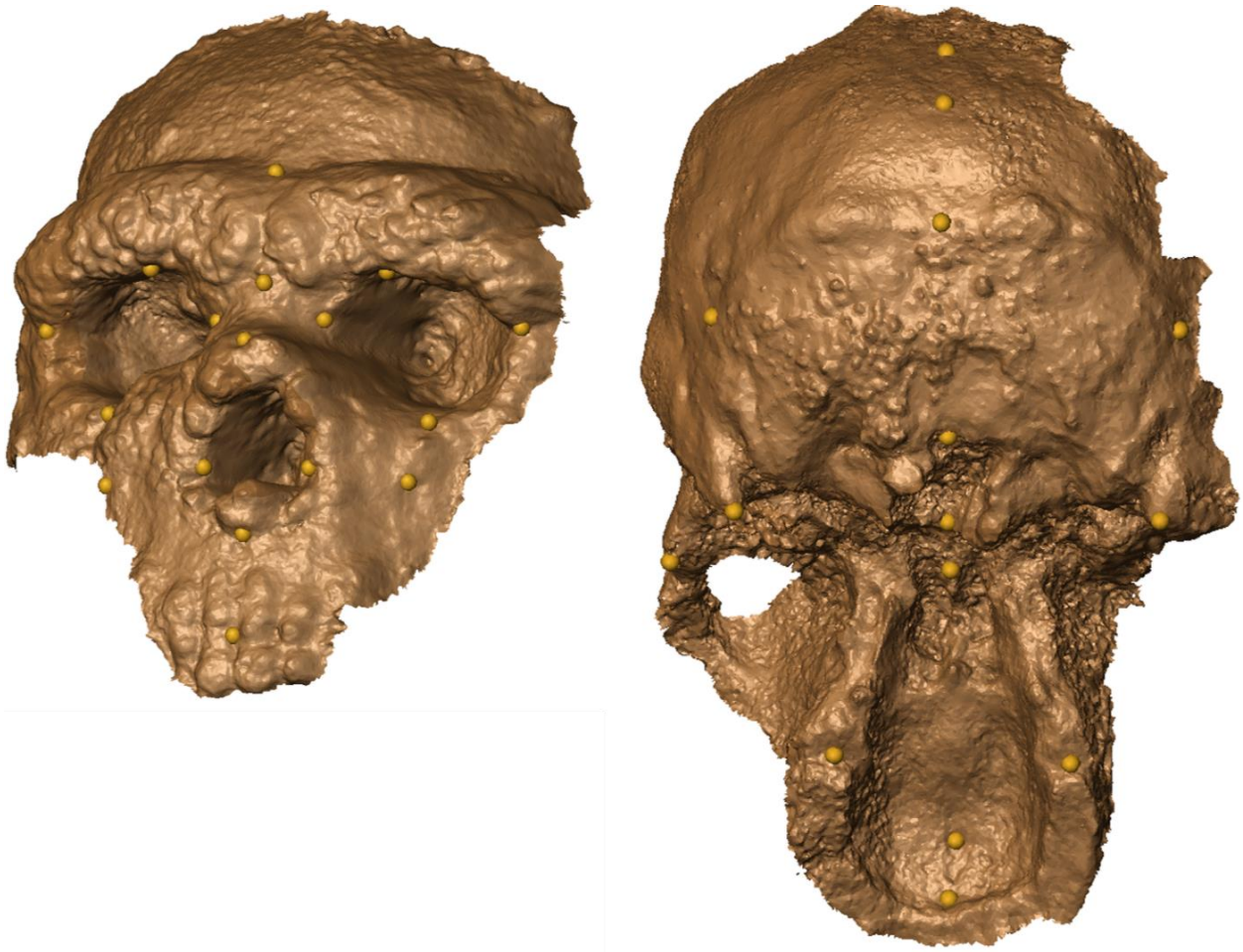

Figure 2.2 - Configurations for the front side (left) and the rear side (right) of Altamura, used for Section 3.3.2 (Digital alignment) and Section 3.3.3 ('combin3d')

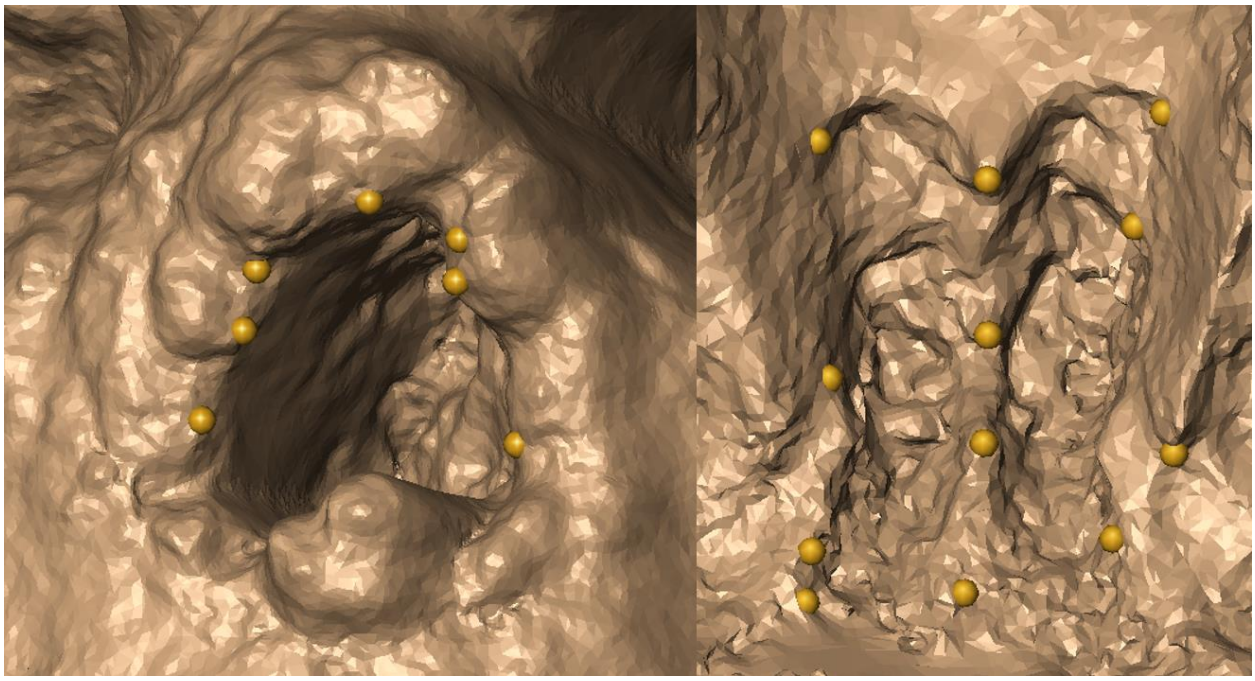

Figure 2.3 - Configurations used in Section 3.2.4 for the alignment of the nasal cavity; anterior model (left), posterior model (right)

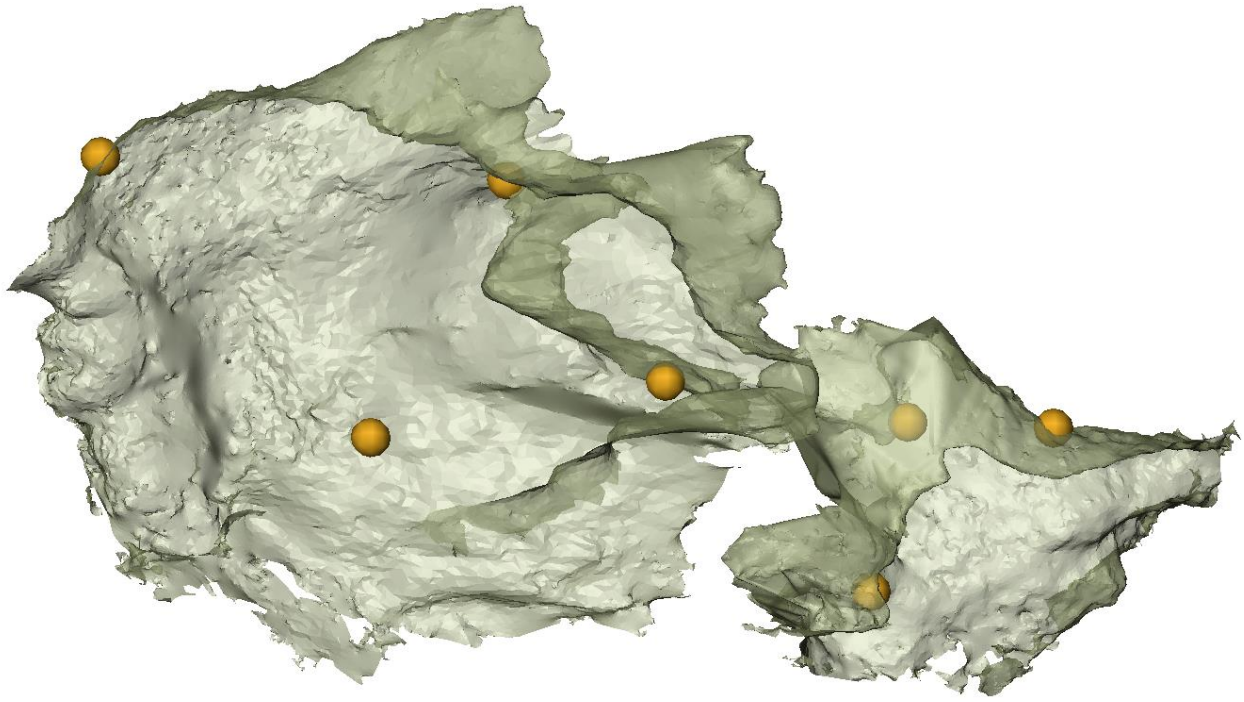

Figure 2.4 – Configuration used in section 3.3 (Reconstruction of the nasal cavity). Only the mid-sagittal and right lateral landmarks are visible.

2.2 GEOMETRIC MORPHOMETRICS

This research has been carried out by using a Geometric Morphometrics (GM) approach (Rohlf and Marcus, 1993; Adams et al., 2004), which embraces the methods to sample, process and analyse the shape variables retaining all information contained by the data (Slice, 2006). As stated by Bookstein (1997a), "the objects of morphometric study are not the forms themselves, but rather their associations, causes, and effects"; GM allows to extract the information from the shape by approximating it by an outline (Rohlf, 1990) or, as is nowadays most commonly used, as a configuration of two- or three-dimensional points (landmarks) that satisfy a criterion of geometric homology (Adams et al., 2004; Gunz et al., 2005). The 'geometric homology' (Mitteroecker and Gunz, 2009) differs slightly from the strict biological concept of homology by adding to the developmental and phylogenetic criteria a topological one expressing the relationships among locations of structures across the sample; in this sense it is rooted in the transformation grids proposed by Thompson in 1917 (Thompson, 1992; Gunz et al., 2005).

A repeatable procedure of definition, location and collection of the landmarks is the first aim of GM (Bookstein, 1997a), followed by the recording of the landmark coordinates in a defined coordinate system (Slice, 2006). Landmarks are defined by Bookstein (1997a) as belonging to three types:

- type 1 correspond to juxtaposition of tissues (e.g. where three sutures meet);
- type 2 are defined as maxima of curvature or other local morphogenetic processes, as tips of extrusions and valleys of invaginations;
- type 3 are extremal points the definitions of which refer to information at diverse, finitely separated locations, as in the case of farthest points from given other points, or intersections of segments defined by other points, or centroids.

One additional approach is that of geometric points (semilandmarks), evenly spaced and defined, along an outline or a surface, on the basis of a landmark configuration (Bookstein, 1997b; Gunz et al., 2005). Semilandmarks allow to quantify the shape also on structures which lack traditional landmarks (Schlager, 2017).

The semilandmarks approach is based on two of the 'cornerstones' of GM: Procrustes analysis and Thin-plate spline (Bookstein, 1997b).

Procrustes superimposition is a technique to obtain the best fitting superimposition of the configurations of the sample by minimizing the sum of squared distances of their parameters for location and orientation (Bookstein, 1997a); it is also possible to apply a "full Procrustes analysis", by scaling all specimens to a standard size by the same least-squares estimate (Slice, 2006). In GM, it is also referred to as Generalised Procrustes Analysis (GPA, Gower, 1975).

Thin-plate spline is a tool for the interpolation of scattered data, based on the bending energy which deforms a grid formed by fixed nodes (Bookstein, 1989); it can be applied for the estimation of missing landmarks either by using the landmarks that are present in the same configuration (e.g. by warping the symmetric points in case of bilateral landmarks), or by statistically predicting the location of missing coordinates using multiple multivariate regressions based on a sample of complete specimens (Gunz et al., 2009).

For both geometric morphometrics and the statistical analysis of this research has been used the statistical software R (R Development Core Team, 2016) and specifically the packages Arothron (Profico et al., 2015), Morpho and Rvcg (Schlager, 2017).

2.2.1 The automatic segmentation – CA-LSE and AST-3D

Among the outputs of the present thesis there is the development of a R-based tool for the automatic segmentation of inner cavities. For the analysis of maxillary sinuses of the

present thesis a 2D GM approach was eventually chosen, because dealing with broken and/or sediment-filled cavities of fossils; the methodology here presented has revealed to be very effective in segmenting empty cavities, and was here used for better defining empty portions in fossil maxillary sinuses and to implement reconstructions of the modern human nasal cavity.

The protocol usually applied to isolate and render three dimensional meshes from digital specimens, whether they are structural parts, soft tissues or hollow spaces, demands the manual segmentation of the CT-scan data (Weber and Bookstein, 2011): proceeding through sequential CT slices, the operator defines a mask of each region of interest, subsequently performing a triangulation of the segmented slices, thus obtaining a 3D mesh. In the case of inner cavities, the operator must digitally 'fill' the hollow spaces, by a procedure that is time-consuming and prone to generating topological artefacts (Profico et al., 2016; Veneziano et al., 2018), due to the almost unavoidable inaccuracies in the manual processing (closure) of holes and gaps, such as foramina or missing portions (Huotilainen et al., 2014; Nicolielo et al., 2017).

On the other hand, the isolation of the external surface could be useful to virtually restore incomplete/damaged specimens, for example by using TPS interpolation (Gunz et al., 2009). Commercial software commonly used for segmentation and mesh editing are often expensive, while the methods here presented are developed in R environment and hence available for free. They automatically reproduce virtual images of both inner and outer surfaces of skeletal remains.

The first method, Computer-Aided Laser Scanner Emulator (CA-LSE), provides the reconstruction of the external portions of a 3D mesh, being a replacement for laser scanners, and it further allows the reconstruction of internal surfaces by subtraction.

The second method, Automatic Segmentation Tool for 3D objects (AST-3D), performs the digital reconstruction of anatomical cavities, and further allows the reconstruction of the outer surface by subtraction.

Both methods require the definition of a set of points of view (POVs) in order to delineate the outer surface of the digital object of interest, subsequently producing a mesh of the visible (from the POVs perspective) surface. This operation is an implementation of the "Hidden Point Removal" (HPR) operator method developed by Katz, Tal & Basri (2007).

There is no restriction upon the definition of POVs under CA-LSE, which are automatically placed on a sphere containing and not intersecting the 3D mesh. Conversely, under AST-3D the POVs set has to be manually defined within the cavity of interest by using an imaging software to define a configuration of landmarks which will represent the references for the POVs (fig. 2.5). In both cases, the number of POVs will be instrumental in defining the final quality of the mesh 'extraction' process. The more POVs, the better the final result.

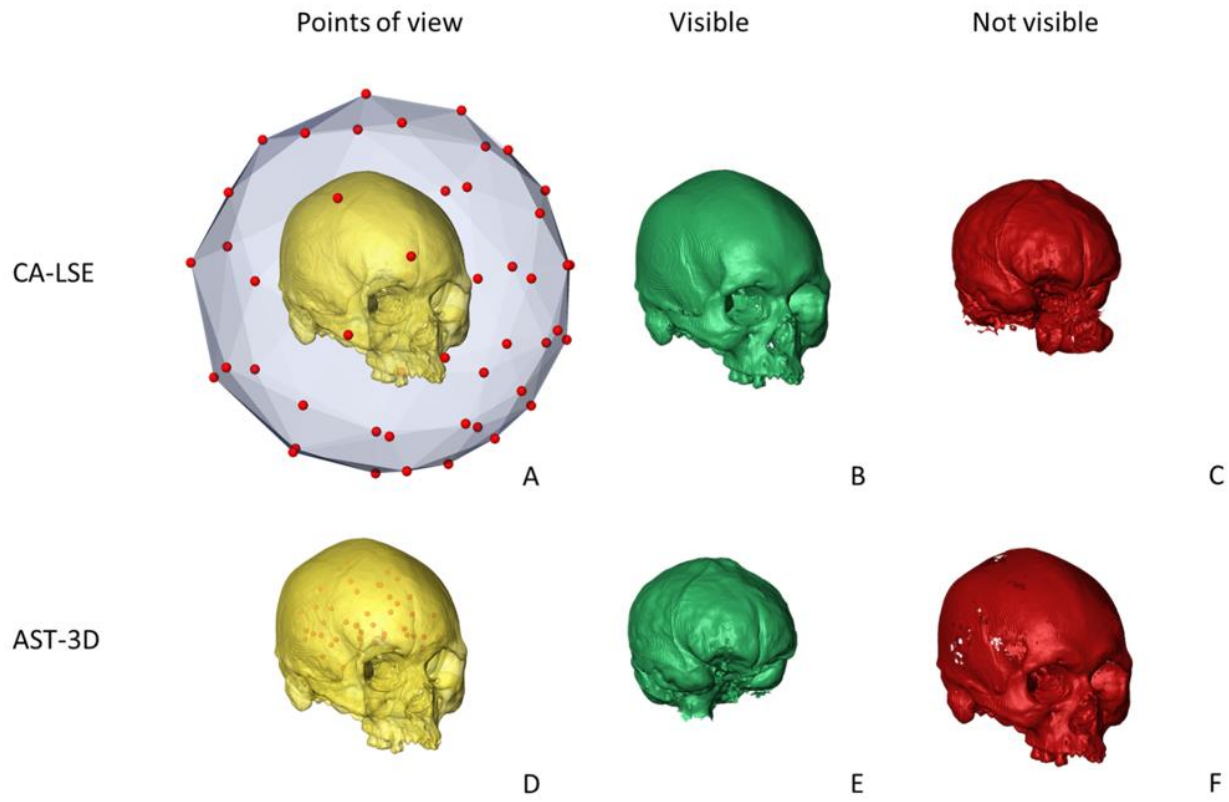

Figure 2.5 - Functioning of the two tools for automatic segmentation, CA-LSE (above) and AST-3D (below). Definition of the POVs (A, D); extraction of the visible surface (B,E); extraction of the not visible surface (C,F)

HPR is a two-step process: the first is the 'spherical flipping', which reflects each vertex of the mesh onto a sphere centred on a POV, and the second is the 'convex hull', which is built taking into account the POV (i), the vertices of the mesh (ii) and the reflected vertices of the mesh obtained from the spherical flipping (iii). A vertex of the mesh is marked as visible from the POV perspective if its reflected point lies on the convex hull.

CA-LSE is designed to work both using automatic definition of the POVs or user-selected POVs; for the former, the argument default in the function *ext.int.mesh()* has to be set to TRUE. Under the latter, the arguments default and method have to be set respectively to FALSE and "calse". To perform the AST-3D method the user has to set the arguments default and method respectively to FALSE and "ast3d". It is possible also to import the coordinates of the POVs from external software (e.g., Slicer3d, ImageJ, Amira) setting the arguments *default* and *import.pov* on FALSE and TRUE, respectively.

2.2.2 2D Geometric morphometrics

Internal structures of human fossil crania are often badly preserved, broken or completely missing (Schwartz and Tattersall, 2002; Gunz et al., 2009; Profico et al., 2019a) and among them, maxillary sinuses are particularly subjected to gaps because delimited by thin walls of bone (Lieberman, 2011). In dealing with fossils it is thus necessary to overcome such issues; one of the possible ways is to use a proxy of the actual shape.

Nowadays are available segmentation techniques which allow to extract an inner surface with no artefacts derived from manual closing of missing portions, as the aforementioned tools CA-LSE and AST-3D (Profico et al., 2018b); nonetheless this approach is not always suitable - as in the case of some of the fossil specimens used for the study of the present thesis – because fossils can present themselves filled with

unremovable – physically nor digitally – sediment; in these cases, a manual segmentation of the cavity is needed, instead. A third option is that to apply a simpler 2d approach, used in this case to identify a 'Neanderthal sinus profile' characterising the general shape.

Such approach derives from Rak (1986), but is equally debtor to Heim (1989), who used 2D tomographic sections to highlight the peculiar profile of the facial morphology in a Neanderthal specimen – La Chapelle-aux-Saints - and it is here applied with some modifications with the purpose to intercept a profile distinguishing different fossil and extant human groups.

In geometric morphometrics the use of 2D landmarks configurations is longstanding - having represented the first and most common approach - but it is still proficiently used thanks to its simplicity, low cost and easiness (Cardini, 2014). It can be applied, for example, to dataset based on pictures instead of 3D models, often more difficult to collect. Also, 2D has several advantages in terms of analysis: an effective visualization of shape change by TPS (Bookstein, 1991; Cardini, 2014), the possibility to be performed only on the most informative views as the lateral one (e.g. mid-sagittal profiles), in order to make maximum use of type 3 landmarks (Bookstein, 1997a) and/or to easily cross-check for 3D analysis (Bruner, 2004).

Maxillary sinuses feature only one landmark of type 1, which coincides with the *ostium*, the opening connecting the sinus itself with the nasal cavity (Rae and Koppe, 2004); when dealing with archaeological or fossil collections, such structure and the thin wall it is located onto are often damaged or not preserved. The shape of maxillary sinuses makes difficult to apply GM by using only one homologous point, so a 2D study can overcome this issue by using type 3 landmarks and semilandmarks.

We adopted the same, easily definable, transversal plane to intercept in all individuals the sinus variability: the plan cuts the cranium by passing by the two *poria* and the upper margin of the uppermost infra-orbital foramen (in case of low asymmetry of the

cranium, has always been used the right one). The section thus obtained was used to define a bi-dimensional profile of both maxillary sinuses.

The operation was carried out by using the software Thermo Scientific Amira® (https://www.fei.com/software/amira/ , Stalling et al., 2005). The sections were scaled by using a metric reference of the software. For each specimen were sampled two landmark configurations: one consisting of three landmarks, located in the extremal points (respectively the most anterior, distal and posterior); the other consisting of 100 equidistant semilandmarks sampled along the profile, interpolating the lacking portions, if needed, on the basis of the nearest preserved points.

2.2.3 Digital Tool for Alignment (DTA)

Biostratinomic and/or taphonomic processes often determine in fossils deformation stresses (Hughes and Jell, 1992; Arbour and Currie, 2012; Schlager et al., 2018) which can lead to breakage and subsequently to missing portions (Ogihara et al., 2006; Arbour and Brown, 2014; Di Vincenzo et al., 2017). The cranium of Altamura has not been affected by these processes and present itself undamaged and undeformed; still, the karstic flow in which it is encompassed precluded part of the cranial morphology to the digital acquisition. For this reason, it has been treated as a cranium disassembled in two portions.

As previously mentioned in section 2.2, missing morphological information can be digitally recovered either by using the preserved shape information on the deficient specimen (e.g., by exploiting biological symmetry) or through the use of a 3D comparative sample of phylogenetically close species, conspecifics, or individuals of the same sex (Gunz et al., 2009). Several case-studies are reported in the literature (Zollikofer et al., 2005; Benazzi et al., 2014; Amano et al., 2015; Di Vincenzo et al., 2017),

and the use of virtual reconstructions is now becoming commonplace, but its efficiency is rarely quantified (Ogihara et al., 2006; Tallman et al., 2014; Schlager et al., 2018).

For the research here presented has been developed the Digital Tool for Alignment (DTA), a new landmark-based procedure to align disassembled portions of a same broken specimen. DTA is written in R language and embedded in the Arothron package (Profico et al., 2018c) and is designed for aligning two portions of a 3D mesh – or the disarticulated model (DM) - by using a reference sample or model (RM) for comparison (fig 2.6).

To run DTA, a set of anatomical landmarks is defined first on the two separated portions; then each landmark is moved to the nearest vertex of the mesh triangles to allow its identification by a number corresponding to a row of the vertex matrix of the mesh, and eventually track its position on the 3D models moved in the Cartesian coordinate system.

The second step is the alignment via GPA of each part of the DM on each RM of the comparative sample, where the same landmark configuration has been previously defined. The specimens of the reference sample are scaled to the mean of the single scale factors calculated for each of the two portions of the DM separately, and symmetrized via reflection and relabelling, thereby producing a symmetrical, bilateral and scaled landmark configuration (to avoid errors due to asymmetry).

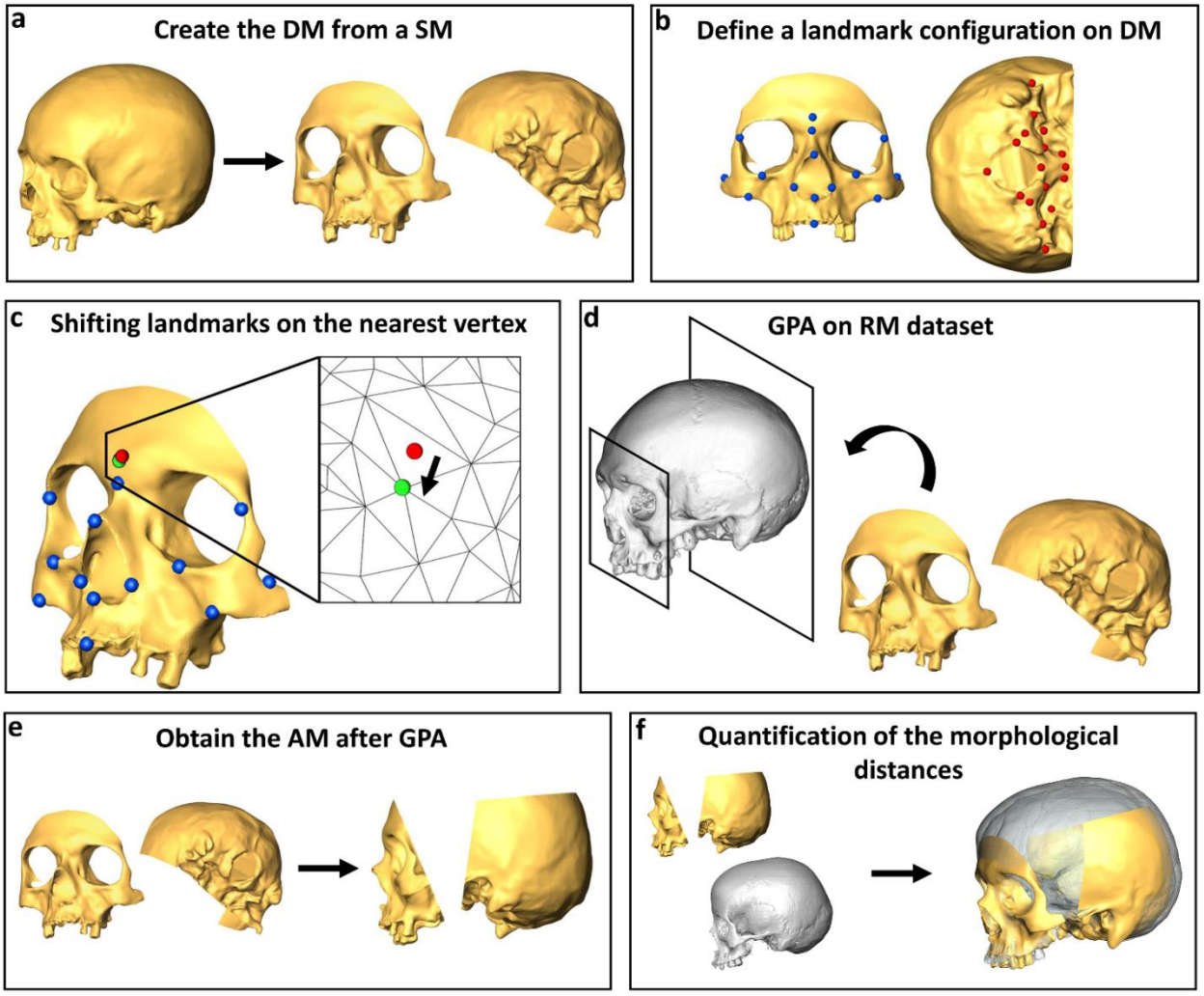

Figure 2.6 - Functioning of the DTA: the steps of the process are ordered from a to f

The third step consists of quantifying the morphological distances between each part of the DM and the corresponding landmark configurations on each item in the RM sample. DTA allows calculation of the morphological distance using either one of two different metrics: the total displacement (Euclidean distance) and/or the Procrustes distance.

Then, the single specimen in the reference set with the lowest morphological distance to DM is selected as the best RM for the digital alignment to reconstruct the integral shape of the target.

2.2.4 'Combin3D' analysis

As mentioned in section 2.2.2, 2D geometric morphometrics is a useful tool to simplify shape analysis or overcome difficulties coming from the collection of 3D data; it is also useful to check the results coming from 3D data analysis (Bruner, 2004). Altamura represented a good case study for a new statistical approach developed contextually to this thesis work. The method, called *combinland* (Profico et al., 2019c) is applicable to cases - as Altamura - in which the complete extraction of the specimen and thus its overall acquisition is not – or not yet - possible. *combinland* is a new R tool which combines the morphological information coming from different landmark sets acquired on different configurations. These configurations can be 2D sections or norms of a 3D object or even a mix of 2D and 3D configurations.

The Centroid Size (CS) - the quadratic mean of the vector difference between each landmark and the centroid – which is used for the scaling of a same-configuration dataset, cannot be similarly used for comparing the size of shapes identified by different number of landmarks; a size correction is thus needed (Dryden and Mardia, 2016). This is because the value of CS is influenced by the total number of landmarks defining the shape.

combinland combines multiple datasets into a unique matrix that can be subjected to ordination analyses encoding the whole morphological information; *combinland* works with different number of landmarks in both 2D and/or 3D configurations. It is based on a technique originally proposed by Adams (1999), but introduces a new size correction to guarantee a proper combination of multiple landmark configurations weighting sizes for the number of landmarks and dimensions (fig. 2.7), specifically by re-multiplying coordinates (that were originally divided by their proper CS) by the square root of their number of landmarks (that vary among different configurations) times their number of dimensions (that would be 2, in the case of 2D datasets, 3 for 3D datasets).

For Altamura, no 2D configurations were used; have been used, instead, 3D configurations of landmarks, recognizable despite the concretions, on the two models acquired (more on the acquisition in section 2.3), the same used for DTA. The configurations thus concerned the face – on the Apse side - and the rear portion including occipital, cranial base and palate. The same configurations have been taken on the reference sample and a GPA has been performed on each set.

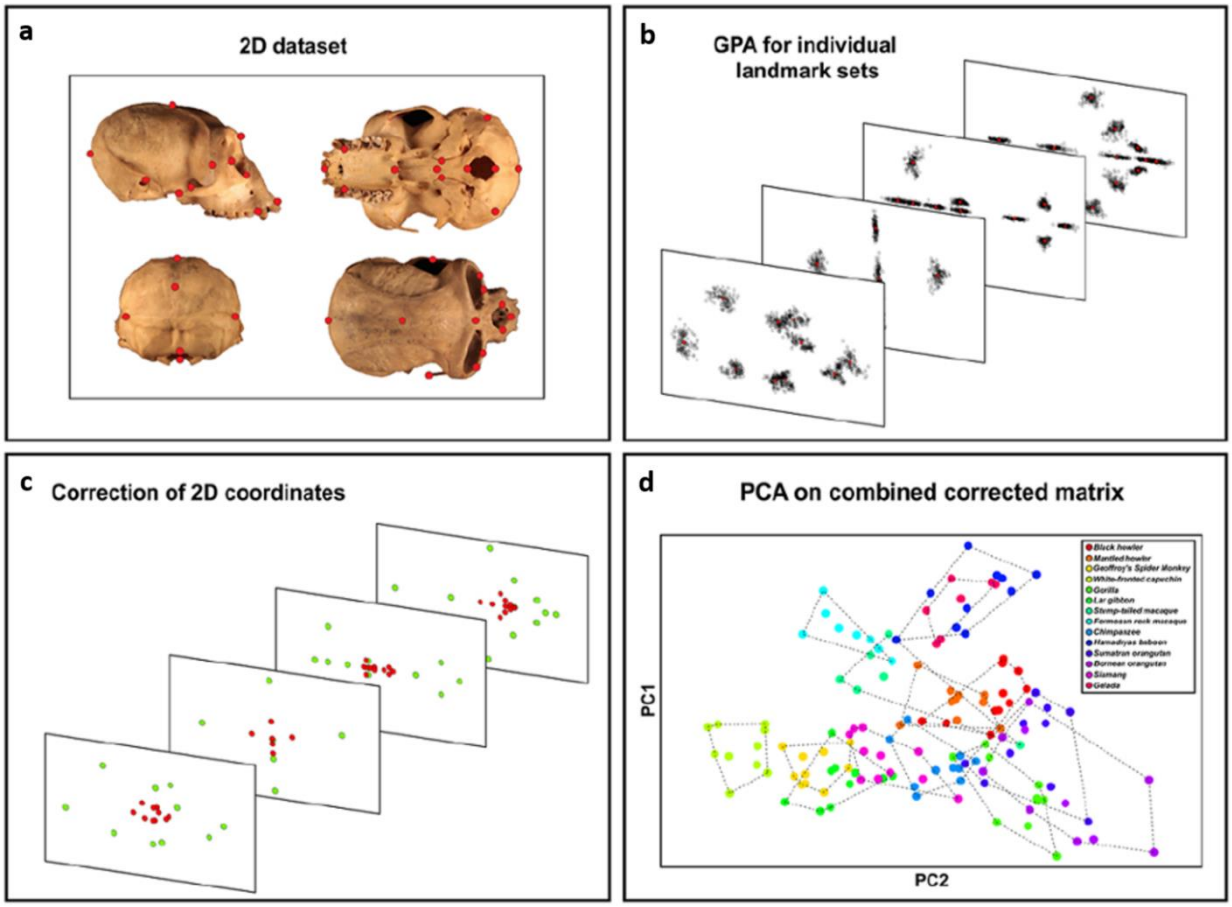

Figure 2.7 - Functioning of the combinland tool. The steps of the process are ordered from a to d

2.3 DIGITAL ACQUISITION IN THE KARSTIC ENVIRONMENT

The candidate has been conducting some of the required work of investigation in the Lamalunga cave. The descents into the Lamalunga cave took place as part of the K.A.R.S.T. research project (see section 1.4), under the coordination of the project director Prof. Giorgio Manzi and with the logistic and speleological assistance of the C.A.R.S. speleological group, on April and October 2018 and April 2019.

Part of the project concerned the analysis of the microclimate and the geological context of the cave; other activities were carried out on the paleoanthropological material, by high resolution digital acquisition of the nasal cavity, coanae, brain cavity and points of contact between cranium and the flowstones. In addition, has been performed a further superficial acquisition, both via laser scanner and photogrammetry, of the small chamber behind the Apse.

To perform the activities with minimum invasiveness and to reduce further contaminations as much as possible - both from microbiological agents and exogenous DNA - in the Apse was used medical surgical equipment: sterile drapes, gloves, masks and caps; moreover, clean shoe covers were brought to the ante-Apse to be put on at every access to the location of the skeleton.

Prior to any activity on the cranium, an amount of water naturally present in the endocranial cavity was removed and collected; its volume has been observed to vary during the year between 600 to 760 ml (data recorded between 2017 and 2018); a known quantity of the water has been collected for biochemical analysis, while the rest has been regularly put back inside the cranial cavity.

During the sessions of activities, there has been a turnover of the operators and the speleological staff between the two contiguous chambers – Apse, and ante-Apse (see figure 1.12) – in order to have no more than three people operating in the Apse and two in the ante-Apse providing assistance.

2.3.1 Digital acquisition of the cranial portions

The digital acquisition of the cranium surface was performed in a previous campaign. Two different methodologies have been used : the front side (from now on, FS), that is visible and accessible from the Apse of Man, was acquired via laser scanning, by a Konica Minolta range7, at a resolution of 40 μm; the rear side (from now on, RS) was acquired via photogrammetry by a GoPro camera mounted on a probe. The chamber behind the apse, in fact, is accessible from the Apse only by small slots opening in the flowstones, of which the larger ones (>20 cm high and >10 cm wide circa) are some 80 cm far from the cranium, on the upper right of the wall (see figure 1.14). The GoPro images have been subsequently processed by using the software Agisoft Photoscan.

2.3.2 Digital acquisition of the nasal cavity

The acquisition was made in several sessions by using endoscopic probes. The equipment used was an Olympus IPLEX NX IV9635N with 3.5 m long probes with diameters of 6 mm and 4 mm and 120D/NF lens with a 120° angle; the base unit was an 8.4-inch daylight view LCD touchscreen monitor (https://www.olympus-global.com/news/2016/nr160404iplexe.html).

Prior to the acquisition by Olympus equipment, test acquisitions were made with an Ambu aScope 3 bronchoscope with LCD monitor aView (https://www.ambu.com/products/flexible-endoscopes/bronchoscopes).

The acquisition, made both by photos and videos, concerned the details of the nasal cavity and the structures there preserved (e.g. turbinates, vomer), the cranial base, the endocranial cavity, the right ear canal, the superior dental arch and the points of contact between the cranium and the concretions (fig. 2.8). The probes were also used to explore

the assemblage of bones below the cranium, with detailed shots of the mandible there located and of the dental arch.

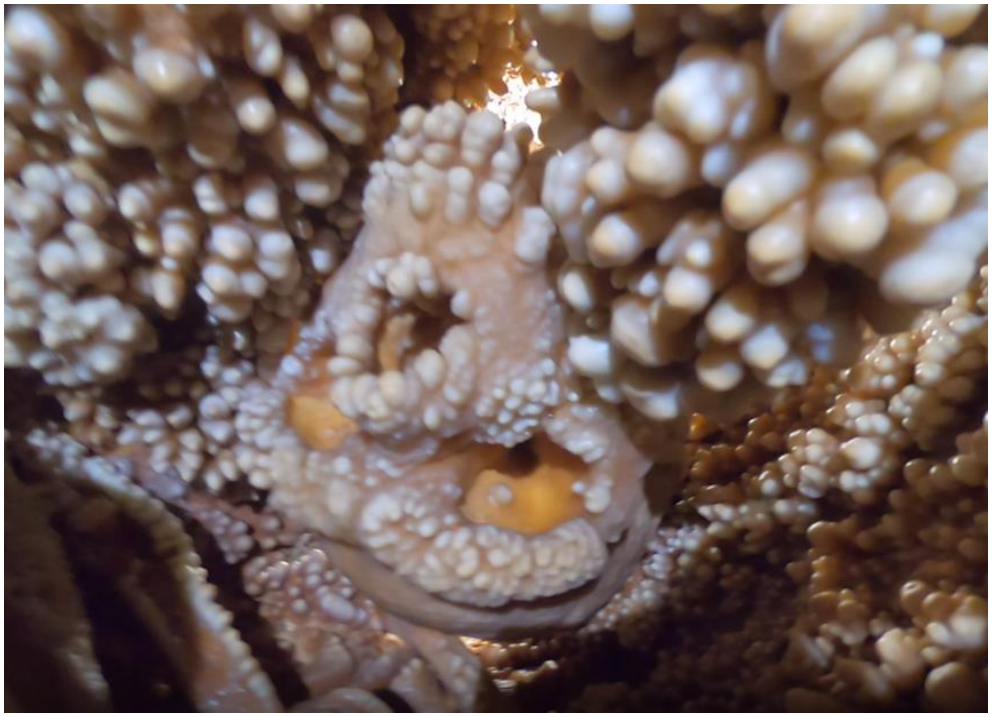

Figure 2.8 - A frame showing the points of contact between cranium and concretions and the passage near the palate in where the probe was passed. Slight deformation due to the fisheye of the lens.

The nasal cavity has been video recorded by Olympus IPLEX both on the FS and the RS; in the latter acquisition, the probe was passed through a small hole opening between the maxillary dental arch and the flowstone above, slid parallel to the cranial base and recorded the coanae by a 180° rotation of the camera. The HD videos of the endoscopy were subsequently processed by ImageJ software (Ferreira and Rasband, 2012) to eliminate the wide-angle effect by deforming the image according to a reference grid acquired prior to the sessions. 50 frames have been eventually extracted from each video and processed by Agisoft Photoscan software.

3 RESULTS

[...] y tenía una cara como una bendición.

Miguel de Cervantes, *Don Quijote de la Mancha*

3.1 FOSSIL MAXILLARY SINUSES

The fossil maxillary sinuses were studied by a 2D GM approach. The study took into consideration the ensemble of the two sinuses as the shape of study: for this reason, were chosen fossil specimens in which both sinuses were preserved and not subject to strong deformation.

The first two landmarks of the first configuration sampled (8 landmarks) were defined on a metric reference, known and constant for all the specimens, in order to scale the whole sample, prior to the data processing, according with these two landmarks. Then, the curves of 100 landmarks were created separately on each sinus, left and right, by using the second configuration sampled along the sinus profile as reference. The curves were built by using the *equidistantcurve()* function, from 'Morpho' R package. For each specimen the sinus configurations - left and right - were aligned onto the six-point configurations defined on the extreme points.

The GPA has been subsequently performed on the sample, by the function *procsym()* ('Morpho' package) without scaling (scale = FALSE) and eventually a PCA was performed; in figure 3.1 is reported the plot relative to first two PCs, which account for more than 70% of the variance (tab. 3.1). The shape variations relative to the two first PCs are reported in figure 3.2.

The sample was then investigated for the intra-group variability: it was divided in three groups, respectively *H. sapiens* (SAP), *H. neanderthalensis* (NEA) and Mid- Pleistocene

humans (or *H. heidelbergensis*, HEI). A mean shape for each group was defined; the shape variations between groups are presented in figures 3.4 to 3.6.

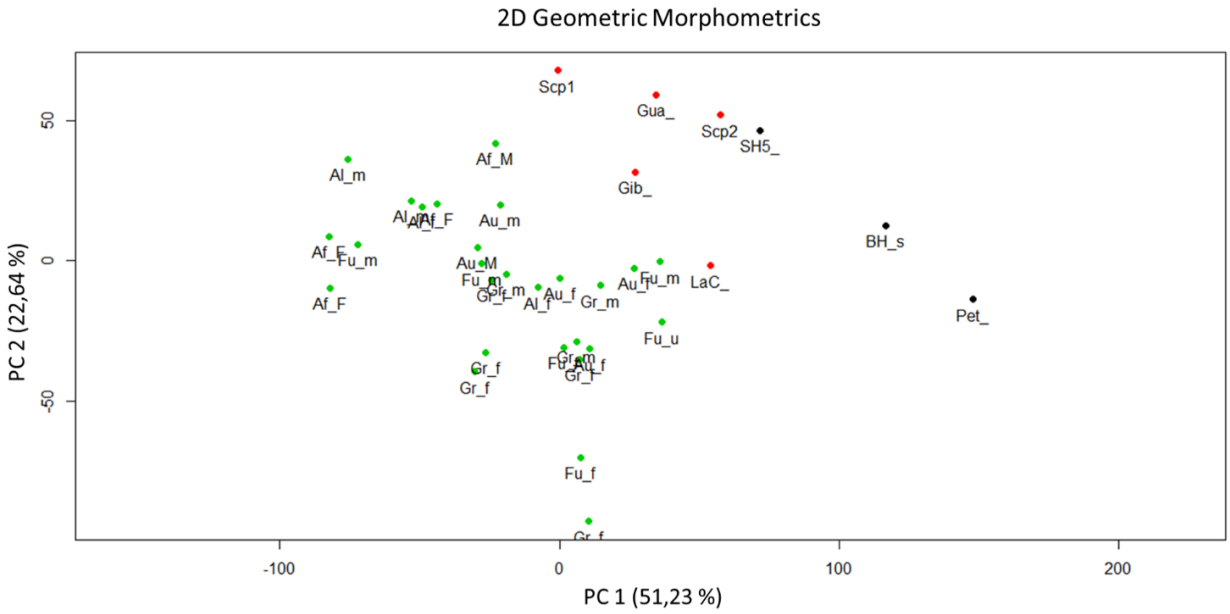

Figure 3.1 - PCA analysis for the 2D profile of maxillary sinuses. Green: H. sapiens (Af = Africa; Al = Alaska; Au = Australia; Fu = Fuegians; Gr = Greenland); Red: H. neanderthalensis; Black: Mid-Pleistocene humans

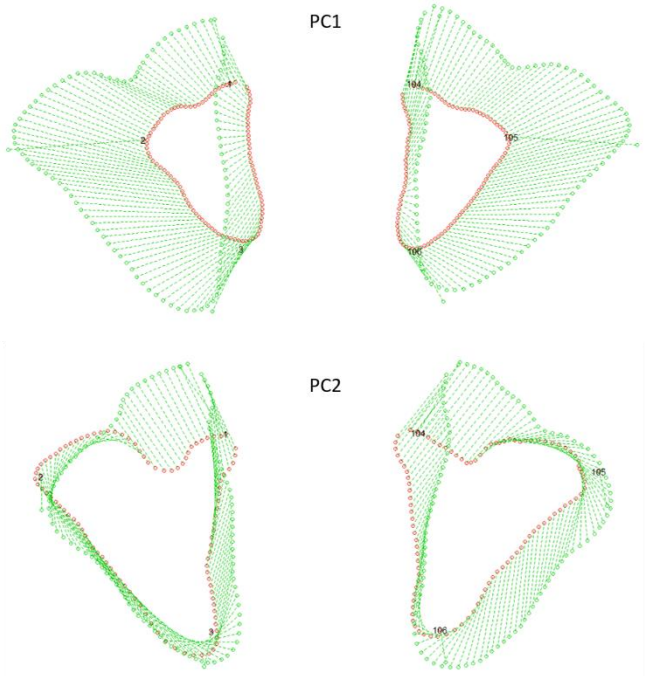

Figure 3.2 - Shape variation for the PC1 (above) and PC2 (below) of the 2D profiles of maxillary sinuses. In red, negative values; in green, positive values

Table 3.1 - Eigenvalues from principal components analysis of 2D maxillary sinus shape. The first 6 PCs are reported, accounting for more than the 90% of variability

PC	EIGENVALUES	VARIANCE (%)	CUMULATIVE (%)
1	2693,19	51,23	51,23
2	1190,43	22,64	73,88
3	360,56	6,86	80,73
4	231,06	4,4	85,13
5	196,68	3,74	88,87
6	146,36	2,78	91,66

By looking at the first two PCs, the 2D analysis returned the sample divided in rather defined clusters: in the plot reported in figure 3.1 it can be seen how modern humans are grouped in the negative values of the PC1, spreading instead along the y-axis (PC2).

Neanderthals cluster in the neutral-to-positive values along the PC1 and in the extreme positive values of PC2, while the Mid-Pleistocene humans – here labelled as *H. heidelbergensis* - spread across the central values of PC 2 and represent the extreme

individuals on the first component. SH5 falls at the limit of the Neanderthal cluster for the PC2 and at the lowest values of PC1 for *H. heidelbergensis*.

For what concerns PC1, the variability of Neanderthals and Mid-Pleistocene humans overlaps slightly along the neutral-to-positive values, with modern humans more clearly spreading along the negative values (fig. 3.3a); in the PC2 the three distribution are more clearly separated, with the Mid-Pleistocene humans isolated from the other groups (fig. 3.3b).

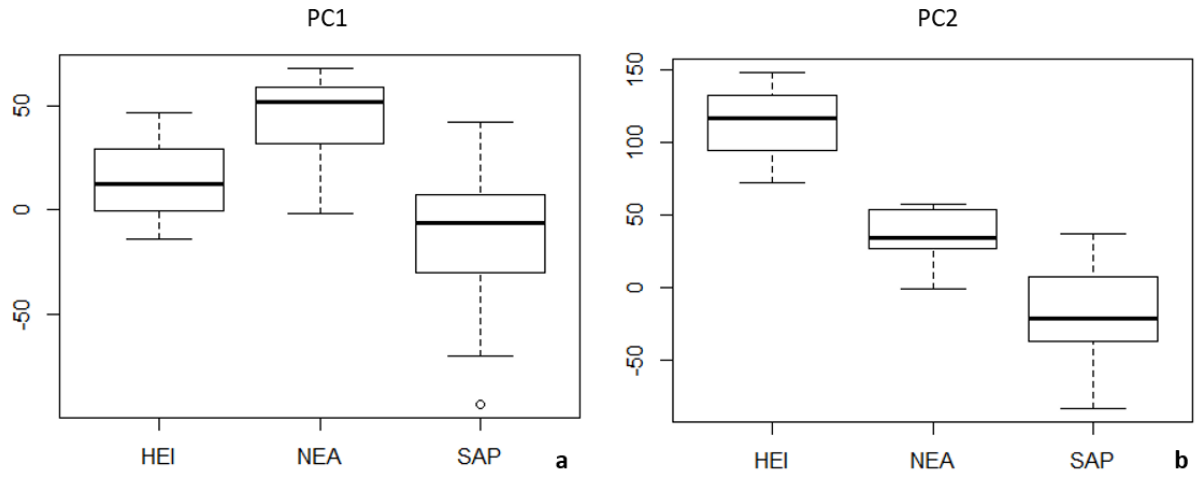

Figure 3.3 - Box plot for PC1 (a) and PC2 (b), variability between groups

The mean shape of the sample (not scaled GPA) was deformed to represent respectively the maximum and minimum shapes along the PCs (fig. 3.1): the first component is clearly driven by allometry, with the maximum values representing a more robust sinus. For the second component, it is registered the antero-posterior elongation of the sinus shape, which, looking at the sample, appears to be related with the mid-facial prognathism.

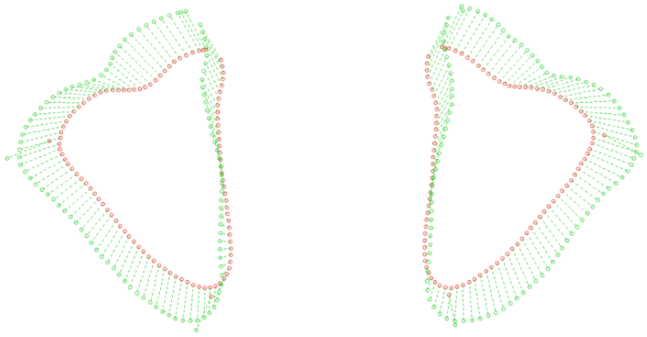

Figure 3.4 - Shape variations between H. sapiens (red) and H. neanderthalensis (green)

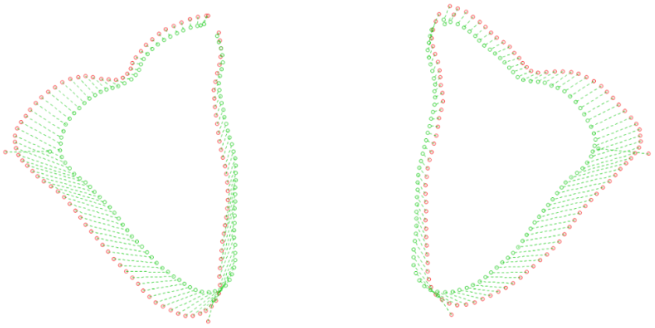

Figure 3.5 - Shape variations between H. heidelbergensis (red) and H. neanderthalensis (green)

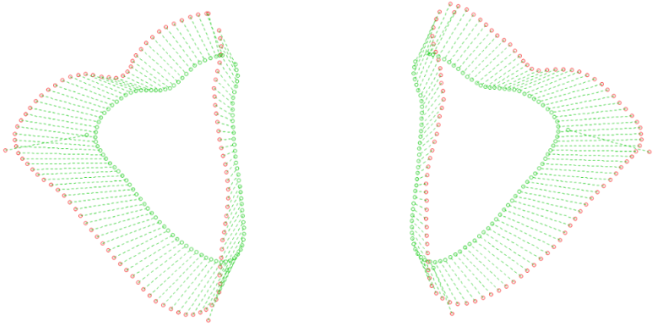

Figure 3.6 - Shape variations between H. heidelbergensis (red) and H. sapiens (green)

3.2 THE ALTAMURA CRANIUM

3.2.1 The acquired portions

The laser scanner acquisition of the FS had to deal with undercut problems due to the concretions. As it is visible from figure 3.7a, the position of the cranium and the presence of concretions determined an optimal acquisition only for the surfaces orthogonal to the laser beam, while some imperfections emerged in the case of the surfaces not sufficiently angled with it (e.g. some walls of cavities as orbits and nose, the farthest portions of the parietals). Minor undercut flaws affected the supero-lateral portions of the supraorbital torus, while the central portion resulted to be well defined.

The final acquisition of the FS here presented includes the midface, the anterior portion of the frontal bone (the bregma was not accessible) and the left zygomaxillary region. The details of the nasal cavities acquired separately by the Olympus probe have been less affected by undercut problems, thanks to the high mobility of the probe head: it has been acquired roughly the anterior half of the nasal cavity, while the nasal floor was not sufficiently visible to be reconstructed with high detail (fig. 3.8 a).

The RS acquired by photogrammetry presents a slight decrease of quality in the anterior portion of the palate, because of the impossibility to take the picture with a sufficiently orthogonal axis; for the same reason, the dental arch is not as defined as the occipital region. The foramen magnum seemingly 'closed' is a predictable flaw inherent to the photogrammetry acquisition, but does not affect the general reconstruction, given also the fact that the foramen magnum margin is among the zones in the basioccipital region of Altamura more covered by concretions (fig. 3.7b).

The acquisition of the coanae provided a good model of the supero- posterior half of the nasal cavity, while the posterior portion of the turbinates has been acquired with a notable definition (fig 3.8b).

Figure 3.7 - Digital acquisition of the front side (a) by laser scanner and rear side (b) by photogrammetry

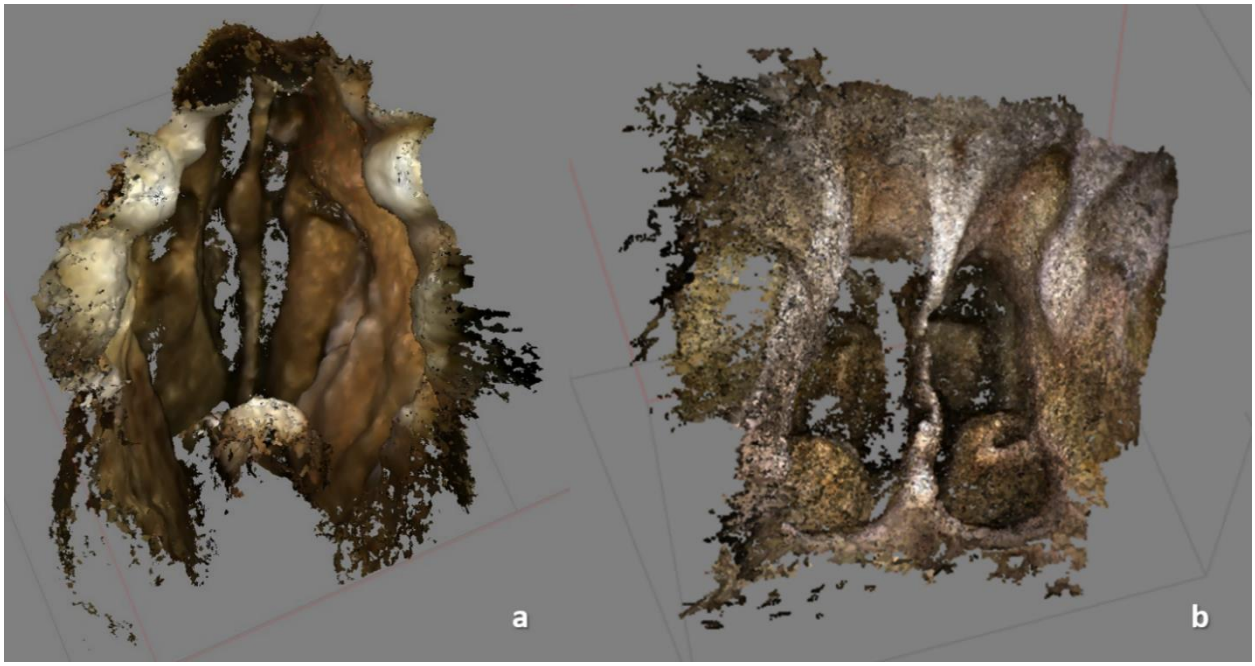

Figure 3.8 - Reconstruction of the nasal cavity (reversed): anterior portion (a), coanae (b)

3.2.2 Digital alignment

For performing the DTA on Altamura the choice of the landmarks was constrained by the anatomical points recognizable on the fossil specimens despite concretions. Any deficient landmark configuration of the reference sample was estimated by Thin-plate-spline interpolation, by using the *fixLMtps()* function (package 'Morpho'). The separate configurations of Altamura, as well as the two 3D models (FS and RS), were processed and the bi-lateral landmarks were defined; conversely, the complete configurations of the reference specimens were processed as separated in two modules each and symmetrized.

The DTA performs an analysis of the Procrustes distance of the specimens from the reference sample, based on the shape of both the FS and RS. It was also calculated the Euclidean distance (mm) of each specimen from Altamura on the basis of the separate configurations and were identified those characterized by the minor morphological distance. The results are reported in detail in figure 3.9 (Procrustes distance) and table 3.2 (Euclidean distance).

The morphologically closest specimen to Altamura resulted to be SH5, followed by three 'classic' Neanderthals - respectively La Chapelle, La Ferrassie and Guattari - and by a discontinuity of the curve; after this gap are respectively Amud and Scp1 and lastly the other *H. heidelbergensis* followed by modern humans.

Four different reconstruction were performed, based on the four closest specimens, plus one based on a 'consensus' of the three 'classic' Neanderthals (figs. 3.10 – 3.14).

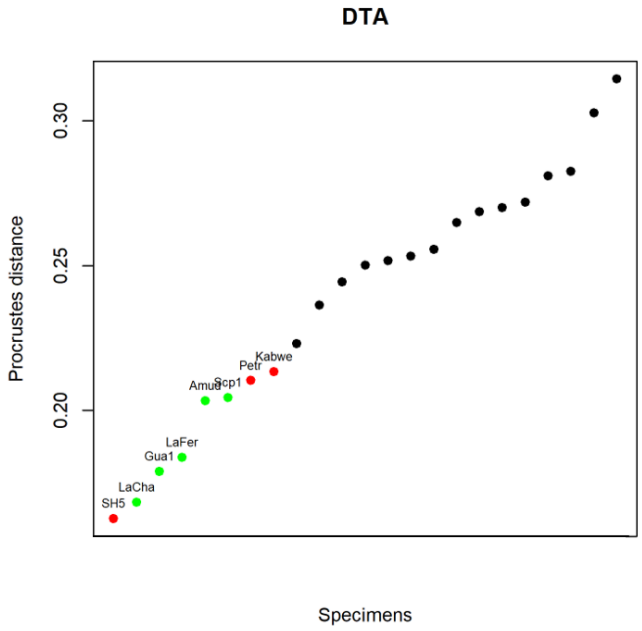

Figure 3.9 - Procrustes distance between Altamura and the reference sample. In red, Mid-Pleistocene humans; in green, Neanderthals; in black, modern humans

Table 3.2 - Euclidean distance of the reference sample from Altamura

SPECIMEN	EUCLIDEAN DISTANCE (mm)
SH5	105.37
La Cha	120.29
La Fer	128.67
Gua	129.15
Scp1	142.89
Pet	143.62
Amud	148.98
BH	150.44
ULAC012	173.93
ULAC039	191.88
ULAC060	195.95
ULAC953	198.58
ULAC019	200.48
ULAC909	201.96
ULAC057	205.89
ULAC904	211.82
ULAC033	213.03
ULAC013	215.98
ULAC066	225.38
ULAC920	225.65
ULAC954	233.79
ULAC016	245.80
ULAC955	249.36

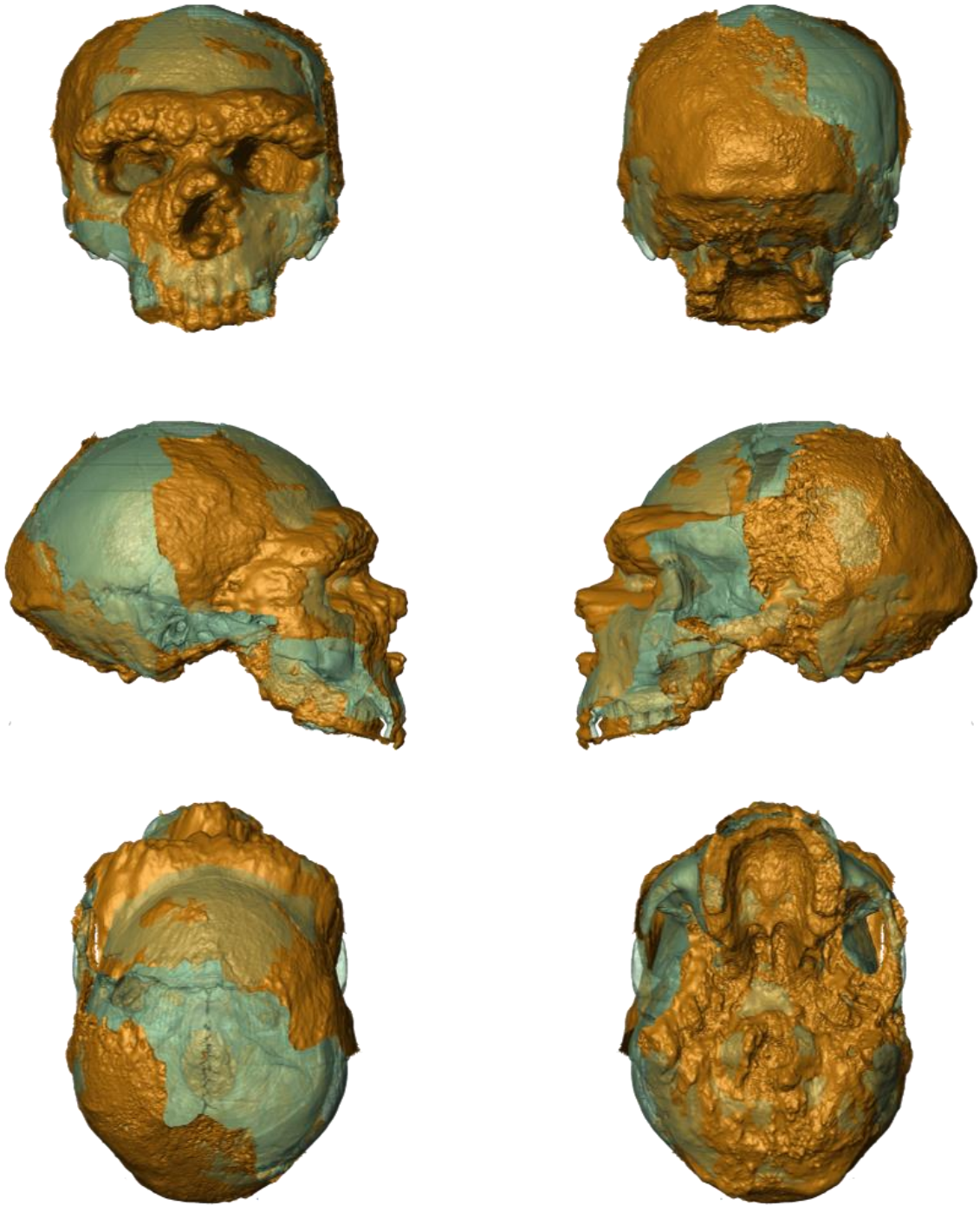

Figure 3.10 - Altamura reconstruction on SH5 (light blue)

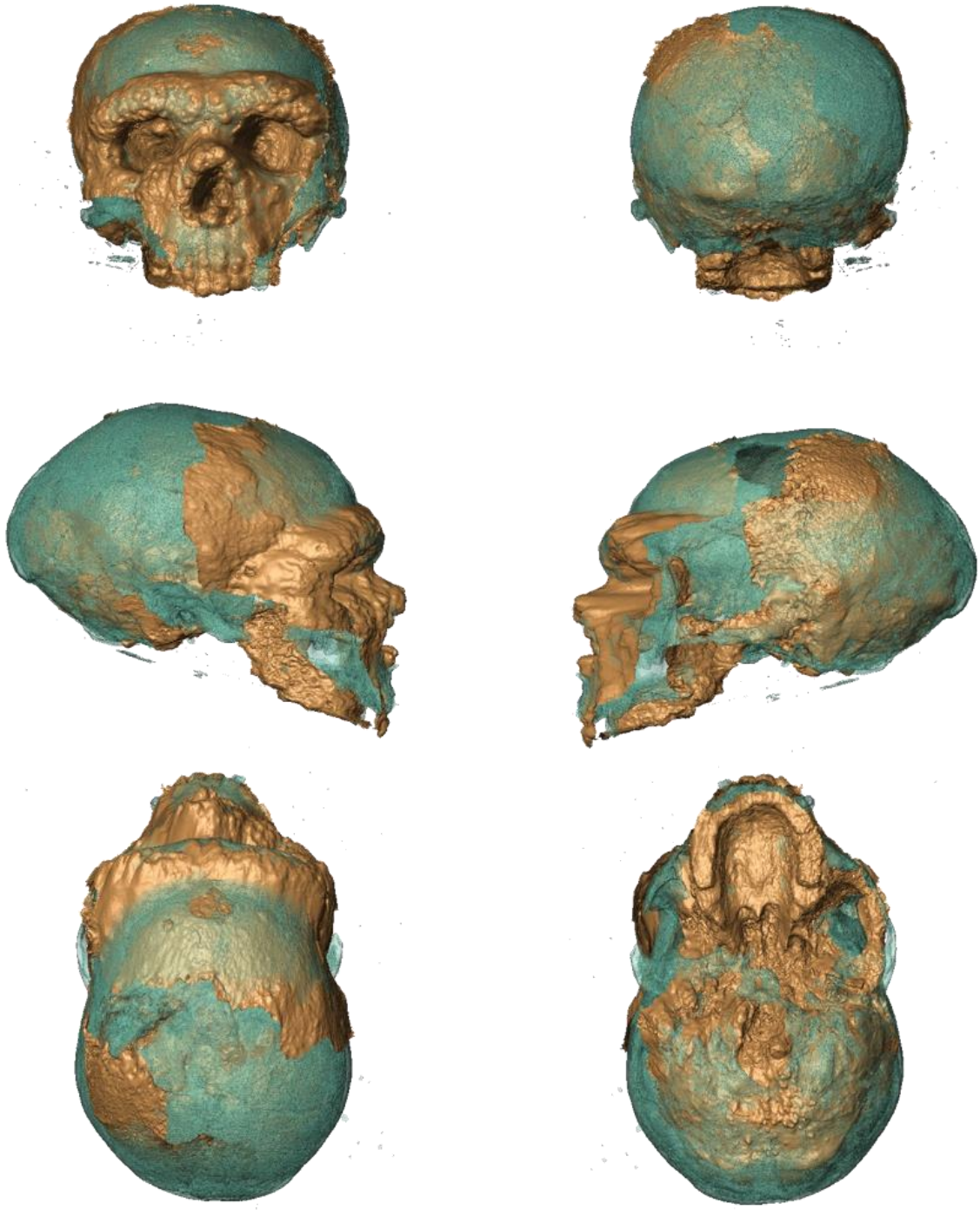

Figure 3.11 - Altamura reconstruction on La Chapelle (light blue)

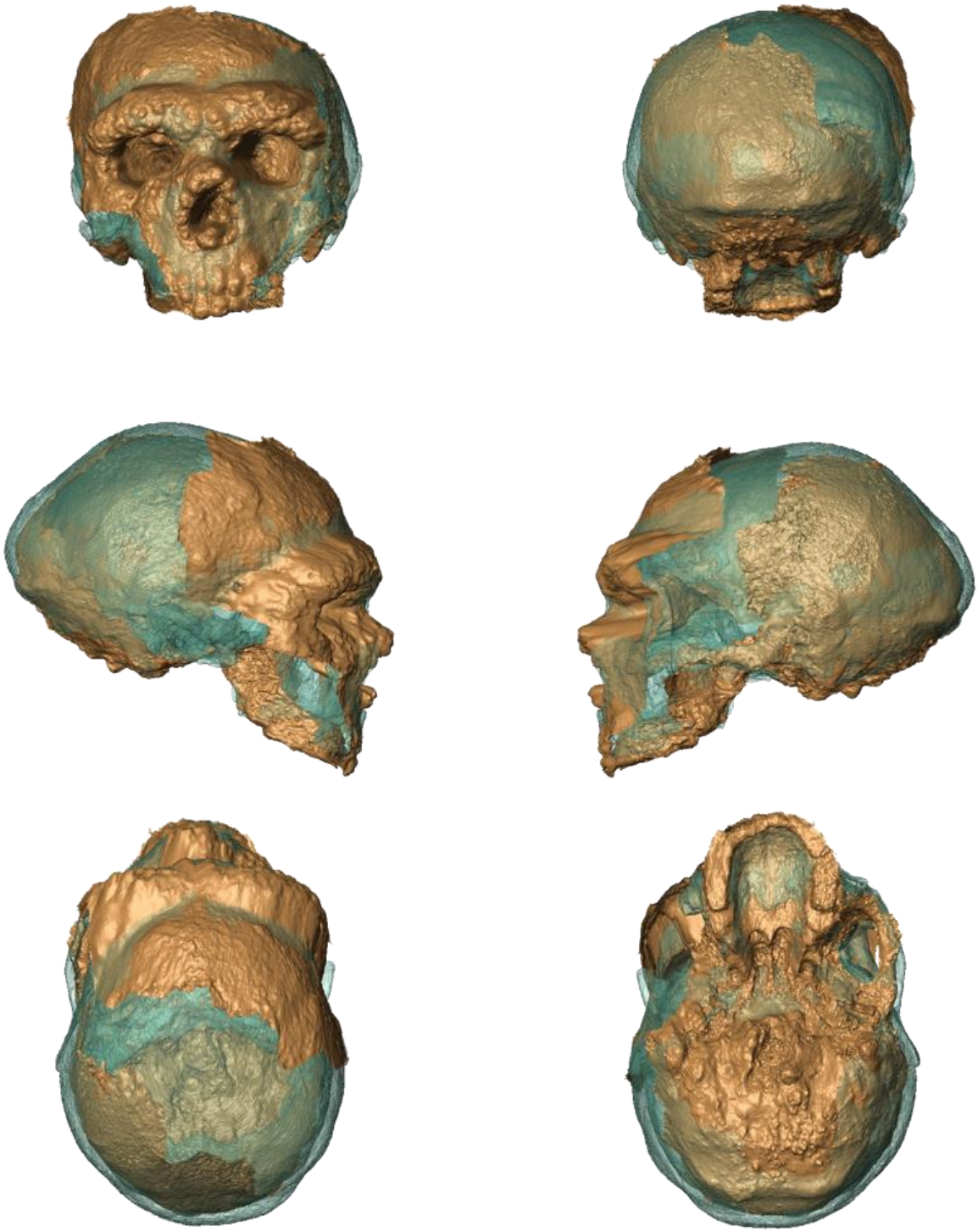

Figure 3.12 - Altamura reconstruction on Guattari 1 (light blue)

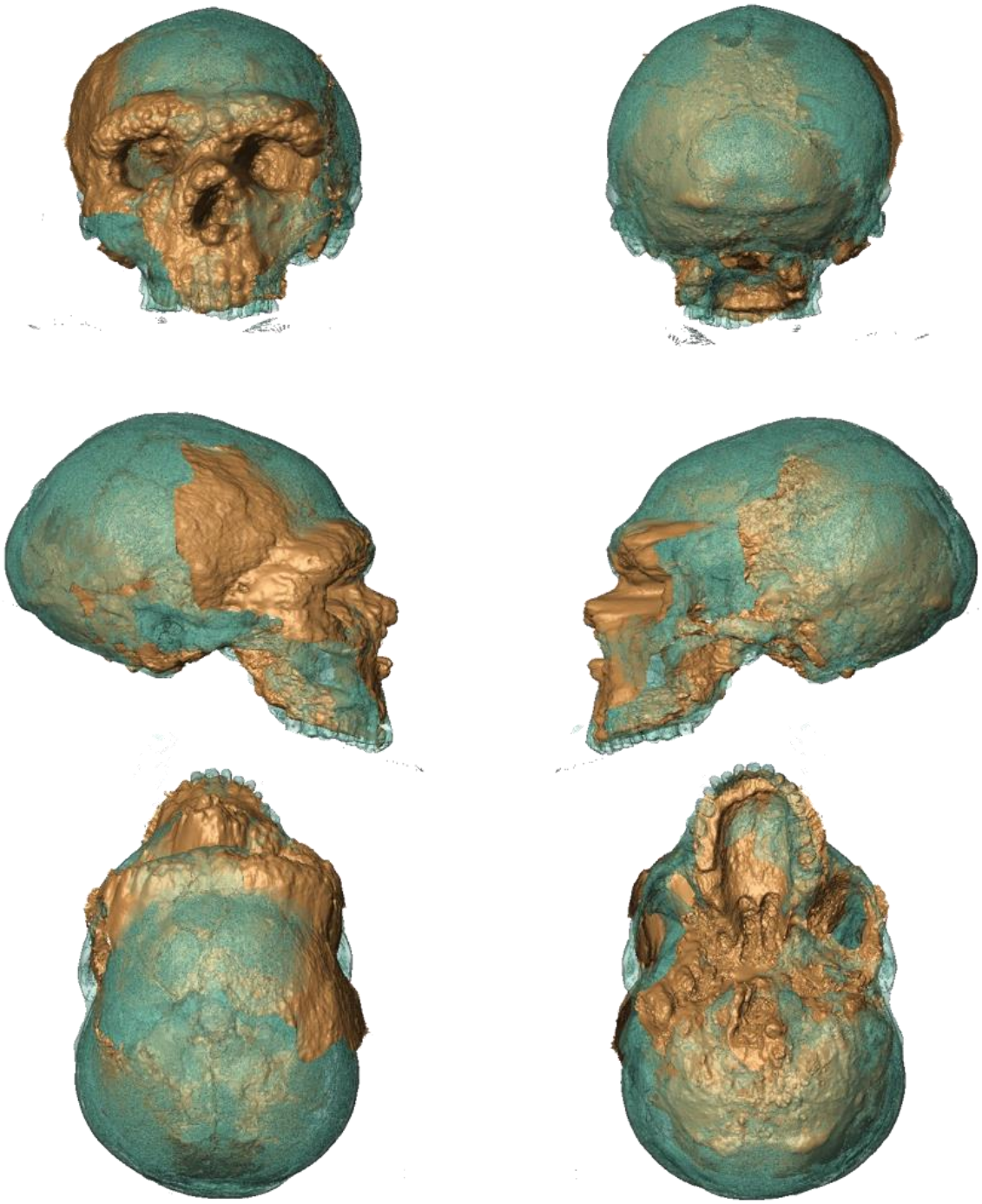

Figure 3.13 - Altamura reconstruction on La Ferrassie (light blue)

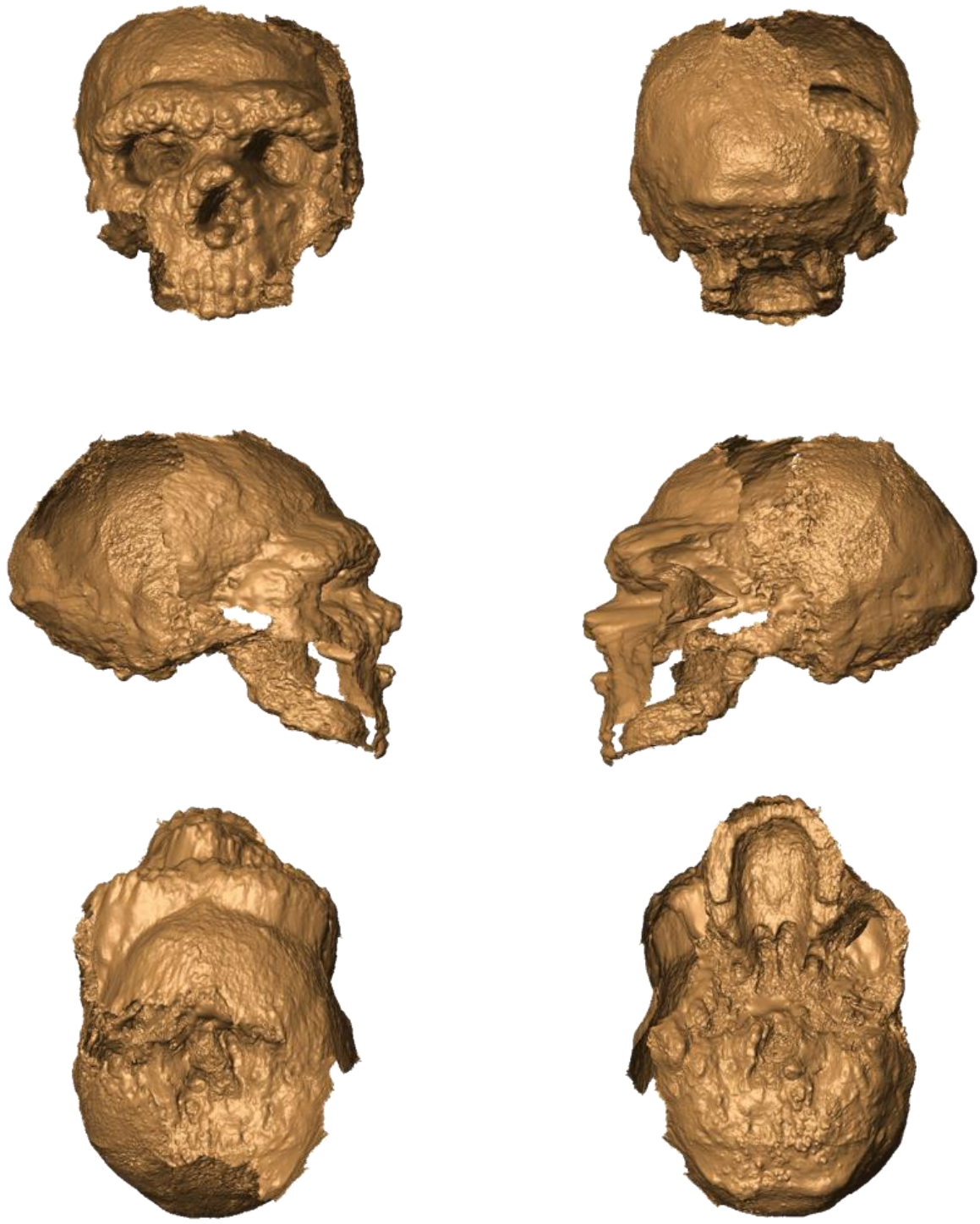

Figure 3.14 - Altamura aligned on a consensus shape of 'classic Neanderthals

A PCA was performed on the whole sample, including the reconstructions (fig. 3.15); since the presence of the five reconstructions could have conditioned the covariance matrix, another PCA was performed by predicting the presence of the reconstructions (fig. 3.16), for which the eigenvalues are reported in table 3.3. The shape variations for the entire configuration in the first two components are presented in figure 3.17.

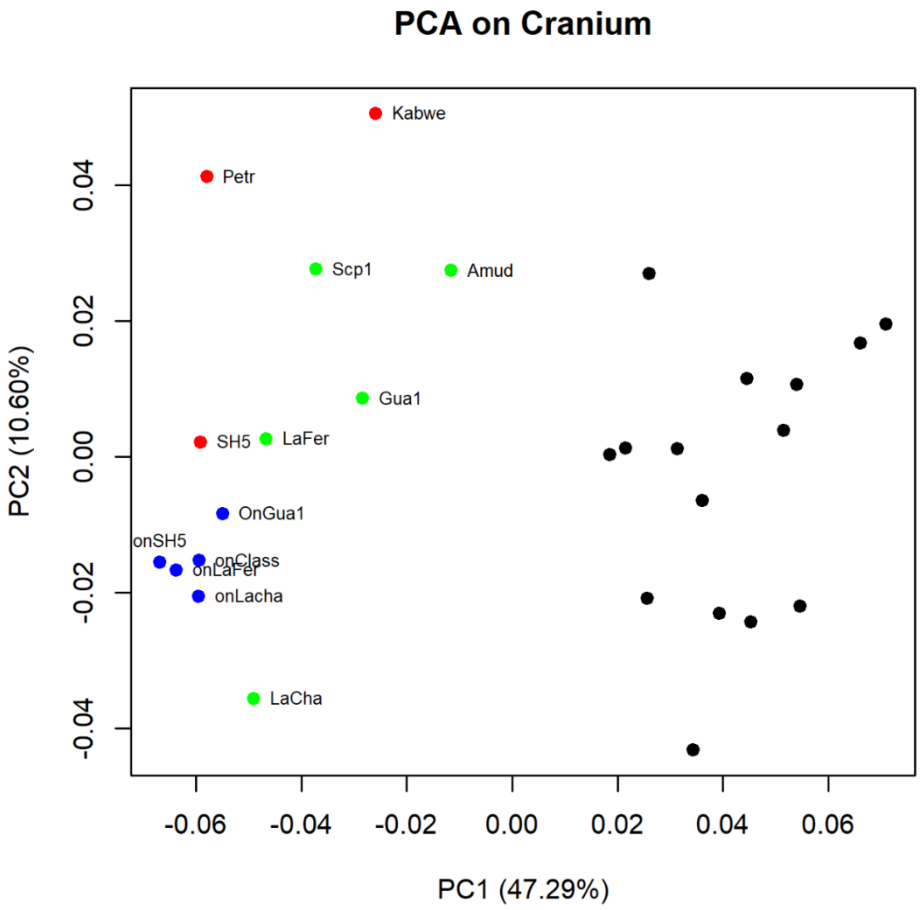

Figure 3.15 - PCA analysis including the aligned reconstructions (blue); in green, Neanderthals; in red, Mid-Pleistocene humans; in black, modern Europeans

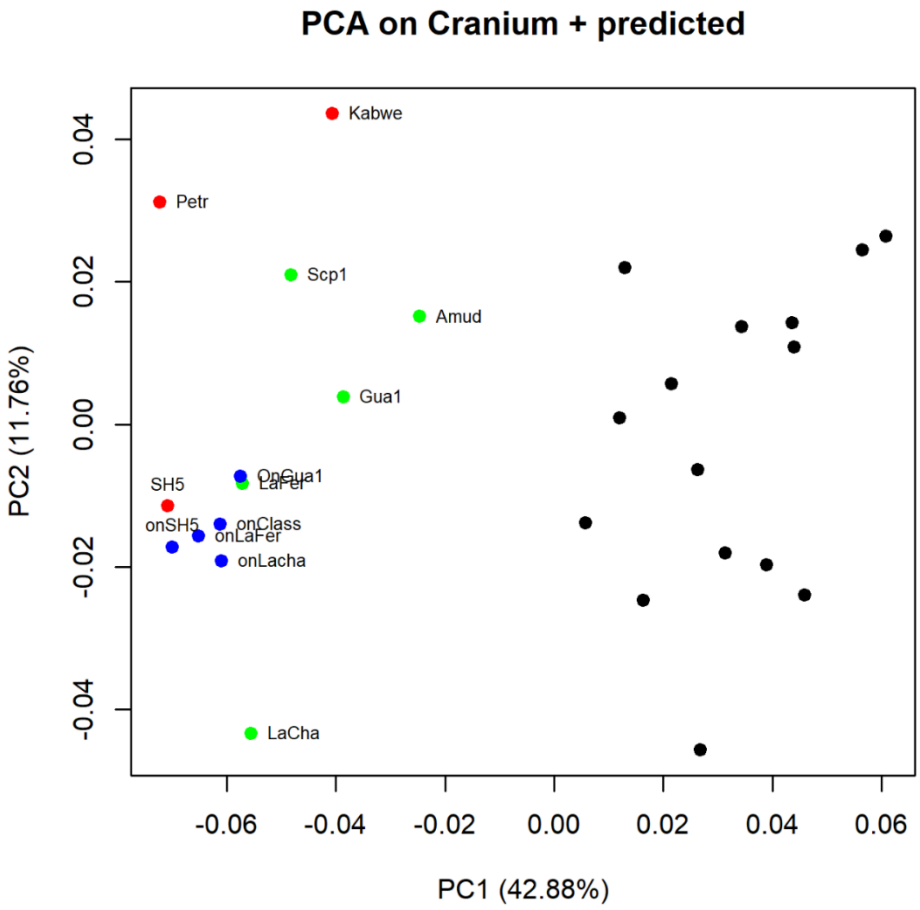

Figure 3.16 - PCA analysis including the predicted aligned reconstructions (blue); in green, Neanderthals; in red, Mid-Pleistocene humans; in black, modern Europeans

Table 3.3 - Eigenvalues from principal components analysis of DTA including the reconstructions (the farthest reconstructions are predicted). Are reported the first 11 PCs, accounting for more than 90% of variability

PC	EIGENVALUES	VARIANCE (%)	CUMULATIVE (%)
1	4,53	42,88	42,88
2	2,37	11,76	54,63
3	2,05	8,74	63,38
4	1,69	5,95	69,32
5	1,63	5,57	74,89
6	1,28	3,44	78,33
7	1,22	3,12	81,45
8	1,12	2,60	84,05
9	1,10	2,54	86,59
10	0,99	2,05	88,64
11	0,94	1,83	90,47

The PCA clearly shows a separation of the modern humans from the fossils along the PC1, respectively clustering at positive and negative values. From the shape variations can be gathered that the fossils are characterized by a general lowering of the neurocranium and the emergence of mid-facial prognathism.

The group of fossil humans appears to divide slightly along the PC2, with SH5 falling within the Neanderthal variability. The second component records the height of the face, with an increase in the flexion of the upper nasal region in correspondence with the negative values; an increased flexion of the basioccipital region can be seen in correspondence of the positive values, matched by a flattening of the occipital squama.

For their rates of expression of these morphological variations, both the reconstructions - and SH5 as well - fall within the 'classic' Neanderthals cluster.

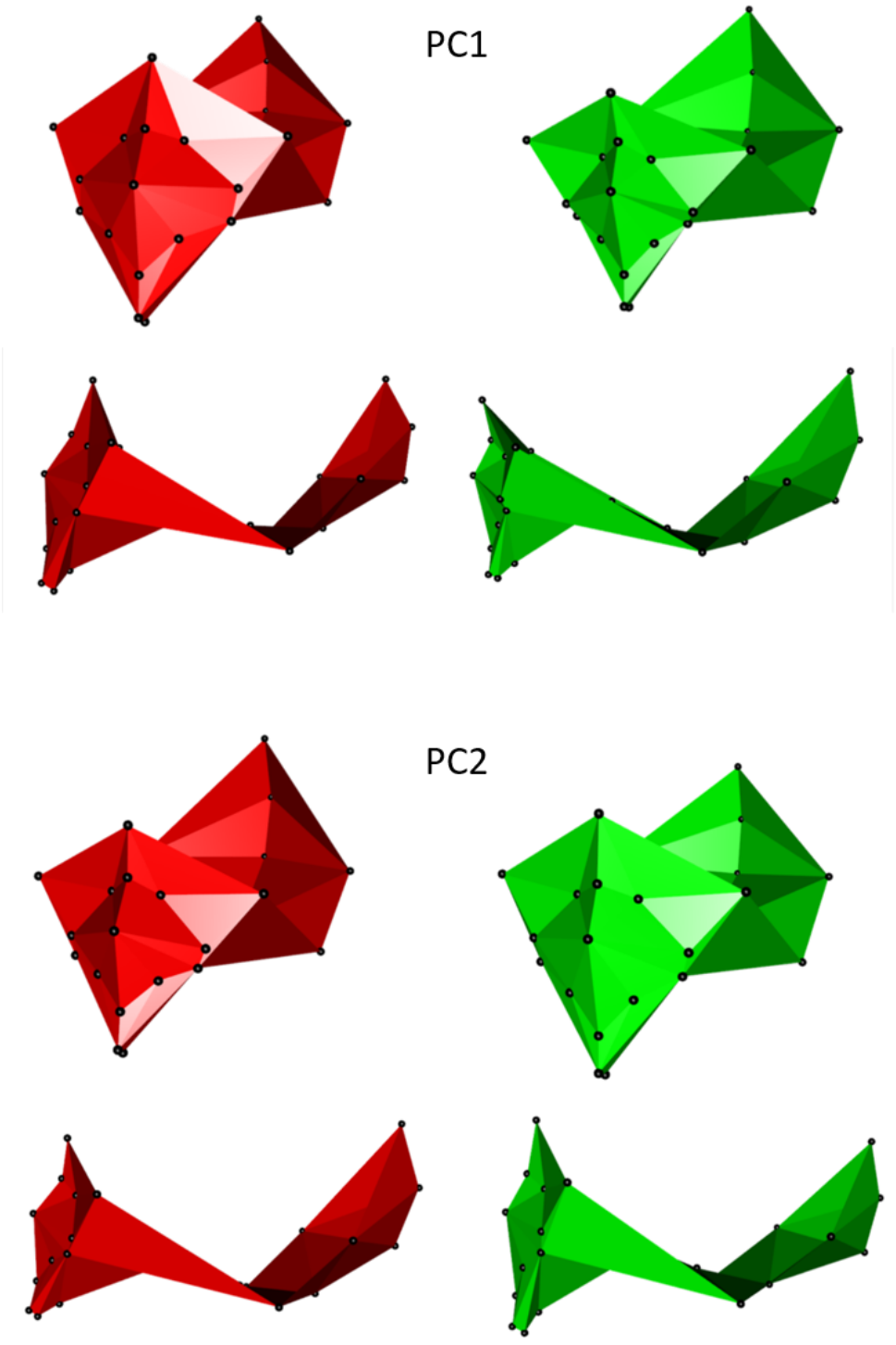

Figure 3.17 - Shape variations for DTA; PC1 (above), PC2 (below) In red, negative values; in green, positive values

3.2.3 'combin3D' analysis

To apply the *combinland()* tool and perform the analysis by combining the 3D configurations of the two districts, were used the same landmark configurations used for the DTA. These underwent to Procrustes registration separately (function *procsym()* of the package 'Morpho'). A PCA analysis has been thus performed (fig 3.18); the first two PCs resulted to account for more than 50% (table 3.4)

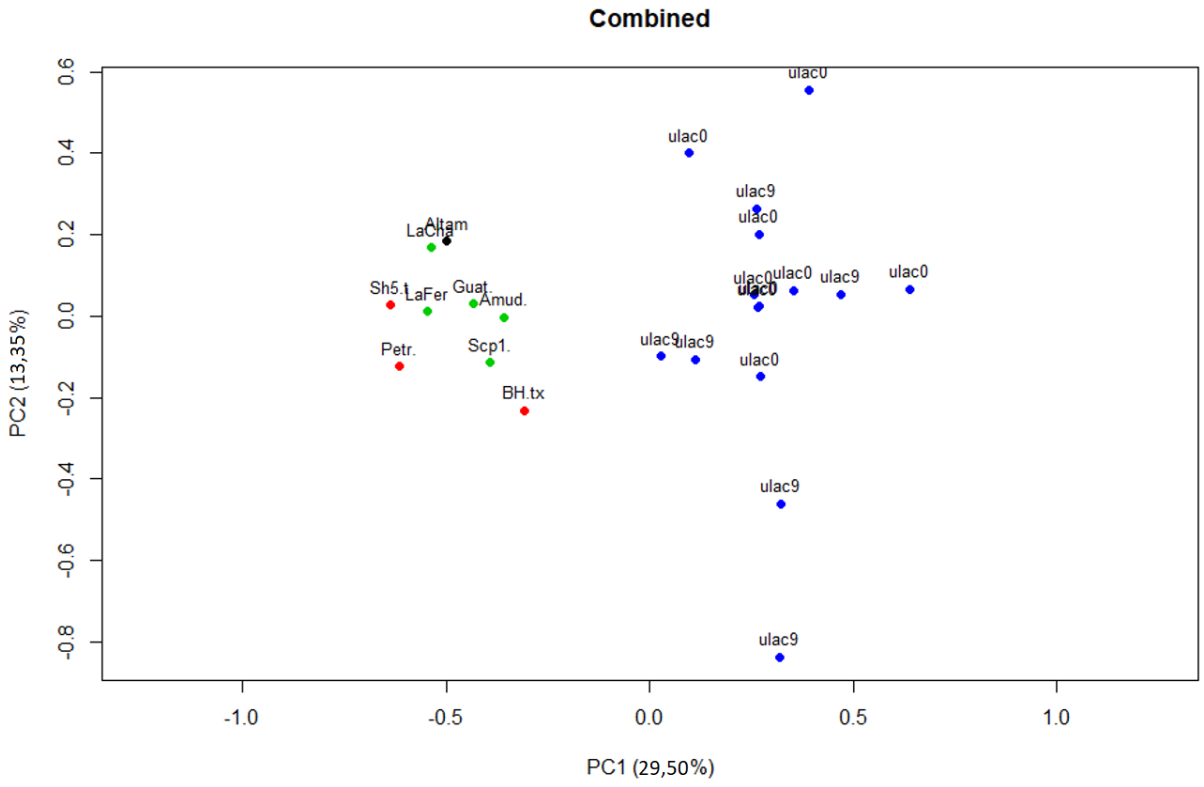

Figure 3.18 - PCA analysis performed with the combinland tool. In black, Altamura; in green, the Neanderthals; in red, the Mid-Pleistocene humans

Table 3.4 - Eigenvalues from principal components analysis of 'combin3D'. Are reported the first 12 PCs, accounting for more than 90% of variability

PC	EIGENVALUES	VARIANCE (%)	CUMULATIVE (%)
1	40,34	29,5	29,5
2	27,13	13,35	42,84
3	22,38	9,08	51,92
4	19,53	6,91	58,83
5	18,83	6,43	65,26
6	16,83	5,13	70,4
7	15,88	4,57	74,97
8	14,42	3,77	78,73
9	13,78	3,44	82,18
10	12,8	2,97	85,15
11	12,27	2,73	87,88
12	11,26	2,3	90,17

The plot presents a well distinct grouping of respectively modern and fossil humans; the latter appear strongly clustered, with no clear internal separations except for a slight trend along the PC2, determining for *H. heidelbergensis* to be at the inferior limit of the cluster.

Lastly, the shape variations were calculated for each configuration along the first two PCs (fig. 3.19).

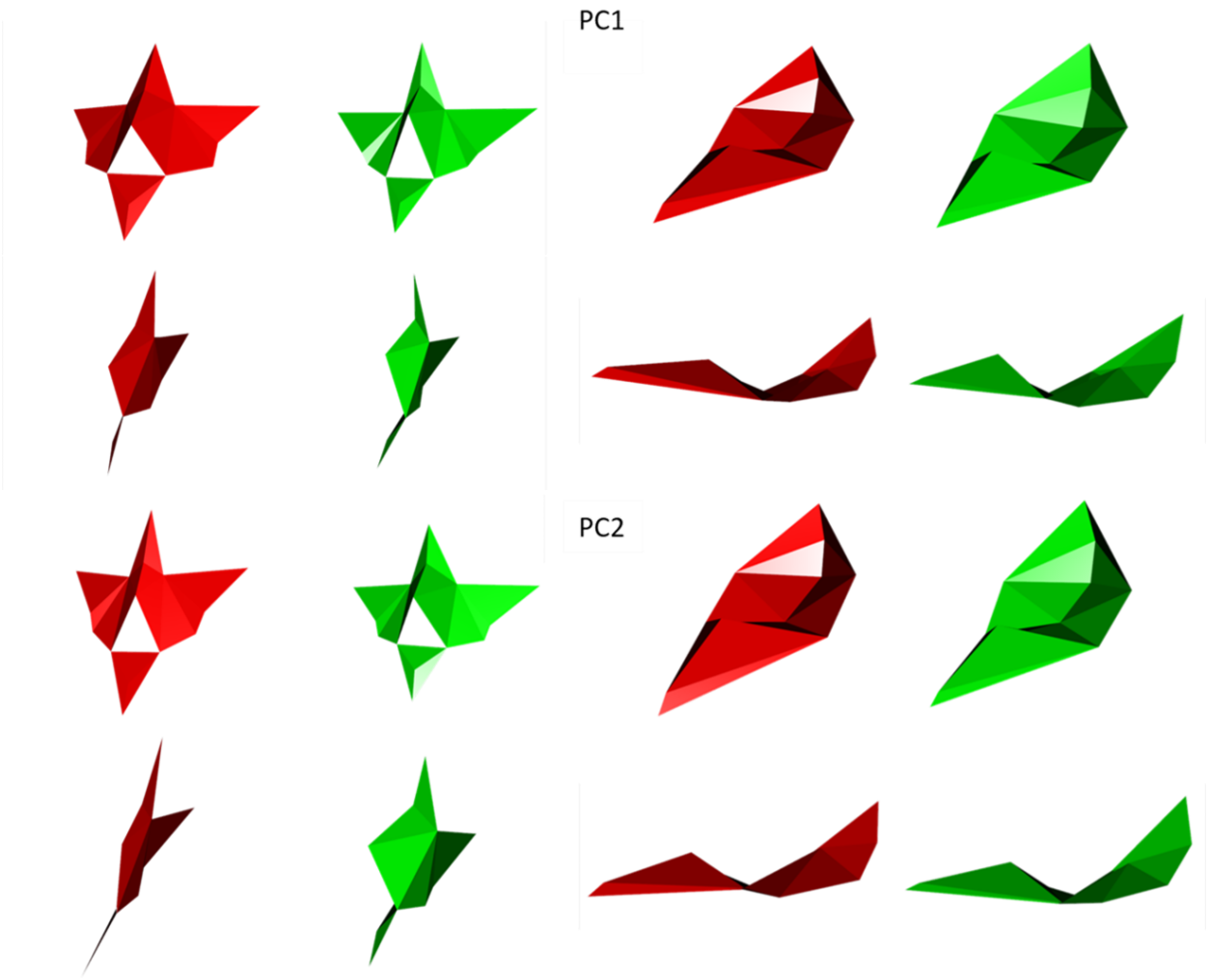

Figure 3.19 - Shape variations of the two separate sides: PC1 (above), PC2 (below). In red, negative values; in green, positive values

While the shape variations along the PC1 are self-evidently displaying the major morphological differences among modern humans and the rest of the sample (fig. 3.18), according to the abrupt separation along the component, it is interesting to see how, although separated, the shape variations along the PC2 are similar to those obtained by the analysis of the DTA: the main differences among *H. neanderthalensis* and *H. heidelbergensis* faces can be recorded at the level of *nasion*, while in the cranial base concern the flexion of the palate and of the occipital squama.

3.2.4 Reconstruction of the nasal cavity

The nasal cavity was reconstructed by assembling the two models - anterior part and coanae - onto the SH5-based reconstruction of Altamura. The anterior portion has been aligned on the reconstructed cranium by the function *rotmesh.onto()* of the Morpho R package by using a landmark configuration built on 'homologous' concretions located in the nose opening and recognizable on both the surfaces; the same function was used to align the posterior portion and the coanae, by using, in this case, anatomical points (see figure 2.3).

The reconstructed inner portions seem very similar to those of a modern human in their general organization and lack the presence of a derived autapomorphy like that recognised by Schwartz and Tattersall (2002). The reconstruction is presented in figure 3.20.

A TPS warping from a modern human inner nose was eventually performed, by using a configuration of anatomical points recognizable in the inner nose of Altamura; this procedure, carried out by the function *tps3D()* of the package Morpho, consists in the warping by TPS of a 3D mesh from a starting configuration to a target one. The warping is intended to provide a proxy for the gaps in the reconstruction of the Altamura nose, as well as a check for differences and/or anomalies in respect to a modern human nose.

The general morphology of the nasal cavity in Altamura appears stretched antero-posteriorly and supero-inferiorly, in respect to that of the modern human: by the TPS warp of modern human soft tissues, the turbinates appear slightly shorter, medially ticker and more angled in respect to the nasal cavity (fig. 3.21).

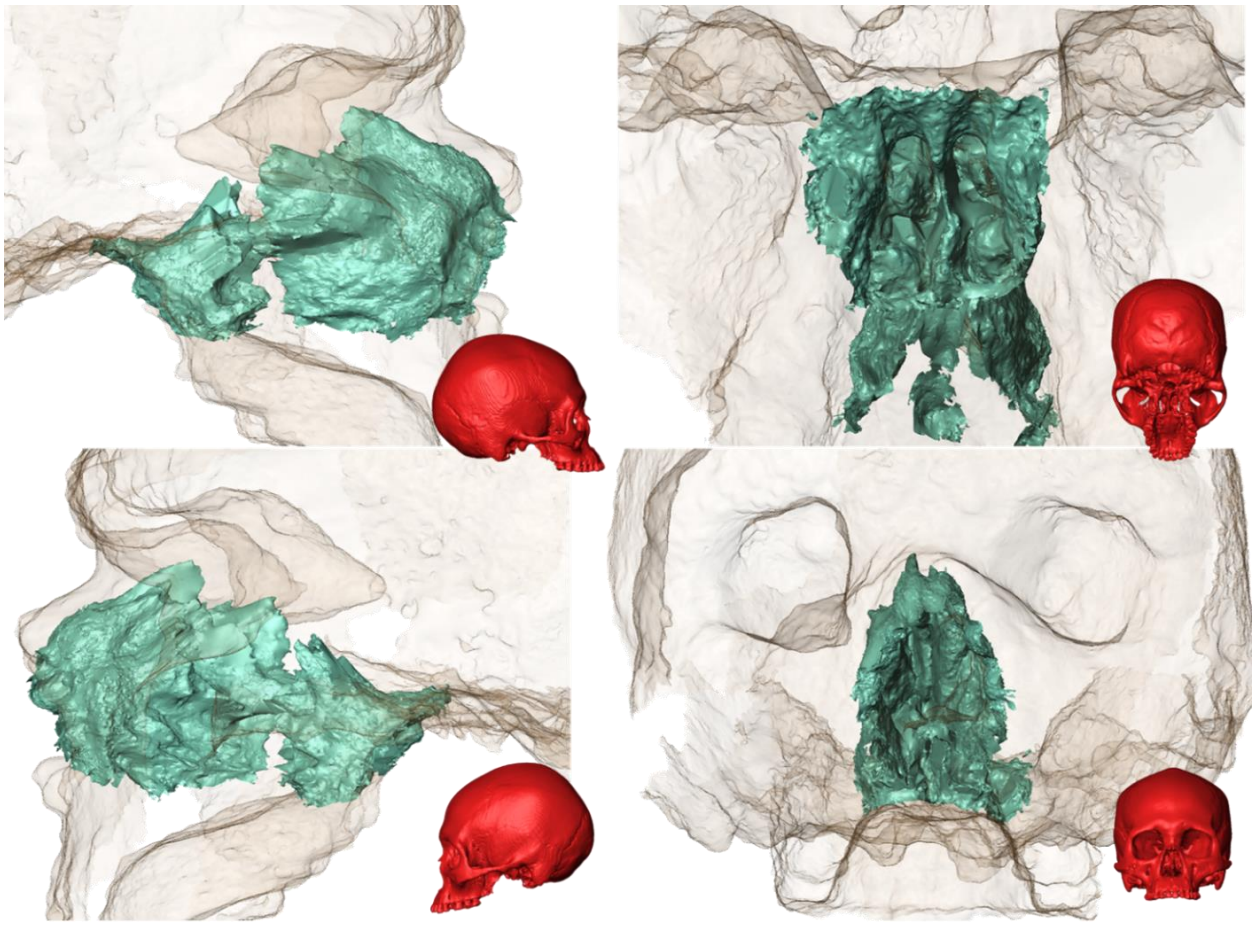

Figure 3.20 - Reconstruction of the nasal cavity of Altamura. In transparent brown, the reconstruction on SH5. The skulls in red indicate the norms

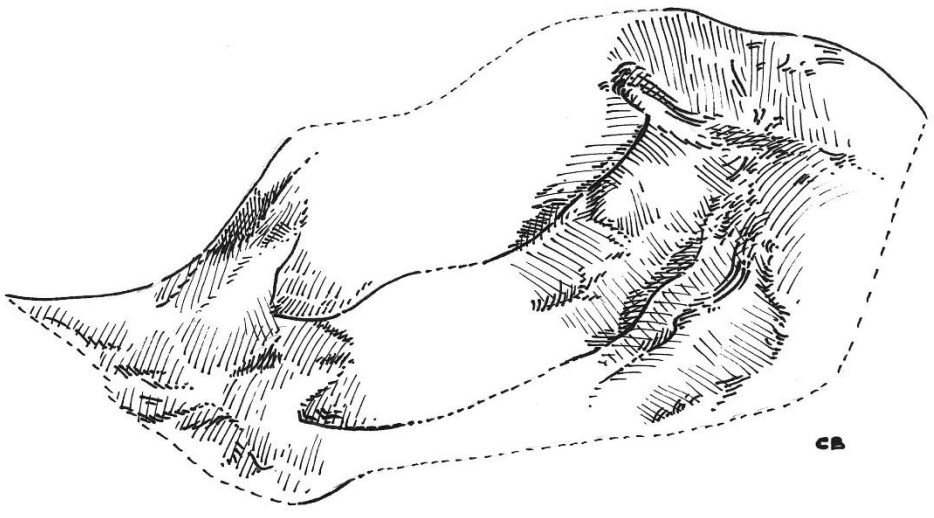

3.21 - Graphic representation of the nasal cavity of Altamura, left side, section parallel to the vomer. The dotted lines in the middle and at the bottom represent the unreconstructed portions. Drawing of the author

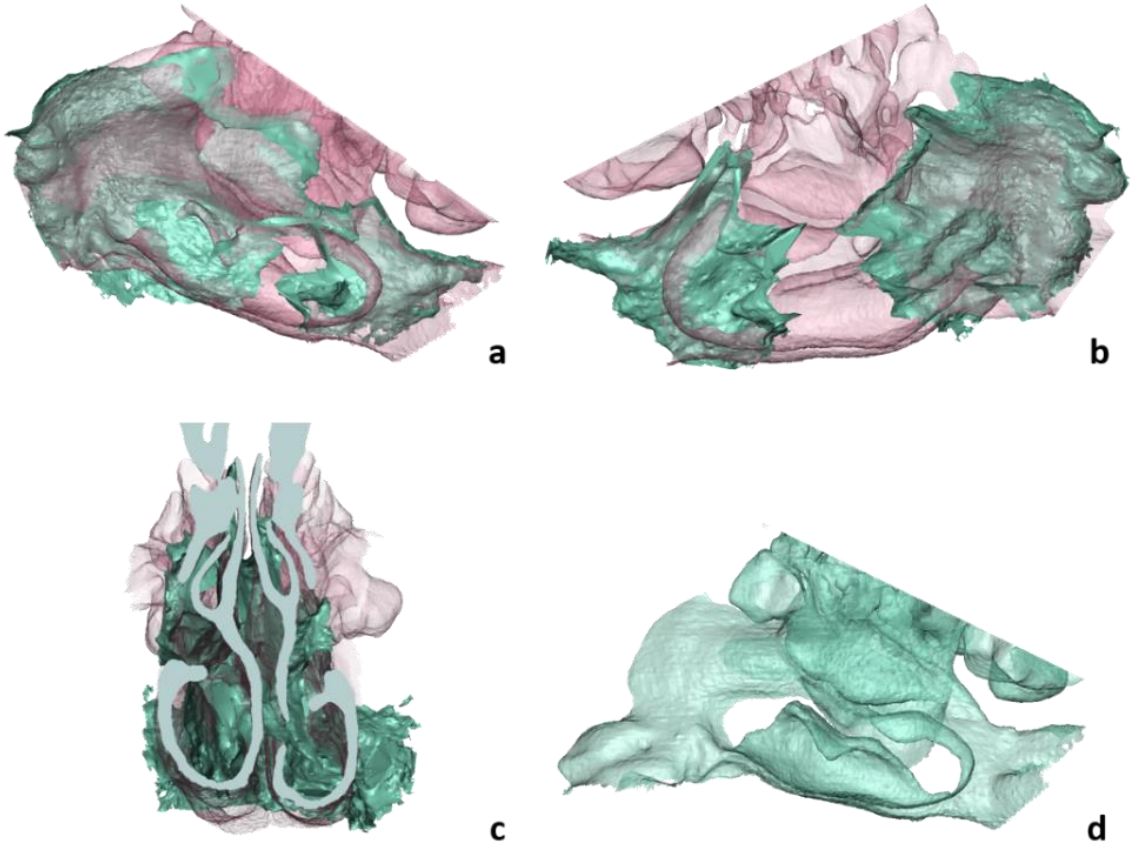

Figure 3.22 - Modern human nose (pink) warped on Altamura (green). ***a:*** *right lateral,* ***b:*** *left lateral (sections parallel to the vomer);* ***c:*** *coronal section of the nasal cavity (medial);* ***d:*** *warped modern human nose (right lateral section)*

4 DISCUSSION

This thesis has a manifold purpose. First, it introduces new methodologies aimed at overcoming issues related with the morphometric study of fossil and extant species; second, it describes some solutions for the digital acquisition applied to a specimen available only *in situ*, in a problematic environmental context as the Lamalunga Cave is; lastly, it provides a first morphological and comparative study on the unique - but still overlooked - specimen known as 'Altamura Man' (or, more simply, Altamura), beside presenting, through this specimen, the first characterization and reconstruction of the internal nose of the Neanderthals.

The approach used was that of Geometric Morphometrics (GM) and the data were processed in R statistical environment.

The cranium of Altamura is still embedded in karstic concretions inside the cave, thus some of the internal regions of the facial skeleton (e.g. the maxillary sinuses) were not available. Still, it was relevant to take these inner cavities into account for a study focused on the facial skeleton of Neanderthals. For this purpose, it was used a 2D GM approach.

Concerning the 2D analysis of the maxillary sinuses (figure 3.1), the first aspects to discuss is the variability of the Mid-Pleistocene humans (although represented by only three specimens): the width of the related cluster seems to reflect in fact a relatively higher variability of the group, if compared to the cluster of the Neanderthals, which reflects a less variable morphology.

Taking into consideration the principal components, the first one appears to be driven by the allometry, a variable that contributes to the clear distinction – with the expected 'exception' of SH5 - between Neanderthals and the specimens referred to *H. heidelbergensis*. By looking at the distribution of these individuals, it becomes clear how

much the morphology of the inner structures can represent a further source of information, with a consistent diagnostic value, supporting and/or implementing the data coming from the external cranial morphology. A proper example is represented by the Mid-Pleistocene specimens considered here. The rate of mid-facial prognathism in Petralona has been long discussed in terms of evolutionary implications, with different points of view between scholars on its 'Neanderthal-likeness' (Stringer et al., 1979; Murrill, 1981; Harvati, 2009). The facial pneumatization, on the other hand, corroborates the scenario of a stronger relationship between Petralona and Kabwe with respect to SH5, whose mid-facial prognathism is more likely to be ancestral to that of Neanderthals. On the contrary, the extreme pneumatization of Petralona, instead of being the result of a derived facial morphology – as it seems in the sample from Atapuerca Sima de Los Huesos – determines the obliteration of the canine fossa and the slight 'inflation' of the infraorbital plate in a still generalised facial pattern, as proposed by Rak (1986). With this scenario is consistent the distribution of Mid-Pleistocene humans along the PC1 (Figure 3.1), in which SH5 falls at the limit of the Neanderthal cluster, while Kabwe and Petralona express respectively higher levels of allometry, with the latter representing an 'extreme' condition. Such condition determines a peculiar facial morphology that can be put in relation with the Neanderthal mid-facial prognathism, if seen only from the 'outside'.

The modern humans also spread along the PC1 accordingly with allometry: females, in fact tend to fall roughly along the extremely negative values of the principal component, suggesting a certain rate of sexual dimorphism that can be recorded in the sinus profile. This factor, not investigated here, seems to contribute to the greatest part of the variability in modern humans, while another driving factor appears to be the geographical origin, through a possible adaptative pressure on the face. Geographical factors seems to be at the basis, in fact, of the variation of the modern humans along the PC2: it is interesting to point out that, although densely grouped, the less 'cold-adapted' humans (i.e. Africans and aboriginal Australians) tend – with some exceptions - to fall

in the upper part of the cluster, across the neutral to positive values of the PC2, while the cold-adapted ones tend to spread below.

At the same time, Neanderthals cluster across the extreme positive values of the PC2. This suggest that the shape of the sinuses may not be similarly influenced by climatic factors - at least in Neanderthals - or that, otherwise, different morphologies lead to different solutions in response to the same adaptative pressure; an 'Ockham's razor'-based approach would suggest that, more simply, maxillary sinuses variations follows those affecting the external facial morphology.

For what concerns the shape variations, the component mostly defining a 'Neanderthal profile' resulted to be the second one, related with the antero-posterior elongation of the sinus shape, accompanied by the presence of a medial-anterior 'compartment' already recognizable – although with a different shape - in the more archaic SH5. The analysis suggests that La Chapelle may represent an exception, probably due to the incompleteness of the sinuses – with the posterior portion almost absent and thus subject to a strong profile approximation – and because of pathological reasons as the notable dental resorption: several studies found a relation between dental conditions and modifications of sinuses (Rogers and Waldron, 1989; Soikkonen and Ainamo, 1995; Abrahams and Glassberg, 1996; Dias et al., 2007) and these aspects are often taken into consideration in dental implantology (Hürzeler et al., 1996; Chiapasco et al., 2008)

It is interesting to notice how the anterior profile of the maxillary sinuses confirms that the coronal orientation of the infraorbital plate is an archaic feature present in *H. heidelbergensis* and retained in the more derived modern humans, while the Neanderthal morphology - with a more angled infraorbital plate - seems to be a derivative feature, characterising the species and already incipient in a specimen like SH5.

SH5, preluding to Neanderthals for the external morphology, displays a sinus shape consistent with this scenario (PC2), but falling at the limit of the Neanderthal cluster and at the lowest values for *H. heidelbergensis* for what concerns the allometry (PC1).

Lastly, the shape variations were defined for the specific groups to see how the mean shape of each differs from the others (figures 3.4 – 3.6): the highest difference in shape can be seen between Neanderthals and *H. sapiens*, with the more angled infraorbital margin and the backward shift of the zygomatic arch; between *H. heidelbergensis* and Neanderthals the differences are expressed by an antero-posterior elongation and a latero-lateral narrowing; lastly, the difference between *H. heidelbergensis* and *H. sapiens* seems to be only influenced by size, with a very similar mean shape, only bigger in *H. heidelbergensis*.

The results suggest that the profile of maxillary sinuses is strictly related with the external facial shape; moreover, it is highlighted how little the modern human sinus shape diverges from that of the Mid-Pleistocene humans of the sample, while the Neanderthal profile is the most derived, being characterised by a significant rotation of the infraorbital plate - which reaches a sub-parallel orientation in respect to the sagittal plane - matched by an antero-posterior 'stretching' mainly expressed by an anterior projection of the nasal margin of the sinuses. Unsurprisingly, the Mid-Pleistocene individual most related with the Neanderthal lineage, SH5, falls close to the variability of the Neanderthals.

These results appear to be interesting even though obtained by a limited sample. While Neanderthals confirm to display a derived shape strongly characterised by a constant set of features, the most informative potential resides in the Mid-Pleistocene humans, displaying the highest morphological variability also in terms of inner structures. Unfortunately, the specimens referred to the species *H. heidelbergensis* well preserved and available are few; the specimens Bodo and Steinheim were first considered for the sample, but they appear badly distorted, to a degree that would have undermined the morphological analysis. In the case of Steinheim, the deformation of the skull still represent, in some cases, a reason of debate about its actual morphology (Arsuaga et al., 2019). The application of protocols of retro-deformation was not feasible in the case of

these specimens because their taphonomic modification is not symmetrical (Di Vincenzo et al., 2017; Profico et al., 2018a).

Other specimens that would contribute to further evaluate the evolutionary meaning of the maxillary sinuses shape are the other adult individuals from Sima de Los Huesos in which maxillary region is preserved (e.g. cranium 15, cranium 17; Sala et al., 2016); these specimens were not available at the moment of the definition of the sample, while the cranium 5 (or SH5) was already available and ultimately represented one of the main subject of the present research.

As a matter of fact, SH5 revealed to be, once again, a key specimen also for the digital alignment of Altamura.

The results of the DTA, seemingly not consistent with neither chronology nor phylogeny, are conversely more interesting if read in the light of cranial morphology: the archaic features of Altamura appear to be very similar to those of SH5, even more if looking at the neurocranium (figure 3.7, b), that displays an 'angled' coronal profile with a reduced lateral inflation (*en bombe* shape).

The RS appears thus to influence the morphological distance much; the subsequent specimens, which are all 'classic' Neanderthals, confirm that a Neanderthal morphological 'signal' is indeed present in Altamura, but the specimen appears to be strongly characterised by the morphology of neurocranium, that is also the portion less affected by the presence of concretions.

The position of Amud and Scp1 just before the phylogenetically farther Mid-Pleistocene humans (as confirmed also by the internal morphology studied in the previous section), can be explained by some peculiarities of these specimens: Scp1 represents an *unicum* because of the archaic morphology of the face, matched by a more rounded neurocranium, while Amud is an extremely encephalised and *'en bombe'*d' Neanderthal. Indeed, they both are the less complete specimens – in some of the regions of interest - and thus their position may have been more influenced by the TPS interpolation to

some extent. Nonetheless, the grouping together of these two crania would make sense in the light of the proposed phylogenetic affinity between 'early' and Near-eastern Neanderthals (Stringer, 1990; Rak, 1993; Harvati, 2015).

It can be suggested that southern Italy represented during the Pleistocene a *refugium* (Sommer and Nadachowski, 2006; Gavin et al., 2014), acting as an 'island', from the point of view of ecology and demography, and preserving archaic features in more modern populations (as has been proposed about Ceprano; Manzi, 2016; Di Vincenzo et al., 2017). This could explain how an individual that can be clearly defined as Neanderthal - both for molecular data and dating (Lari et al., 2015) - may bear features very similar to those of previous, possibly ancestral, populations (e.g. Sima de Los Huesos).

One of the main outputs of this research was to perform a 'virtual extraction' of a fossil cranium that is still unavailable to a full digital acquisition (e.g. CT scan). As described in the introduction (section 1.4.2), a further difficulty in digitising the specimen was represented by the flowstone enclosing it; a digital protocol to 'reassemble' the two halves – treated as two fragments of a disassembled skull – was designed for the purpose and published (Profico et al., 2019b).

As previously described, a first passage of the DTA is the identification of the morphologically nearest references for the subsequent reconstruction. Figure 3.10 shows the two halves of Altamura (brown) as aligned on SH5 (light blue). An apparent similarity is evident in all the six norms: whereas it is self-evident that the mid-sagittal profile of the reconstruction is a result of the alignment on SH5, the most interesting features can be seen on the regions of Altamura that are complete. It is the case of the left parietal region (as seen in the posterior norm), which is almost symmetrical with the right parietal region of SH5, filling the same region that is missing in Altamura. The main differences in this profile concern the temporo-parietal junction, where Altamura displays the incipient 'inflation' that can be seen in some of the 'early' Neanderthals: this trait determines the mastoids to be sensibly shifted toward the basioccipital in a

marked difference from those of SH5, which retains a more archaic condition. Nonetheless, as appears clear from figure 3.7 (b), the mastoids in Altamura keep a notably archaic morphology, apparently being more protruding than any other Neanderthal specimen, included the chronologically 'nearest' ones, Saccopastore 1 and 2.

The facial morphology similarly shows an interesting pattern of overlapping traits, although some regions appear influenced by the presence of concretions (e.g. supraorbital arches, right infraorbital plate of Altamura) or pathologies (alveolar region of SH5); nonetheless, can be appreciated how Altamura shows receding zygomatic arches and frontal squama compared to those of SH5, whereas the occipital region shows a marked *chignon* with a well-developed suprainiac fossa. The result, by looking at the two specimens combined, is that Altamura appears as an antero-posteriorly 'stretched' variant of SH5, in a way that appears consistent with the noticeable emergence of Neanderthal traits: the anterior projection of the mid-facial portion of the face, the lowering of the cranial vault, the apparent reduction of the mastoids. It is important to notice that the symmetry with which the two portions overlap with the skull of SH5 (with the expected exception of the right infraorbital plate, presenting an accumulation of concretion) assesses the quality of both the acquisition and the digital alignment.

The most notable defect of the digital acquisition can be seen in the reconstruction on SH5, but can be best appreciated in the alignments on the 'classic' Neanderthals: the anterior portion of the right parietal – thus the most posterior margin of the FS - seems to be 'over-inflated' also when superimposed on specimens like Guattari or La Ferrassie. This is an effect due to the undercut in the most difficult area of the FS to acquire via laser scanner (see figure 1.17): the presence of the flowstone prevented to align the device with an optimal angle; this minor flow anyway does not undermine the goodness of the reconstruction, nor affected the DTA to the point to misrepresent the results (e.g. by overestimating the latero-lateral inflation of the parietals).

Figures 3.11 to 3.13 present the alignment of Altamura on three 'classic' Neanderthals, identified by the tool as the morphologically nearest references, respectively: La Chapelle, Guattari and La Ferrassie. By looking at the three reconstructions together it can be seen the evolutionary pattern of the accretion and fixation of Neanderthal features: the differences can be registered mostly on the neurocranium, which – apart from the afore mentioned flaw of the right parietal of Altamura – shows an overall enlargement more evident in the occipital squama, with the marked expression of the occipital bun. The antero-lateral shift of the infraorbital plate can also be recorded, whereas the rest of the face seems to be more 'conservative' in respect to Altamura, although the strong presence of concretions on the face does not allow a detailed definition of the differences.

It is interesting to notice that the basioccipital appears to be in all reconstruction the less changing district, consistently with its nature of region more 'stable' from an evolutionary point of view. In addition, thanks to the rendering of the reconstructions (figures 3.10 to 3.13) it can be appreciated that – in accordance with Haeckel's recapitulation theory (Gould, 1977) - the main differences between the 'classic' Neanderthals and their more archaic counterpart, Altamura, seems to express themselves by following a Neanderthal ontogenetic pattern, which sees, as proposed by Trinkaus and Lemay (1982), the posterior part of the brain as the last region in which growth happens.

A PCA was then performed to validate the reconstruction made on the best fitting specimen, that is SH5. Were added to the analysis also the other reconstructions on La Chapelle, Guattari, La Ferrassie, and the reconstruction made on the morphological consensus between all the three 'classic' Neanderthals. The first component recorded the main differences between modern humans and the other human species, consisting mainly in the rate of mid-facial prognathism and the neurocranial shape. The most interesting differences are recorded along the PC2, where in the context of a generalized archaic human shape (figure 1.9) common to the fossils, it can be appreciated a number

of differences at the level of the mid-face (flexion of the nasals following to the development of the nose for the negative values) and the occipital, with a variation concerning the presence and expression of the occipital bun.

The plots (figures 3.14 – 3.15) display how the morphology of Altamura is consistent with a Neanderthal shape, but affected by its archaic features, which are in turn consistent with those characterising SH5 that in the PCA falls – as expected – within the Neanderthal variability.

The 'combin3D' method was specifically designed to overcome possible difficulties in obtaining a 3D volume from an actual biological shape. The method can work by combining different configurations acquired both by 3D and 2D, with a variable number of landmarks. By using 'combin3D' it has been possible to look at the ensemble of the districts of study without forcing them into a reconstruction, thus allowing to put the 'plain' Altamura along the other specimens. On the other hand, 'combin3D' does not display the co-variation factors influencing the overall cranial shape.

The results are thus affected by the lack of a *datum* determined by the co-variation of the two regions; nonetheless, although with slight differences and lacking the detail of the previous analyses, they confirm the results of DTA. Although more closely clustered, the fossils show a trend in which the Mid-Pleistocene humans are roughly 'peripherical' to the cluster, along with Altamura, which confirms to have a Neanderthal morphology bearing peculiar traits.

By looking at the shape variations (figure 3.19), it can be seen how the PC1 is dominated, in the face, by the rate of flexion and thus how much the nasal bones are less protruding from a more vertical face (modern humans, positive values) whereas in fossil humans the face as a whole is more shifted anteriorly, presenting a less 'flexed' profile. The modifications in the nasal opening show a supero-inferior elongation and latero-lateral shortening towards the positive values. For what concerns the palate-basioccipital, the shape variations show mostly the apparent elongation of the

basioccipital, and its general shortening in the extremely positive values, related with modern humans. The combination of the two put two *H. heidelbergensis* – SH5 and Petralona – at the negative extreme of the fossil cluster and, interestingly, Kabwe (BH) shifted towards H. sapiens; Altamura falls in the middle values of the cluster, between the Neanderthals. On the other hand, the shape variations recorded on the PC2, show modifications in the relative rate of mid-facial prognathism – expressed here by the angle supra-glabellar depression-*nasion-rhinion* – which seems to increase towards the positive values; by looking at the trend in the fossil subsample, this is more interesting as SH5, again, falls among the Neanderthals. In the palate-basioccipital, the shape variations relative to the PC2 show slight changes in the flexion of the basioccipital.

The results of the combin3D analysis are similar to those of the DTA: the specimens more morphologically relatable to Altamura are SH5 along with La Chapelle, Guattari and La Ferrassie. The only difference between the results of the two analyses is that SH5 falls farther, while La Chapelle appears to be the more similar, from the plot.

Can be suggested that this is a 'secondary' effect of the recombination of the reference sample in two separate configurations by the *combinland()* tool: the missing information from the covariation of the two parts of the crania gives as a result a 'turnover' between SH5 and La Chapelle; at the same time is confirmed the validity of the *combinland()* tool as a proxy for analysis on difficult samples, as the rest of the fossils fall in the plot consistently with the results obtained by the DTA.

The reconstruction of the nasal cavity represented a case study for a novel approach to digital acquisition: photogrammetry was the sole technique viable in the context; at the same time, being performed in those conditions, it was the less accurate and prone to undercut problems. Thanks to the size and mobile structure of the probes, these problems were overcome, obtaining from one side and the other of the nasal cavity two halves consistent with each other and allowing to see the inner general morphology (fig. 3.20).

The Neanderthal nasal cavity, visible for the first time in its internal structures, seems very similar to that of modern humans in its general morphology: are recognizable the three nasal conchae, oriented roughly as in modern humans and the vomer dividing the cavity. The similarities between modern human and Neanderthal nose suggests a common 'blueprint' for the internal structure of the two species; moreover, the Altamura nose may be interpreted as a 'consensus' between a strongly derived morphology – as that determined by the mid-facial prognathism in later Neanderthals – and the generalised face (Rak, 1986) of the more archaic forms. For this reason, Altamura may reveal to be the best specimen with which try to operate a further reconstruction: to warp its nose according to cranial landmark configurations of other fossils and attempt the reconstructions of their nose.

By comparing the shape of a modern human nose with that obtained by the TPS warping of a modern human nasal cavity on Altamura, we can see that the latter is strikingly similar to the 'cold and dry' model described by Noback and colleagues (2011) and illustrated in figure 1.6: Altamura nasal cavity appears to be higher and latero-laterally narrower in respect to many modern human noses; in addition, also the midsagittal profile of the coanae appears to be less angled with the floor line of the nasal cavity. Such 'convergence' may be attributable to an adaptation resulting from the 'bottleneck' of MIS 6 (figure 1.7), that is consistent, in turn, with the dating of Altamura.

It is interesting to notice that turbinates seem to follow the general pattern of the nasal cavity, by becoming thicker supero-inferiorly, narrower latero-laterally and more angled in respect of the nasal floor; this suggests a variation only in the pattern of distribution of the epithelium, without neither apparent increase nor reduction of the surface area.

These observations contribute to shed new light on the possible adaptative changes in the nose among Mid-to-Late-Pleistocene humans; unfortunately, the incompleteness of nasal cavities in the fossil sample do not allow to clearly assess the general morphology of their noses like it was possible to do with Altamura. On the other hand, Altamura

does not display any presence of additional bony structures as those described by Schwartz and Tattersall (2002); at the same time, it seems not to exist any broken margin suggesting the loss of a similar structure due to taphonomy.

The completeness of Altamura nose can shed light on the actual presence of such structures, instead. The nasal 'rim' was clearly recognised by Schwartz and Tattersall on the Forbes' Quarry specimen from Gibraltar, for long time considered one of the last 'classic' Neanderthals, despite it was suggested to be archaic because its morphology by Condemi (1992) among others, and has been recently revised by molecular studies (Bokelmann et al., 2019) which put Forbes' Quarry among 60 to 120 ka old Neanderthals. Therefore, by looking at the preserved nose of Altamura, the existence of such structure could be put in doubt both as a plesiomorphic or as a derived trait characterising all Neanderthals.

* * *

In conclusion, this study highlighted how much a single as well as, at the same time, exceptionally preserved specimen, can provide information and data for inferences, after a study conducted only *in situ* and with surface acquisitions. In a sense, the investigation on Altamura until now 'scratched the surface', yet many and very interesting are the data obtained.

Generally speaking, Altamura provided critical information about an early stage of Neanderthal evolution and unique data on anatomical structures of this species that where unknown before.

Moreover, new tools of Virtual Anthropology were designed and presented in this work, aimed to overcome issues related with the particular conditions of study of this very peculiar specimen; these new methods can be applied on other case studies, providing useful instruments for morphological analysis.

The study of maxillary sinuses presented here applied an approach based on Rak (1986) and Heim (1989) to define a 2D 'basic shape' for Mid-to-Late Pleistocene and modern

humans: not only a basic shape species-related is recognizable, but also bears a phylogenetic meaning. The Neanderthal derived shape starts to develop in the Sima de Los Huesos sample, while the cranial derived shape of *H. sapiens* preserves an archaic morphology for the maxillary pneumatization already present in *H. heidelbergensis* specimens different from Sima de los Huesos (or, at least, from SH5). The peculiar development of the maxillary sinuses appears to follow passively the external shape of the facial skeleton, seemingly validating the hypothesis by Witmer (1999)

Interesting conclusions can also be drawn from the DTA made on Altamura: the cranium displays a Neanderthal morphology, characterised strongly by some archaic features – particularly visible in the neurocranial shape – shared with SH5, an individual belonging to a population of the Middle Pleistocene featuring a set of traits that anticipate the Neanderthal morphology (Arsuaga et al., 2014). At the same time, Altamura seems to diverge from the morphology of another 'early' Neanderthal from central Italy (Scp1) – similarly to a specimen like Ceprano, which differs from coeval representatives of *H. heidelbergensis* – by keeping ancestral characters. This suggests that southern Italy acted more than once as a *refugium*, producing isolation and subsequent retention of archaic features in the human populations of this region.

The DTA was necessary to obtain a 'virtual extraction' of the cranium and the subsequent alignment of the acquired portions of the nose, which revealed to be – as expected – different from that of modern humans, but with characters referable to a 'cold and dry' nasal pattern. In addition, DTA and the subsequent reconstruction of the nose provided the first representation of the internal nasal structures in a Neanderthal.

Altamura is still resting (let us say) in its site, but not in the same conditions that allowed its exceptional preservation; among the reasons for this, can be cited its remarkable visual appearance, which contributed to ingenerate in part of the local people suspicion and diffidence against the researchers working on – and working 'for' – the specimen, a circumstance that brought several problems in the activities and contributing to prevent so far its extraction for a proper study.

Still, the scientific and cultural potential of Altamura can be of advantage to the local population as well as to the scientific community only by extracting it from the cave, as soon as the contextual conditions will allow it.

Until that moment, Altamura may be considered among the paleoanthropological specimens that have been more studied so far in its environment of deposition and preservation; the present thesis is just one of the outputs of such a great effort.

PUBLISHED MATERIAL

Part of the subchapter 1.2 is published in:

Profico, A., Schlager, S., Valoriani, V., **Buzi, C.**, Melchionna, M., Veneziano, A., Raia, P., Moggi-Cecchi, J., Manzi, G., 2018a. *Reproducing the internal and external anatomy of fossil bones: Two new automatic digital tools.* American Journal of Physical Anthropology.

Profico, A., Bellucci, L., **Buzi, C.**, Di Vincenzo, F., Micarelli, I., Strani, F., Tafuri, M.A., Manzi, G., 2018. *Virtual Anthropology and its Application in Cultural Heritage Studies.* Studies in Conservation.

Part of subchapter 1.5 is published in:

Profico, A., Bellucci, L., **Buzi, C.**, Di Vincenzo, F., Micarelli, I., Strani, F., Tafuri, M.A., Manzi, G., 2018. *Virtual Anthropology and its Application in Cultural Heritage Studies.* Studies in Conservation.

Part of section 2.2.1 is published in:

Profico, A., Schlager, S., Valoriani, V., **Buzi, C.**, Melchionna, M., Veneziano, A., Raia, P., Moggi-Cecchi, J., Manzi, G., 2018a. *Reproducing the internal and external anatomy of fossil bones: Two new automatic digital tools.* American Journal of Physical Anthropology.

Part of section 2.2.3 is published in:

Profico, A., **Buzi, C.**, Davis, C., Melchionna, M., Veneziano, A., Raia, P., Manzi, G., 2019. *A New Tool for Digital Alignment in Virtual Anthropology.* The Anatomical Record.

Part of section 2.2.4 is published in:

Profico, A., Piras, P., **Buzi, C.**, Del Bove, A., Melchionna, M., Senczuk, G., Varano, V., Veneziano, V., Raia, P., Manzi, G., 2019. *Seeing the wood through the trees. Combining shape information from different landmark configurations.* Hystrix.

BIBLIOGRAPHY

Abrahams, J.J., Glassberg, R.M., 1996. Dental disease: A frequently unrecognized cause of maxillary sinus abnormalities? American Journal of Roentgenology.

Adams, D.C., 1999. Methods for shape analysis of landmark data from articulated structures. Evolutionary Ecology Research.

Adams, D.C., Rohlf, F.J., Slice, D.E., 2004. Geometric morphometrics: Ten years of progress following the 'revolution.' Italian Journal of Zoology. 71, 5–16.

Agostini, S., 2010. Lineamenti geomorfologici della Grotta di Lamalunga. DiRe in Puglia 2, Direzione Regionale BCA della Puglia, Bari. 17–21.

Alciati, G., Pesce Delfino, V., Vacca, E., 2005. Catalogue of Italian fossil human remains from the Palaeolithic to the Mesolithic. Istituto Italiano di Anthropologia, Roma.

Amano, H., Kikuchi, T., Morita, Y., Kondo, O., Suzuki, H., Ponce De Leõn, M.S., Zollikofer, C.P.E., Bastir, M., Stringer, C.B., Ogihara, N., 2015. Virtual reconstruction of the Neanderthal Amud 1 cranium. American Journal of Physical Anthropology.

Arbour, J.H., Brown, C.M., 2014. Incomplete specimens in geometric morphometric analyses. Methods in Ecology and Evolution.

Arbour, V.M., Currie, P.J., 2012. Analyzing taphonomic deformation of ankylosaur skulls using retrodeformation and finite element analysis. PLoS ONE.

Arsuaga, J.L., Martínez, I., Arnold, L.J., Aranburu, A., Gracia-Téllez, A., Sharp, W.D., Quam, R.M., Falguères, C., Pantoja-Pérez, A., Bischoff, J.L., Poza-Rey, E.M., Parés, J.M., Carretero, J.M., Demuro, M., Lorenzo, C., Sala, N., Martinón-Torres, M., García, N., Alcázar De Velasco, A., Cuenca-Bescós, G., Gómez-Olivencia, A., Moreno, D., Pablos, A., Shen, C.C., Rodríguez, L., Ortega, A.I., García-González, R.,

Bonmatí, A., Bermúdez De Castro, J.-M., Carbonell, E., 2014. Neandertal roots: Cranial and chronological evidence from Sima de los Huesos. Science.

Arsuaga, J.L., Martínez, I., Gracia, A., Lorenzo, C., 1997. The Sima de los Huesos crania (Sierra de Atapuerca, Spain). A comparative study. Journal of Human Evolution.

Arsuaga, J.L., Martinón-Torres, M., Santos, E., 2019. Homo steinheimensis, a comparison between the Steinheim skull and the Atapuerca Sima de los Huesos fossils. In: Proceedings of the European Society for the Study of Human Evolution 8. European Society for the study of Human Evolution, p. 7.

Aust, R., Stierna, P., Drettner, B., 1994. Basic experimental studies of ostial patency and local metabolic environment of the maxillary sinus. Acta Oto-Laryngologica.

Azzaroli, Radina, B., Ricchetti, G., Valduga, A., 1968. Note Illustrative della Carta Geologica d'Italia, Foglio 189. Servizio Geologico d'Italia. 21.

Bastir, M., O'Higgins, P., Rosas, A., 2007. Facial ontogeny in Neanderthals and modern humans. Proceedings of the Royal Society B: Biological Sciences.

Bastir, M., Rosas, A., Stringer, C.B., Manuel Cuétara, J., Kruszynski, R., Weber, G.W., Ross, C.F., Ravosa, M.J., 2010. Effects of brain and facial size on basicranial form in human and primate evolution. Journal of Human Evolution.

Bates, K.T., Falkingham, P.L., Rarity, F., Hodgetts, D., Purslow, T., Manning, P.L., 2010. Application of high-resolution laser scanning and photogrammetric techniques to data acquisition, analysis and interpretation in palaeontology. International Archives of Photogrammetry, Remote Sensing and Spatial Information Sciences. XXXVIII, 68–73.

Beaudet, A., Bruner, E., 2017. A frontal lobe surface analysis in three archaic African human fossils: OH 9, Buia, and Bodo. Comptes Rendus Palevol.

Benazzi, S., Gruppioni, G., Strait, D.S., Hublin, J.-J., 2014. Technical Note: Virtual reconstruction of KNM-ER 1813 Homo habilis cranium. American Journal of

Physical Anthropology.

Blaney, S.P.A., 1990. Why paranasal sinuses? The Journal of Laryngology & Otology.

Bokelmann, L., Hajdinjak, M., Peyrégne, S., Brace, S., Essel, E., de Filippo, C., Glocke, I., Grote, S., Mafessoni, F., Nagel, S., Kelso, J., Prüfer, K., Vernot, B., Barnes, I., Pääbo, S., Meyer, M., Stringer, C.B., 2019. A genetic analysis of the Gibraltar Neanderthals. Proceedings of the National Academy of Sciences. 116, 15610–15615.

Bookstein, F.L., 1989. Principal warps: thin-plate splines and the decomposition of deformations. IEEE Transactions on Pattern Analysis and Machine Intelligence. 11, 567–585.

Bookstein, F.L., 1991. Thin-Plate splines and the atlas problem for biomedical images. In: Lecture Notes in Computer Science (Including Subseries Lecture Notes in Artificial Intelligence and Lecture Notes in Bioinformatics). Springer-Verlag, Berlin/Heidelberg, pp. 326–342.

Bookstein, F.L., 1997a. Morphometric tools for landmark data: geometry and biology. Cambridge University Press.

Bookstein, F.L., 1997b. Landmark methods for forms without landmarks: Morphometrics of group differences in outline shape. Medical Image Analysis.

Bookstein, F.L., Schäfer, K., Prossinger, H., Seidler, H., Fieder, M., Stringer, C.B., Weber, G.W., Arsuaga, J.L., Slice, D.E., James Rohlf, F., Recheis, W., Mariam, A.J., Marcus, L.F., 1999. Comparing frontal cranial profiles in archaic and modern homo by morphometric analysis. Anatomical Record.

Borsato, A., Miorandi, R., Zandonati, M., 2010. Progeto di datazione radiometrica del reperto Neandertaliano della Grotta di Lamalunga e speleotemi associati. DiRe in Puglia 2, Direzione Regionale BCA della Puglia, Bari. 63–66.

Boyer, D.M., Gunnell, G.F., Kaufman, S., McGeary, T.M., 2016. Morphosource: Archiving and sharing 3-D digital specimen data. The Paleontological Society

Papers. 22, 157–181.

Bradtmöller, M., Pastoors, A., Slizewski, A., Weniger, G.-C., 2010. NESPOS - A digital archive and platform for Pleistocene archaeology. In: Proceedings of the Data Management Workshop. pp. 13–18.

Bruner, E., 2004. Geometric morphometrics and paleoneurology: Brain shape evolution in the genus Homo. Journal of Human Evolution.

Bruner, E., 2007. Cranial shape and size variation in human evolution: Structural and functional perspectives. Child's Nervous System.

Bruner, E., Lozano, M., Lorenzo, C., 2016. Visuospatial integration and human evolution: The fossil evidence. Journal of Anthropological Sciences.

Bruner, E., Mantini, S., Manzi, G., 2004. A geometric morphometric approach to airorhynchy and functional cranial morphology in Alouatta (Atelidae, Primates). Journal of Anthropological Sciences. 82, 47–66.

Bruner, E., Manzi, G., 2006a. Saccopastore 1: the earliest Neanderthal? A new look at an old cranium. In: Neanderthals Revisited: New Approaches and Perspectives. Springer, Dordrecht, pp. 23–36.

Bruner, E., Manzi, G., 2006b. Digital Tools for the Preservation of the Human Fossil Heritage: Ceprano, Saccopastore, and Other Case Studies. Human Evolution. 21, 33–44.

Bukreeva, I., Mittone, A., Bravin, A., Festa, G., Alessandrelli, M., Coan, P., Formoso, V., Agostino, R.G., Giocondo, M., Ciuchi, F., Fratini, M., Massimi, L., Lamarra, A., Andreani, C., Bartolino, R., Gigli, G., Ranocchia, G., Cedola, A., 2016. Virtual unrolling and deciphering of Herculaneum papyri by X-ray phase-contrast tomography. Scientific Reports. 6, 27227.

Burton, D., Dunlap, D.B., Wood, L.J., Flaig, P.P., 2011. Lidar Intensity as a Remote Sensor of Rock Properties. Journal of Sedimentary Research. 81, 339–347.

Buzi, C., Micarelli, I., Profico, A., Conti, J., Grassetti, R., Cristiano, W., Di Vincenzo, F., Tafuri, M.A., Manzi, G., 2018. Measuring the shape: performance evaluation of a photogrammetry improvement applied to the Neanderthal skull Saccopastore 1. ACTA IMEKO.

Cardini, A., 2014. Missing the third dimension in geometric morphometrics: How to assess if 2D images really are a good proxy for 3D structures? Hystrix.

Cardini, A., Elton, S., 2008. Does the skull carry a phylogenetic signal? Evolution and modularity in the guenons. Biological Journal of the Linnean Society.

Cartmill, M., Smith, F.H., 2009. The human lineage. John Wiley & Sons.

Cave, A.J.E., 1967. Observations on the platyrrhine nasal fossa. American Journal of Physical Anthropology.

Chiapasco, M., Zaniboni, M., Rimondini, L., 2008. Dental implants placed in grafted maxillary sinuses: A retrospective analysis of clinical outcome according to the initial clinical situation and a proposal of defect classification. Clinical Oral Implants Research.

Chirchir, H., Kivell, T.L., Ruff, C.B., Hublin, J.-J., Carlson, K.J., Zipfel, B., Richmond, B.G., 2015. Recent origin of low trabecular bone density in modern humans. Proceedings of the National Academy of Sciences.

Churchill, S.E., 2014. Thin on the Ground: Neandertal Biology, Archeology and Ecology, Thin on the Ground: Neandertal Biology, Archeology and Ecology.

Conde-Valverde, M., Quam, R., Martínez, I., Arsuaga, J.L., Daura, J., Sanz, M., Zilhão, J., 2018. The bony labyrinth in the Aroeira 3 Middle Pleistocene cranium. Journal of Human Evolution.

Condemi, S., 1992. Les hommes fossiles de Saccopastore (Italie) et leurs relations phylogénétiques. CNRS Editions, Paris.

Condemi, S., 1998. The Neanderthals: A cold-adapted European middle Pleistocene population? Anthropologie (1962-). 35–42.

Conroy, G.C., Vannier, M.W., 1984. Noninvasive three-dimensional computer imaging of matrix-filled fossil skulls by high-resolution computed tomography. Science (New York, N.Y.). 226, 456–8.

Conroy, G.C., Vannier, M.W., 1987. Dental development of the Taung skull from computerized tomography. Nature. 329, 625–7.

Copes, L.E., 2012. Comparative and experimental investigations of cranial robusticity in mid-Pleistocene hominins. Arizona State University.

Cunningham, J.A., Rahman, I.A., Lautenschlager, S., Rayfield, E.J., Donoghue, P.C.J., 2014. A virtual world of paleontology. Trends in Ecology and Evolution. 29, 347–357.

Dart, R.A., 1925. Australopithecus africanus The Man-Ape of South Africa. Nature 1925 115:2884.

de Azevedo, S., González, M.F., Cintas, C., Ramallo, V., Quinto-Sánchez, M., Márquez, F., Hünemeier, T., Paschetta, C., Ruderman, A., Navarro, P., Pazos, B.A., Silva de Cerqueira, C.C., Velan, O., Ramírez-Rozzi, F. V., Calvo, N., Castro, H.G., Paz, R.R., González-José, R., 2017. Nasal airflow simulations suggest convergent adaptation in Neanderthals and modern humans. Proceedings of the National Academy of Sciences. 114, 12442–12447.

de Lumley, M.-A., Bailon, S., Cauche, D., Echassoux, A., El Guennouni, K., Grimaud-Hervé, D., Hanquet, C., Khatib, S., de Lumley, H., Manzano, A., Mestour, B., Michel, V., Moigne, A.-M., Valensi, P., Voisin, J.-L., Pollet, G., Saos, T., 2018. Les restes humains fossiles de la grotte du Lazaret. Nice, Alpes-Maritimes, France. CNRS Editions.

Dean, D., Hublin, J.-J., Holloway, R.L., Ziegler, R., 1998. On the phylogenetic position of

the pre-Neandertal specimen from Reilingen, Germany. Journal of Human Evolution.

Demes, B., 1987. Another look at an old face: biomechanics of the Neandertal facial skeleton reconsidered. Journal of Human Evolution. 16, 297–303.

Dennell, R.W., Martinón-Torres, M., Bermúdez De Castro, J.-M., 2011. Hominin variability, climatic instability and population demography in Middle Pleistocene Europe. Quaternary Science Reviews.

Di Vincenzo, F., Churchill, S.E., Buzi, C., Profico, A., Tafuri, M.A., Micheli, M., Caramelli, D., Manzi, G., 2018. Distinct among Neanderthals: The scapula of the skeleton from Altamura, Italy. Quaternary Science Reviews.

Di Vincenzo, F., Profico, A., Bernardini, F., Cerroni, V., Dreossi, D., Schlager, S., Zaio, P., Benazzi, S., Biddittu, I., Rubini, M., Tuniz, C., Manzi, G., 2017. Digital reconstruction of the Ceprano calvarium (Italy), and implications for its interpretation. Scientific Reports. 7.

Dias, G.J., Prasad, K., Santos, A.L., 2007. Pathogenesis of apical periodontal cysts: Guidelines for diagnosis in palaeopathology. International Journal of Osteoarchaeology.

Diniz-Filho, J.A.F., Raia, P., 2017. Island rule, quantitative genetics and brain-body size evolution in homo floresiensis. Proceedings of the Royal Society B: Biological Sciences.

Dryden, I.L., Mardia, K. V., 2016. Statistical shape analysis, with applications in R: Second edition, Statistical Shape Analysis, with Applications in R: Second Edition.

Esteve-Altava, B., 2017. In search of morphological modules: a systematic review. Biological Reviews.

Evteev, A., Cardini, A.L., Morozova, I., O'Higgins, P., 2014. Extreme climate, rather than population history, explains mid-facial morphology of Northern Asians. American

Journal of Physical Anthropology.

Falk, D., Hildebolt, C., Smith, K., Morwood, M.J., Sutikna, T., Brown, P., Jatmiko, Saptomo, E.W., Brunsden, B., Prior, F., 2005. The brain of LB1, Homo floresiensis. Science.

Falkingham, P.L., 2012. Acquisition of high resolution three-dimensional models using free, open-source, photogrammetric software. Palaeontologia Electronica. 15, 1–15.

Ferreira, T., Rasband, W., 2012. ImageJ User Guide User Guide ImageJ. Image J user Guide.

Flottes, L., Clere, P., Rui, R., Devila, F., 1960. La physiologie des sinus (Societe Francaise D'Oto-Rhino-Laryngologie), Paris: Libraire Arnette.

Friess, M., Marcus, L.F., Reddy, D.P., Delson, E., 2002. The use of 3D laser scanning techniques for the morphometric analysis of human facial shape variation. BAR Int Series. 1049, 31–5.

Gavin, D.G., Fitzpatrick, M.C., Gugger, P.F., Heath, K.D., Rodríguez-Sánchez, F., Dobrowski, S.Z., Hampe, A., Hu, F.S., Ashcroft, M.B., Bartlein, P.J., Blois, J.L., Carstens, B.C., Davis, E.B., de Lafontaine, G., Edwards, M.E., Fernandez, M., Henne, P.D., Herring, E.M., Holden, Z.A., Kong, W. seok, Liu, J., Magri, D., Matzke, N.J., Mcglone, M.S., Saltré, F., Stigall, A.L., Tsai, Y.H.E., Williams, J.W., 2014. Climate refugia: Joint inference from fossil records, species distribution models and phylogeography. New Phytologist.

Giacobini, G., Manzi, G., 2018. Lazaret 24 and the human fossil record in Europe between MIS 7 and MIS 5: towards a re-evaluation of Homo neanderthalensis aniensis Sergi, 1934. In: de Lumley, M.-A. (Ed.), Les Restes Humains Fossiles de La Grotte Du Lazaret (Nice, Alpes-Maritimes): Des Homo Erectus Européens Évolués En Voie de Néandertalisation. CNRS Editions, Paris.

Gkantidis, N., Halazonetis, D.J., 2011. Morphological integration between the cranial

base and the face in children and adults. Journal of Anatomy.

Gorjanović-Kramberger, D., 1906. Der diluviale Mensch von Krapina in Kroatien. Ein Beitrag zur Paläoanthropologie, Studien u̇ber die Entwicklungsmechanik des Primatenskelletes, Volume II. CW Kreidel.

Gould, S.J., 1977. Ontogeny and phylogeny. Harvard University Press, Cambridge, Massachussetts.

Gower, J.C., 1975. Generalized procrustes analysis. Psychometrika.

Gunz, P., Harvati, K., 2007. The Neanderthal "chignon": Variation, integration, and homology. Journal of Human Evolution.

Gunz, P., Mitteroecker, P., Bookstein, F.L., 2005. Semilandmarks in Three Dimensions. In: Modern Morphometrics in Physical Anthropology. Kluwer Academic Publishers-Plenum Publishers, New York, pp. 73–98.

Gunz, P., Mitteroecker, P., Neubauer, S., Weber, G.W., Bookstein, F.L., 2009. Principles for the virtual reconstruction of hominin crania. Journal of Human Evolution. 57, 48–62.

Gunz, P., Neubauer, S., Maureille, B., Hublin, J.-J., 2010. Brain development after birth differs between Neanderthals and modern humans. Current Biology.

Harvati, K., 2009. Petralona: link between Africa and Europe? Hesperia Supplements. 43, 31–47.

Harvati, K., 2015. Neanderthals and their contemporaries. In: Handbook of Paleoanthropology, Second Edition.

Heim, J.-L., 1989. La nouvelle reconstitution du crâne néandertalien de la Chapelle-aux-Saints. Méthodes et résultats. Bulletins et Mémoires de la Société d'anthropologie de Paris. 1, 95–118.

Holton, N.E., Yokley, T.R., Butaric, L., 2013. The Morphological Interaction Between the

Nasal Cavity and Maxillary Sinuses in Living Humans. Anatomical Record.

Howell, F.C., 1957. The Evolutionary Significance of Variation and Varieties of "Neanderthal" Man The Quarterly Review of Biology. Source: The Quarterly Review of Biology.

Huang, H.L., Hsu, J.T., Fuh, L.J., Tu, M.G., Ko, C.C., Shen, Y.W., 2008. Bone stress and interfacial sliding analysis of implant designs on an immediately loaded maxillary implant: A non-linear finite element study. Journal of Dentistry.

Hublin, J.-J., 2005. Climatic Changes, Paleogeography, and the Evolution of the Neandertals. In: Neandertals and Modern Humans in Western Asia.

Hughes, N.C., Jell, P.A., 1992. A statistical/computer-graphic technique for assessing variation in tectonically deformed fossils and its application to Cambrian trilobites from Kashmir. Lethaia.

Huotilainen, E., Jaanimets, R., Valášek, J., Marcián, P., Salmi, M., Tuomi, J., Mäkitie, A., Wolff, J., 2014. Inaccuracies in additive manufactured medical skull models caused by the DICOM to STL conversion process. Journal of Cranio-Maxillofacial Surgery.

Hürzeler, M.B., Kirsch, A., Ackermann, K.-L., Quiñones, C.R., 1996. Reconstruction of the severely resorbed maxilla with dental implants in the augmented maxillary sinus: a 5-year clinical investigation. International Journal of Oral & Maxillofacial Implants. 11.

Ibrahim, N., Sereno, P.C., Dal Sasso, C., Maganuco, S., Fabbri, M., Martill, D.M., Zouhri, S., Myhrvold, N., Iurino, D.A., 2014. Semiaquatic adaptations in a giant predatory dinosaur. Science.

Jankowski, R., 2011. Revisiting human nose anatomy: Phylogenic and ontogenic perspectives. Laryngoscope.

Katz, S., Tal, A., Basri, R., 2007. Direct visibility of point sets. In: Proceedings of the ACM SIGGRAPH Conference on Computer Graphics.

Keir, J., 2009. Why do we have paranasal sinuses? Journal of Laryngology and Otology.

King, W.B.R., 1864. The reputed fossil man of the Neanderthal. Quaterly Journal of Science.

Kirihene, R.K.D.R.A., Rees, G., Wormald, P.-J., 2018. The Influence of the Size of the Maxillary Sinus Ostium on the Nasal and Sinus Nitric Oxide Levels. American Journal of Rhinology.

Klingenberg, C.P., 2013. Cranial integration and modularity: Insights into evolution and development from morphometric data. Hystrix.

Koca, O.L., Eskitascioglu, G., Usumez, A., 2005. Three-dimensional finite-element analysis of functional stresses in different bone locations produced by implants placed in the maxillary posterior region of the sinus floor. Journal of Prosthetic Dentistry.

Lari, M., Di Vincenzo, F., Borsato, A., Ghirotto, S., Micheli, M., Balsamo, C., Collina, C., De Bellis, G., Frisia, S., Giacobini, G., Gigli, E., Hellstrom, J.C., Lannino, A., Modi, A., Pietrelli, A., Pilli, E., Profico, A., Ramirez, O., Rizzi, E., Vai, S., Venturo, D., Piperno, M., Lalueza-Fox, C., Barbujani, G., Caramelli, D., Manzi, G., 2015. The Neanderthal in the karst: First dating, morphometric, and paleogenetic data on the fossil skeleton from Altamura (Italy). Journal of Human Evolution. 82, 88–94.

Lebrun, R., Orliac, M.J., 2016. MORPHOMUSEUM: An online platform for publication and storage of virtual specimens. The Paleontological Society Papers.

Lee, D.-T., Schachter, B.J., 1980. Two algorithms for constructing a Delaunay triangulation. International Journal of Computer & Information Sciences. 9, 219–242.

Lieberman, D.E., 1998. Sphenoid shortening and the evolution of modern human cranial shape. Nature. 393, 158.

Lieberman, D.E., 2000. Ontogeny, homology, and phylogeny in the hominid craniofacial

skeleton: the problem of the browridge. In: Development, Growth and Evolution. Academic Press, pp. 86–115.

Lieberman, D.E., 2011. The evolution of the human head. Harvard University Press.

Lieberman, D.E., Pearson, O.M., Mowbray, K.M., 2000. Basicranial influence on overall cranial shape. Journal of Human Evolution.

Livnat, Y., Shen, H.W., Johnson, C.R., 1996. A near optimal isosurface extraction algorithm using the span space. IEEE Transactions on Visualization and Computer Graphics. 2, 73–84.

Lorensen, W.E., Cline, H.E., 1987. Marching cubes: A high resolution 3D surface construction algorithm. In: Proceedings of the 14th Annual Conference on Computer Graphics and Interactive Techniques - SIGGRAPH '87. ACM Press, New York, New York, USA, pp. 163–169.

Lundberg, J.O., 2008. Nitric oxide and the paranasal sinuses. Anatomical Record.

Lyman, R.L., 1994. Vertebrate taphonomy, Lyman 1994.

Maddux, S.D., Yokley, T.R., Svoma, B.M., Franciscus, R.G., 2016. Absolute humidity and the human nose: A reanalysis of climate zones and their influence on nasal form and function. American Journal of Physical Anthropology.

Maier, W., 2000. Ontogeny of the nasal capsule in cercopithecoids: a contribution to the comparative and evolutionary morphology of catarrhines. In: Old World Monkeys.

Manzi, G., 2004. Human Evolution at the Matuyama-Brunhes Boundary. Evolutionary Anthropology.

Manzi, G., 2016. Humans of the Middle Pleistocene: The controversial calvarium from Ceprano (Italy) and its significance for the origin and variability of Homo heidelbergensis. Quaternary International.

Manzi, G., Bernardini, F., Caramelli, D., Cremaschi, M., Di Vincenzo, F., Galli, C.,

Giacobini, G., Gigli, E., Lari, M., Lo Vetro, D., Martini, F., Muscolino, F., Persico, D., Poggiani Keller, R., Profico, A., Ravara, S., Ravazzi, C., Zanolli, C., Tuniz, C., 2014. The hominin frontal bone recently discovered in the Po Valley, Northern Italy. In: Proceedings of the European Society for the Study of Human Evolution 3. European Society for the study of Human Evolution,.

Manzi, G., Micheli, M., Giacobini, G., 2010. Il cranio dell'Uomo di Altamura: ipotesi di rimozione, documentazione multimediale e studio. DiRe in Puglia 2, Direzione Regionale BCA della Puglia, Bari. 35–40.

Marangoni, A., Belli, M.L., Caramelli, D., Moggi Cecchi, J., Zavattaro, M., Manzi, G., 2011. Tierra del Fuego, its ancient inhabitants, and the collections of skeletal remains in the Museum of Anthropology of Florence and Rome. Museologia scientifica. 5, 88–96.

Marquez, S., Gannon, P.J., Lawson, W., Reidenberg, J.S., Laitman, J.T., 2002. Were Neanderthals full of of" NO" gas? The relationship between paranasal sinus morphology and nitric oxide production. In: Abstracts of AAPA Poster and Podium Presentations. Am. J. Phys. Anthropol., 117: 104-124. WILEY-LISS DIV JOHN WILEY & SONS INC, 605 THIRD AVE, NEW YORK, NY 10158-0012 USA, p. 107.

Marra, F., Ceruleo, P., Jicha, B., Pandolfi, L., Petronio, C., Salari, L., 2015. A new age within MIS 7 for the Homo neanderthalensis of Saccopastore in the glacio-eustatically forced sedimentary successions of the Aniene River Valley, Rome. Quaternary Science Reviews. 129, 260–274.

Martimucci, V., Gueguen, E., Ragone, G., 2010. Grotta di Lamalunga Progetto di ricerca: rilievo topografico speleologico e realizzazione strati informativi. DiRe in Puglia 2, Direzione Regionale BCA della Puglia, Bari. 67–71.

Maureille, B., Bar, D., 1999. The premaxilla in Neandertal and early modern children: Ontogeny and morphology. Journal of Human Evolution.

Micarelli, I., Paine, R., Giostra, C., Tafuri, M.A., Profico, A., Boggioni, M., Di Vincenzo, F., Massani, D., Papini, A., Manzi, G., 2018. Survival to amputation in pre-antibiotic era: A case study from a longobard necropolis (6 th -8 th centuries AD). Journal of Anthropological Sciences.

Mitteroecker, P., Gunz, P., 2009. Advances in Geometric morphometrics. Evolutionary Biology.

Mlynski, R., Grützenmacher, S., Lang, C., Mlynski, G., 2003. Acoustic rhinometry and paranasal cavities: A systematic study in box models. Laryngoscope.

Moran, D.T., Rowley, J.C., Jafek, B.W., Lovell, M.A., 1982. The fine structure of the olfactory mucosa in man. Journal of Neurocytology.

Morrison, E.E., Costanzo, R.M., 1990. Morphology of the human olfactory epithelium. Journal of Comparative Neurology.

Murrill, R.I., 1981. Petralona man: A descriptive and comparative study, with new important information on Rhodesian man. Charles C Thomas Pub Limited.

Neaux, D., 2017. Morphological integration of the cranium in Homo, Pan, and Hylobates and the evolution of hominoid facial structures. American Journal of Physical Anthropology.

Ni, X., Flynn, J.J., Wyss, A.R., 2012. Imaging the inner ear in fossil mammals: High-resolution CT scanning and 3-D virtual reconstructions. Palaeontologia Electronica. 15.

Nicolae, C., Nocerino, E., Menna, F., Remondino, F., 2014. Photogrammetry applied to problematic artefacts. The International Archives of the Photogrammetry, Remote Sensing and Spatial Information Sciences. XL-5: 451-456.

Nicolielo, L.F.P., Van Dessel, J., Shaheen, E., Letelier, C., Codari, M., Politis, C., Lambrichts, I., Jacobs, R., 2017. Validation of a novel imaging approach using multi-slice CT and cone-beam CT to follow-up on condylar remodeling after

bimaxillary surgery. International Journal of Oral Science.

Noback, M.L., Harvati, K., Spoor, F., 2011. Climate-related variation of the human nasal cavity. American Journal of Physical Anthropology.

Ogihara, N., Nakatsukasa, M., Nakano, Y., Ishida, H., 2006. Computerized restoration of nonhomogeneous deformation of a fossil cranium based on bilateral symmetry. American Journal of Physical Anthropology.

Opitz, R., Nuninger, L., 2014. Point Clouds Segmentation of Mixed Scenes with Archeological Standing Remains: A Multi-Criteria and Multi-Scale Iterative Approach. International Journal of Heritage in the Digital Era. 3, 287–304.

Owercowicz, T., Musinsky, C., Middleton, K.M., Crompton, A.W., 2015. Respiratory turbinates and the evolution of endothermy in Mammals and Birds. In: Dial, K.P., Shubin, N., Brainerd, E.L. (Eds.), Great Transformations in Vertebrate Evolution.

Parry, R., 2016. Museums in a Digital Culture.

Pavlidis, G., Koutsoudis, A., Arnaoutoglou, F., Tsioukas, V., Chamzas, C., 2007. Methods for 3D digitization of Cultural Heritage. Journal of Cultural Heritage. 8, 93–98.

Pesce Delfino, V., Vacca, E., 1994. Report of an archaic human skeleton discovered at altamura (Bari), in the “Lamalunga” district. Human Evolution.

Piperno, M., 2010. Totem e Tabù. DiRe in Puglia 2, Direzione Regionale BCA della Puglia, Bari. 23–27.

Pollefeys, M., 2004. Visual 3D Modeling from Images. Vmv.

Ponce De León, M.S., Golovanova, L., Doronichev, V., Romanova, G., Akazawa, T., Kondo, O., Ishida, H., Zollikofer, C.P.E., 2008. Neanderthal brain size at birth provides insights into the evolution of human life history. Proceedings of the National Academy of Sciences.

Preuschoft, H., Witte, H., Witzel, U., 2002. Pneumatized Spaces, Sinuses and Spongy Bones in the Skulls of Primates. Anthropologischer Anzeiger.

Profico, A., Bellucci, L., Buzi, C., Di Vincenzo, F., Micarelli, I., Strani, F., Tafuri, M.A., Manzi, G., 2018a. Virtual Anthropology and its Application in Cultural Heritage Studies. Studies in Conservation.

Profico, A., Buzi, C., Davis, C., Melchionna, M., Veneziano, A., Raia, P., Manzi, G., 2019a. A New Tool for Digital Alignment in Virtual Anthropology. Anatomical Record.

Profico, A., Buzi, C., Davis, C., Melchionna, M., Veneziano, A., Raia, P., Manzi, G., 2019b. A New Tool for Digital Alignment in Virtual Anthropology. The Anatomical Record. 302, 1104–1115.

Profico, A., Piras, P., Buzi, C., Del Bove, A., Melchionna, M., Senczuk, G., Varano, V., Veneziano, A., Raia, P., Manzi, G., 2019c. Seeing the wood through the trees. Combining shape information from different landmark configurations. Hystrix, the Italian Journal of Mammalogy.

Profico, A., Piras, P., Buzi, C., Di Vincenzo, F., Lattarini, F., Melchionna, M., Veneziano, A., Raia, P., Manzi, G., 2017. The evolution of cranial base and face in Cercopithecoidea and Hominoidea: Modularity and morphological integration. American Journal of Primatology. 79.

Profico, A., Schlager, S., Valoriani, V., Buzi, C., Melchionna, M., Veneziano, A., Raia, P., Moggi-Cecchi, J., Manzi, G., 2018b. Reproducing the internal and external anatomy of fossil bones: Two new automatic digital tools. American Journal of Physical Anthropology.

Profico, A., Veneziano, A., Lanteri, A., Piras, P., Sansalone, G., Manzi, G., 2016. Tuning Geometric Morphometrics: an r tool to reduce information loss caused by surface smoothing. Methods in Ecology and Evolution. 7, 1195–1200.

Profico, A., Veneziano, A., Melchionna, M., 2015. Arothron: R Functions for Geometric Morphometrics Analyses. R package version. 314.

Profico, A., Veneziano, A., Melchionna, M., Raia, P., 2018c. Arothron: Geometric Morphometrics Analyses.

Quam, R., Martínez, I., Rosa, M., Bonmatí, A., Lorenzo, C., de Ruiter, D.J., Moggi-Cecchi, J., Conde-Valverde, M., Jarabo, P., Menter, C.G., Thackeray, J.F., Arsuaga, J.L., 2015. Early hominin auditory capacities. Science Advances.

R Development Core Team, 2016. R: A language and environment for statistical computing. R Foundation for Statistical Computing, R Foundation for Statistical Computing, Vienna, Austria.

Rae, T.C., Hill, R.A., Hamada, Y., Koppe, T., 2003. Clinal variation of maxillary sinus volume in Japanese macaques (Macaca fuscata). American Journal of Primatology.

Rae, T.C., Koppe, T., 2004. Holes in the head: Evolutionary interpretations of the paranasal sinuses in catarrhines. Evolutionary Anthropology.

Rae, T.C., Koppe, T., 2008. Independence of biomechanical forces and craniofacial pneumatization in Cebus. Anatomical Record.

Rae, T.C., Koppe, T., Spoor, F., Benefit, B., McCrossin, M., 2002. Ancestral loss of the maxillary sinus in Old World monkeys and independent acquisition in Macaca. American Journal of Physical Anthropology.

Rak, Y., 1986. The Neanderthal: A new look at an old face. Journal of Human Evolution.

Rak, Y., 1993. Morphological Variation in Homo neanderthalensis and Homo sapiens in the Levant. In: Species, Species Concepts and Primate Evolution.

Ramírez-Rozzi, F. V., Bermúdez De Castro, J.-M., 2004. Surpisingly rapid growth in Neanderthals. Nature.

Rogers, J., Waldron, T., 1989. Infections in palaeopathology: the basis of classification

according to most probable cause. Journal of Archaeological Science.

Rohlf, F.J., 1990. Morphometrics. Annual Review of Ecology and Systematics.

Rohlf, F.J., Marcus, L.F., 1993. A revolution in morphometrics. Trends in Ecology and Evolution.

Röntgen, W.C., 1896. On a new kind of rays (English translation). Nature.

Rosas, A., Bastir, M., Martinez-Maza, C., Garcia-Tabernero, A., Lalueza-Fox, C., 2008. Inquiries into Neanderthal craniofacial development and evolution:"accretion" versus "organismic" models. In: Harvati, K., Harrison, T. (Eds.), Neanderthals Revisited: New Approaches and Perspectives.

Rossie, J.B., 2005. Anatomy of the nasal cavity and paranasal sinuses in Aegyptopithecus and early miocene African catarrhines. American Journal of Physical Anthropology.

Rossie, J.B., 2006. Ontogeny and homology of the paranasal sinuses in platyrrhini (Mammalia: Primates). Journal of Morphology.

Rossie, J.B., Simons, E.L., Gauld, S.C., Rasmussen, D.T., 2002. Paranasal sinus anatomy of Aegyptopithecus: Implications for hominoid origins. Proceedings of the National Academy of Sciences.

Ryan, T.M., Ketcham, R.A., 2002. The three-dimensional structure of trabecular bone in the femoral head of strepsirrhine primates. Journal of Human Evolution.

Sala, N., Pantoja-Pérez, A., Arsuaga, J.L., Pablos, A., Martínez, I., 2016. The Sima de los Huesos Crania: Analysis of the cranial breakage patterns. Journal of Archaeological Science.

Schlager, S., 2017. Morpho and Rvcg – Shape Analysis in R. In: Statistical Shape and Deformation Analysis.

Schlager, S., Profico, A., Di Vincenzo, F., Manzi, G., 2018. Retrodeformation of fossil

specimens based on 3D bilateral semi-landmarks: Implementation in the R package "Morpho." PLOS ONE. 13, e0194073.

Schwartz, J.H., Tattersall, I., 2002. Significance of some previously unrecognized apomorphies in the nasal region of Homo neanderthalensis. Proceedings of the National Academy of Sciences.

Scopigno, R., Cignoni, P., Pietroni, N., Callieri, M., Dellepiane, M., 2015. Digital Fabrication Techniques for Cultural Heritage: A Survey. Computer Graphics Forum. 36, 6–21.

Sergi, S., 1936. Die Entdeckung eines weiteren Schädels des Homo neandertalensis var. aniensis in der Grube von Saccopastore (Rom). Anthropologischer Anzeiger. 281–284.

Shea, B.T., 1977. Eskimo craniofacial morphology, cold stress and the maxillary sinus. American Journal of Physical Anthropology.

Shipman, P., 1981. Life History of a Fossil.An introduction to Taphonomy and Paleoecology. % Harvard. Harvard University Press.

Slice, D.E., 2006. Modern Morphometrics. In: Modern Morphometrics in Physical Anthropology.

Soikkonen, K., Ainamo, A., 1995. Radiographic maxillary sinus findings in the elderly. Oral Surgery, Oral Medicine, Oral Pathology, Oral Radiology and.

Sommer, R.S., Nadachowski, A., 2006. Glacial refugia of mammals in Europe: Evidence from fossil records. Mammal Review.

Spoor, F., Hublin, J.-J., Braun, M., Zonneveld, F.W., 2003. The bony labyrinth of Neanderthals. Journal of Human Evolution.

Spoor, F., Zonneveld, F.W., 1995. Morphometry of the primate bony labyrinth: a new method based on high-resolution computed tomography. Journal of anatomy.

Spoor, F., Zonneveld, F.W., Macho, G.A., 1993. Linear measurements of cortical bone and dental enamel by computed tomography: Applications and problems. American Journal of Physical Anthropology. 91, 469–484.

Stalling, D., Westerhoff, M., Hege, H.C., 2005. Amira: A highly interactive system for visual data analysis. In: Visualization Handbook.

Stringer, C.B., 1990. A metrical study of the Guattari and Saccopastore crania. In: Quatern Nov. pp. 621–638.

Stringer, C.B., Howell, F.C., Melentis, J.K., 1979. The significance of the fossil hominid skull from Petralona, Greece. Journal of Archaeological Science.

Tafforeau, P., Boistel, R., Boller, E., Bravin, A., Brunet, M., Chaimanee, Y., Cloetens, P., Feist, M., Hoszowska, J., Jaeger, J.J., Kay, R.F., Lazzari, V., Marivaux, L., Nel, A., Nemoz, C., Thibault, X., Vignaud, P., Zabler, S., 2006. Applications of X-ray synchrotron microtomography for non-destructive 3D studies of paleontological specimens. Applied Physics A: Materials Science and Processing.

Tallman, M., Amenta, N., Delson, E., Frost, S.R., Ghosh, D., Klukkert, Z.S., Morrow, A., Sawyer, G.J., 2014. Evaluation of a New Method of Fossil Retrodeformation by Algorithmic Symmetrization: Crania of Papionins (Primates, Cercopithecidae) as a Test Case. PloS one. 9, e100833.

Tattersall, I., 1972. The functional significance of airorhynchy in Megaladapis. Folia primatologica; international journal of primatology.

Thompson, D.W., 1992. On Growth and Form: The Complete Revised Edition, Book.

Tobias, P. V., 1971. The brain in hominid evolution (James Arthur lecture on the evolution of the human brain, no. 38, 1969). New York, NY: Columbia University Press.

Trinkaus, E., 2007. European early modern humans and the fate of the Neandertals. Proceedings of the National Academy of Sciences.

Trinkaus, E., Lemay, M., 1982. Occipital bunning among later pleistocene hominids. American Journal of Physical Anthropology.

Tuniz, C., Bernardini, F., Caramelli, D., Cremaschi, M., Di Vincenzo, F., Galli, C., Giacobini, G., Gigli, E., Lari, M., Lo Vetro, D., 2014. Frontal bone of Neanderthal morphology recently discovered in the Po valley, Italy. In: Evolution of Modern Humans - From Bones to Genomes.

Vacca, E., 2006. I resti umani di Contrada Lamalunga (Altamura) nel contesto dei ritrovamenti paleoantropologici pugliesi. Ricerche Speleologiche. 1, 28–54.

Vacca, E., Pesce Delfino, V., 2004. Three-dimensional topographic survey of the human remains in Lamalunga Cave (Altamura, Bari, Southern Italy). Collegium Antropologicum.

van Zijverden, W.K., Laan, W.N.H., 2003. Landscape reconstructions and predictive modeling in archaeological research, using a LiDAR based DEM and digital boring databases. Workshop Archaologie and Computer 9. 1–8.

Vanghi, V., Frisia, S., Borsato, A., 2017. Genesis and microstratigraphy of calcite coralloids analysed by high resolution imaging and petrography. Sedimentary Geology.

Veneziano, A., Landi, F., Profico, A., 2018. Surface smoothing, decimation, and their effects on 3D biological specimens. American Journal of Physical Anthropology.

Villmoare, B.A., Kimbel, W.H., 2011. CT-based study of internal structure of the anterior pillar in extinct hominins and its implications for the phylogeny of robust Australopithecus. Proceedings of the National Academy of Sciences.

Weber, G.W., 2001. Virtual anthropology (VA): A call forGlasnost in paleoanthropology. The Anatomical Record. 265, 193–201.

Weber, G.W., 2014. Another link between archaeology and anthropology: Virtual anthropology. Digital Applications in Archaeology and Cultural Heritage.

Weber, G.W., Bookstein, F.L., 2011. Virtual anthropology: a guide to a new interdisciplinary field. Springer Verlag.

Weber, G.W., Recheis, W., Scholze, T., Seidler, H., 1998. Virtual anthropology (VA): methodological aspects of linear and volume measurements--first results. Coll Antropol. 22, 575–584.

Weiner, J.S., 1954. Nose shape and climate. American Journal of Physical Anthropology.

White, T.D., Black, M.T., Folkens, P.A., 2011. Human osteology. Academic press.

White, T.D., Folkens, P.A., 2005. The Human Bone Manual, The Human Bone Manual.

Wilson, P.F., Williams, M.A., Warnett, J.M., Attridge, A., Ketchum, H., Hay, J., Smith, P.M., 2017. Utilizing X-ray computed tomography for heritage conservation: The case of Megalosaurus bucklandii. In: I2MTC 2017 - 2017 IEEE International Instrumentation and Measurement Technology Conference, Proceedings. IEEE, pp. 1–5.

Wind, J., 1984. Computerized X-ray tomography of fossil hominid skulls. American Journal of Physical Anthropology. 63, 265–282.

Wind, J., Zonneveld, F.W., 1985. Radiology of fossil hominid skulls. Hominid Evolution, Past, Present and Future. 437–442.

Wind, J., Zonneveld, F.W., 1989. Computed tomography of an Australopithecus skull (Mrs ples): A new technique. Naturwissenschaften.

Witmer, L.M., 1997. Craniofacial Air Systems. In: Encyclopedia of Dinosaurs.

Witmer, L.M., 1999. The Phylogenetic History of Paranasal Air Sinuses. In: Koppe, T., Nagai, H., Alt, K.W. (Eds.), The Paranasal Sinuses of Higher Primates: Development, Function and Evolution. Quintessence, pp. 21–34.

Wright, J., 1914. A history of laryngology and rhinology, The Laryngoscope.

Yokley, T.R., 2009. Ecogeographic variation in human nasal passages. American Journal

of Physical Anthropology.

Yoshida, T., Vivatbutsiri, P., Morriss-Kay, G., Saga, Y., Iseki, S., 2008. Cell lineage in mammalian craniofacial mesenchyme. Mechanisms of development. 125, 797–808.

Zezza, F., Zezza, T., 1999. Il carsismo in Puglia. Mario Adda.

Zollikofer, C.P.E., de León, M.S.P., Lieberman, D.E., Guy, F., Pilbeam, D., Likius, A., Mackaye, H.T., Vignaud, P., Brunet, M., 2005. Virtual cranial reconstruction of Sahelanthropus tchadensis. Nature. 434, 755–759.

Zollikofer, C.P.E., Ponce De León, M.S., Martin, R.D., 1998. Computer-assisted paleoanthropology. Evolutionary Anthropology: Issues, News, and Reviews. 6, 41–54.

Zollikofer, C.P.E., Ponce De León, M.S., Martin, R.D., Stucki, P., 1995. Neandertal Computer Skulls. Nature. 375, 283–285.

Zollikofer, C.P.E., Ponce de León, M.S., Schmitz, R.W., Stringer, C.B., 2008. New insights into mid-late pleistocene fossil hominin paranasal sinus morphology. Anatomical Record.